Partial Meniscectomy and Osteoarthritis: Evaluation with Quantitative Magnetic Resonance Imaging

By

Megan E. Bowers

B.S.E., University of Connecticut, May 2005

Submitted in partial fulfillment of the requirements for the degree of Doctor of Philosophy in the Program in Biomedical Engineering at Brown University

Providence, Rhode Island

May 2010

This dissertation by Megan E. Bowers is accepted in its present form

by the Department of Biomedical Engineering as satisfying the

dissertation requirement for the degree of Doctor of Philosophy.

Date_____ _____

Braden C. Fleming, Ph.D., Advisor

Date_____ _____

Joseph J. Crisco, Ph.D., Reader

Date_____ _____

Glenn A. Tung, M.D., F.A.C.S., Reader

Date_____ _____

Benjamin B. Kimia, Ph.D., Reader

Date_____ _____

Martha M. Murray, M.D., External Reader

Approved by the Graduate Council

Date_____ _____

Sheila Bonde, Dean of the Graduate School

Curriculum Vitae

Megan E. Bowers was born on August 14, 1983 in Groton, CT to Michael and Donna Bowers. Megan was raised in Gales Ferry, CT with her older brother Robert. She was the valedictorian of Ledyard High School's Class of 2001. She received her Bachelor's of Science in Engineering from the University of Connecticut in 2005, with a major in Biomedical Engineering and a concentration in Bioinformatics. Megan was a University of Connecticut Honors Scholar. During her undergraduate education, Megan was co-captain and treasurer of the University of Connecticut Equestrian Team (UCET), and represented UCET in national competition in 2005, finishing 10^{th} in her division. After graduating from the University of Connecticut in 2005, Megan enrolled in the Ph.D. program at Brown University, where she joined the Bioengineering Laboratory within the Department of Orthopaedics at Brown Alpert Medical School/Rhode Island Hospital. Working with Braden C. Fleming, Ph.D., her dissertation advisor, she has been an author on five original peer-reviewed publications.

CURRICULUM VITAE

MEGAN ELIZABETH BOWERS

Bioengineering Laboratory
CORO West, Suite 404
1 Hoppin Street
Providence, RI 02903

(860)-235-3482 phone
(401)-444-4418 fax
Megan_Bowers@brown.edu
MeganEBowers@gmail.com

Education

Brown University, Providence, RI
Ph.D. Biomedical Engineering, expected May 2010
University of Connecticut, Storrs, CT
B.S.E. Biomedical Engineering, May 2005
Honors Scholar

Original Peer-Reviewed Publications

1. Fleming BC, Oksendahl HL, Mehan WA, Portnoy R, Fadale PD, Hulstyn MJ, **Bowers ME**, Machan JT, Tung GA. Delayed Gadolinium-Enhanced MR Imaging of Cartilage (dGEMRIC) Following ACL Injury. *Osteoarthritis and Cartilage*, In Press.

2. **Bowers ME**, Tung GA, Oksendahl HL, Hulstyn MJ, Fadale PD, Machan JT, Fleming BC. Quantitative Magnetic Resonance Imaging Detects Changes in Meniscal Volume *in Vivo* after Partial Meniscectomy. *The American Journal of Sports Medicine*, In Press.

3. **Bowers ME**, Trinh N, Tung GA, Crisco JJ, Kimia BB, Fleming BC. Quantitative MRI using "LiveWire" to Measure Tibiofemoral Articular Cartilage Thickness. *Osteoarthritis and Cartilage*, 16: 1167-1173 (2008). (PMID: 18407529)

4. **Bowers ME**, Tung GA, Trinh N, Leventhal E, Crisco JJ, Kimia BB, Fleming BC. Effects of ACL Interference Screws on Articular Cartilage Volume and Thickness Measurements with 1.5T and 3T MRI. *Osteoarthritis and Cartilage*, 16: 572-578 (2008). (PMID: 17933559)

5. **Bowers ME**, Tung GA, Fleming BC, Crisco JJ, Rey J. Quantification of Mensical Volume by Segmentation of 3T Magnetic Resonance Images. *Journal of Biomechanics*, 40: 2811-2815 (2007). (PMID: 17391677)

Grants

National Football League Charities Medical Research Grant: ACL Reconstruction using Biologically Enhanced Patellar Tendon Autograft. $124,985 (direct), 1/2009-1/2010, Principal Investigator.

Professional Experience

Department of Orthopaedics, Brown Medical School/Rhode Island Hospital, Providence, RI

— Ph.D. student under Dr. Braden Fleming, *September 2005 - Present*

Hartford Hospital and Connecticut Children's Medical Center, Hartford, CT

— Student researcher, *October 2003– May 2005*

Pfizer, Inc., Groton, CT

— Summer research associate, *May – August 2003*

Teaching Experience

Organ Replacement (Brown University Course BI 1080)

Supplementary Teaching Assistant, *January – May 2008*

— Teaching assistant for Dr. Michael Lysaght's course of approximately 100 undergraduate and graduate-level students

— Tracked students' grades, answered general questions, and adjudicated regrades

Theses and Unrefereed Publications

Bowers ME. The Electronic Esophageal Stethoscope. Honors Thesis, Department of Biomedical Engineering. University of Connecticut, April 2005.

Awards and Honors

Mimics Innovation Award, Presented by Materialise, *May 2008*
University of Connecticut Honors Scholar, *May 2005*
New England Scholar, *April 2005*
Deligeorges Family Scholarship in Biomedical Engineering, *April 2004*
University of Connecticut School of Engineering Scholarship, *August 2003*
Intercollegiate Equestrian Foundation Scholarship, *May 2003*
Connecticut Innovations Technology Scholarship, *June 2001*

Professional Memberships

Orthopaedic Research Society (ORS)

— Associate member, *November 2008 - Present*

American Society of Biomechanics (ASB)

— Student member, *July 2008 - Present*

Osteoarthritis Research Society International (OARSI)

— Student member, *May 2008 - Present*

Sigma Xi

— Associate member, Brown University Chapter, *March 2008 – Present*

University Panels and Memberships

Student Advisory Panel for the Office of BioMed Graduate and Postdoctoral Studies, Brown University

— Biomedical Engineering representative, *September 2007 – 2009*

Women in Science and Engineering (WiSE)

— Mentor to first-year graduate students, *September 2007 – 2009*

University Health Services Emergency Medical Services Manager Hiring Committee

— Student representative on interview and discussion panel, *March – May 2007*

Biomedical Engineering Society (BMES)

— Member, University of Connecticut chapter, *September 2001 – May 2005*

Volunteer Experience

Brown University Emergency Medical Services

— American Heart Association BLS CPR Instructor, *October 2005 – September 2011*

— Volunteer EMT, *September 2005 – December 2008*

— Senior EMT, *September 2006 – September 2008*

— Brown University RIEMT-B Course Laboratory Instructor, *June - August 2007*

St. Margaret's School, East Providence, RI

— Science fair instructor and judge for middle school students, *November 2007 – January 2008*

Abstracts

1. **Bowers ME**, Tung GA, Oksendahl HL, Hulstyn MJ, Fadale PD, Fleming BC. Delayed Gadolinium-Enhanced MRI of Cartilage (dGEMRIC) 12 Months after ACL Reconstruction. Poster presentation, Orthopaedic Research Society, New Orleans, LA, 6-9 March 2010.

2. Tung GA, Mehan WA, Portnoy R, Fadale PD, Hulstyn MJ, **Bowers ME**, Oksendahl HL, Fleming BC. Delayed Gadolinium-Enhanced MR Imaging of Cartilage (dGEMRIC) after ACL Tear. Oral presentation, American Roentgen Ray Society, Boston, MA, 26 April – 1 May 2009.

3. Fleming BC, Portnoy R, Tung GA, Fadale PD, Hulstyn MJ, **Bowers ME**, Oksendahl HL. Delayed Gadolinium-Enhanced MR Imaging of Cartilage (dGEMRIC) after ACL Injury. Podium presentation, Orthopaedic Research Society, Las Vegas, NV, 22-25 February 2009.

4. Mehan WA, Tung GA, Portnoy R, Fadale PD, Hulstyn MJ, **Bowers ME**, Oksendahl HL, Fleming BC. Delayed Gadolinium-Enhanced MR Imaging of Cartilage (dGEMRIC) after ACL Injury. Radiological Society of North America, Chicago, Illinois, 30 November-5 December 2008.

5. **Bowers ME**, Tung GA, Oksendahl HL, Hulstyn MJ, Fadale PD, Fleming BC. Quantifying Meniscal Volume and Articular Cartilage Thickness in Patients Treated with Partial Meniscectomy. Podium presentation, North American Congress on Biomechanics, Ann Arbor, MI, 5-9 August 2008.

6. **Bowers ME**, Tung GA, Oksendahl HL, Hulstyn MJ, Fadale PD, Fleming BC. Quantifying Meniscal Volume and Tibiofemoral Cartilage Thickness after Partial Meniscectomy. Poster presentation, 2nd Annual Workshop on Imaging-Based Measures of Osteoarthritis, Boston, MA, 25-28 June 2008.

7. Portnoy R, Tung GA, Fadale PD, Hulstyn MJ, **Bowers ME**, Oksendahl HL, Fleming BC. Delayed Gadolinium Enhanced MRI of Cartilage (dGEMRIC) After ACL Tear. Poster presentation, 2nd Annual Workshop on Imaging-Based Measures of Osteoarthritis, Boston, MA, 25-28 June 2008.

8. **Bowers ME**, Tung GA, Trinh N, Crisco JJ, Kimia BB, Fleming, BC. Quantitative MRI using "LiveWire" to Measure Tibiofemoral Articular Cartilage Thickness. Poster presentation, Rhode Island Research Alliance Symposium, Providence, RI, 3 June 2008.

9. Portnoy R, Tung GA, Fadale PD, Hulstyn MJ, **Bowers ME**, Oksendahl HL, Fleming BC. Delayed Gadolinium Enhanced MRI of Cartilage (dGEMRIC) in Early Detection of Cartilage Degeneration in Patients with Acute ACL Injury. Podium presentation, Northeast Bioengineering Conference, Providence, RI, 4-6 April 2008.

10. **Bowers ME**, Tung GA, Trinh N, Crisco JJ, Kimia BB, Fleming, BC. Quantitative MRI using "LiveWire" to Measure Tibiofemoral Articular Cartilage Thickness. Poster presentation, Orthopaedic Research Society, San Francisco, CA, 2-5 March 2008.

11. **Bowers ME**, Fleming BC, Tung GA, Leventhal EL, Trinh N, Crisco JJ, Kimia BB. Effects of ACL Interference Screws on Tibiofemoral Articular Cartilage Thickness Measurements with 1.5T and 3T MRI. Poster presentation, Rhode Island Hospital Research Celebration, Providence, RI, 13 November 2007.

12. **Bowers ME**, Fleming BC, Tung GA, Leventhal EL, Trinh N, Crisco JJ, Kimia BB. Effects of ACL Interference Screws on Articular Cartilage Thickness Measurements with 1.5T and 3T MRI. Poster presentation, American Society of Biomechanics, Palo Alto, CA, 22-25 August 2007.

13. Fleming BC, **Bowers ME**, Tung GA, Leventhal EL, Trinh N, Crisco JJ, Kimia BB: Effects of ACL Interference Screws on Femorotibial Cartilage Thickness Measurements using 1.5T and 3T MRI. Poster presentation, Workshop on Imaging-Based Measures of Osteoarthritis, Salzburg, 11-14 July 2007.

14. **Bowers ME**, Tung GA, Fleming BC, Crisco JJ, Rey J. Quantification of Meniscal Volume by Segmentation of 3T MR Images. Poster presentation, Orthopaedic Research Society, San Diego, CA, 11-14 February 2007.

15. **Bowers ME**, Tung GA, Fleming BC, Crisco JJ, Rey J. Quantification of Meniscal Volume by Segmentation of 3T MR Images. Poster presentation, Rhode Island Hospital Research Celebration, Providence, RI, 14 November 2006.

16. McIsaac JH, **Bowers ME**. The Electronic Esophageal Stethoscope. Poster presentation, MEDi2005 Conference and Exhibition, Hartford, CT, October 2005.

Preface and Acknowledgements

My thesis work has been truly enjoyable, and there are many to thank for providing such a wonderful experience. My committee members deserve special thanks. Drs. Crisco, Tung, Kimia, and Murray, I thank you for all of your help and support; I am truly grateful to have such an exceptional team of scholars critique and improve my work. I would also like to thank Dr. Michael Ehrlich and the rest of the Department of Orthopaedics for all of their support.

Of course, my advisor, Braden Fleming, Ph.D., has been essential to my dissertation work. It would be impossible to list everything he has taught me since I began working with him. He has given me a more sound and productive start on my career than I ever imagined. He has made the last five years fun, which is rare for any graduate student. His guidance and incredible work ethic have been invaluable learning tools for me. I am very fortunate to have been a part of his research efforts. A simple thank-you does not suffice.

To my fellow students and colleagues in the Bioengineering Lab: thank you for your support and encouragement. You have made my graduate experience fun, and our “noon-sharp” lunches have kept me grounded.

Those who know me realize that without my furry, four-legged equine friends, I would surely need a professional therapist. The horses that have tolerated and educated me, and maybe even appreciated me during this process deserve special thanks. An equally grateful thank-you goes to the Kil family, who has supported my equine habit, provided me with endless opportunities, and has truly become like a second family to me.

Similarly, I would have been institutionalized long ago without the help and guidance of my friends. It seems they are always there for me, whether it is to support my education or to provide a welcome distraction from it. I am unsure what I have done to deserve such wonderful, unconditional friendships, and I am grateful for them each day.

Finally, there are simply not enough words to thank my parents for their unconditional love and support during my lengthy education. Even on the worst days, my loving family and happy yellow dog have provided sound advice and encouragement. I am profoundly appreciative, even though I may not always find the right way to express it. Without you, Mom and Dad, I would be lost.

Table of Contents

List of Tables

Chapter 2

Chapter 3

Chapter 4

Chapter 5

Chapter 6

List of Figures

Chapter 1

Chapter 2

Chapter 3

Chapter 4

Chapter 5

Chapter 6

Chapter 7

Chapter 1

Introduction

1.1 Overview

The knee is the largest joint in the human body, and is comprised of two joints: the patellofemoral joint, which is the junction between the distal femur and the patella, and the tibiofemoral joint, which is the junction between the distal femur and proximal tibia. The articulating surfaces of the patella, distal femur, and proximal tibia are lined with articular cartilage. Healthy articular cartilage is a smooth tissue that allows functional joint motion with little friction and minimal wear. The knee joint also contains synovial fluid, which provides joint lubrication and cartilage nutrition. The knee has four major ligaments: the anterior cruciate ligament (ACL), the posterior cruciate ligament (PCL), the medial collateral ligament (MCL), and the lateral collateral ligament (LCL) **(Figure 1.1)**. The knee also has two cartilaginous menisci, which act as shock absorbers for the tibiofemoral joint. Both menisci serve to increase contact area, and therefore decrease contact stress, on the articular cartilage of the distal femur and proximal tibia.

Injuries to the tibiofemoral joint, and specifically to the menisci, are common. Meniscal tears are often treated with arthroscopic partial meniscectomy, a common procedure in which the torn area of the meniscus is removed, while the unaffected, stable portion is left intact. A meniscal tear and its surgical treatment may place the knee at risk of developing osteoarthritis (OA) because it may disrupt the load-bearing and protective functions of the meniscus. In the case of a symptomatic meniscal tear, partial resection is routinely performed to eliminate symptoms while attempting to preserve the integrity of the articular cartilage. Although the removal of meniscal tissue may not be the only factor associated with the outcome of a partial meniscectomy, the volume of meniscus removed contributes to functional loss. It is unknown, however, whether there is a critical threshold amount of meniscal tissue that can be removed without diminishing the structure's chondroprotective function.

The long-term objective of this work is to identify whether such a threshold exists by measuring the volume of meniscal tissue removed during partial meniscectomy, and then tracking the development of OA using quantitative magnetic resonance imaging (MRI) to assess articular cartilage thickness. In order to examine the existence of such a threshold, it is necessary to first develop non-invasive techniques to examine meniscal morphometry and articular cartilage thickness *in vivo*. The immediate goals of this work, therefore, were to refine, validate, and apply MR imaging-based methods for quantifying meniscal volume, and for mapping and quantifying changes in articular cartilage thickness within the tibiofemoral joint.

1.2 Background

1.2.1 The Menisci

The menisci are crescent-shaped fibrocartilagenous load-bearing washers that protect the articular cartilage by maximizing contact area and minimizing contact stress within the tibiofemoral joint. The menisci are essential to long-term joint function because they reduce contact stress [1-6], attenuate shock [7-9], and guide knee motion [10-11]. The menisci are also believed to enhance joint lubrication [12] and joint proprioception [12-13]. When the knee is fully extended, 50% of the tibiofemoral compressive load is transmitted through the menisci. The portion of load supported by the meniscus increases to 85% when the knee is flexed at 90^{o} [1]. When the knee is subjected to impact loads, the menisci are squeezed toward the periphery, in turn deforming the resistive circumferential fibers and dissipating energy.

The complete removal of one meniscus ("total meniscectomy") can decrease the contact area by 50 to 70%, which significantly increases the contact stress on the articular cartilage [1]. The shock-absorbing capabilities of the knee are reduced by 20% following total meniscectomy [8]. The menisci also maintain joint congruity and provide stability to the knee [12]. The menisci may also promote hydrodynamic lubrication, which in turn may minimize cartilage wear [12]. Clearly, the chondroprotective function of injured menisci must be restored to preserve the long-term integrity and function of the tibiofemoral joint.

1.2.2 Meniscal Tears

Meniscal tears are typically classified as acute or chronic. The overall meniscal injury rate is reported to be 0.7 per 1000 people per year [14]. Approximately 70% of meniscal tears are “chronic” (i.e. degenerative), while 30% are due to an “acute” injury [15]. Acute tears are most common among younger patients. They frequently occur during sporting activities, and usually take the form of longitudinal or radial tears [16-17]. In contrast, degenerative tears, which typically take the form of horizontal, flap, or complex tears, are more common in older patients [16-17]. 73-81% of all meniscal injuries occur in the medial compartment [14, 16, 18-19]. Meniscal injuries are more prevalent in males (over 3:1) [14-15, 18-19]. The work presented within this dissertation will focus on the treatment of acute medial meniscal tears, rather than chronic tears.

Meniscal tears may place the cartilage at risk of developing OA. When a meniscus is torn, the contact mechanics of the tibiofemoral joint are altered, which disrupts the homeostasis of articular cartilage metabolism, placing the knee at risk for early osteoarthritis. Biomechanical studies have clearly shown that joint contact mechanics are altered following meniscectomy and meniscal transplantation [2, 6, 20-24]. It has been hypothesized, though not proven, that acute tears may be responsible for initiating OA, while chronic tears may be a result of the degenerative process [25]. In older patients undergoing treatment for OA, meniscal tears are extremely common [26] and have been shown to accelerate cartilage degeneration [27]. Similarly, from both functional and radiographic perspectives, patients with degenerative tears who are treated with meniscectomy do not fare as well as patients with acute tears who undergo similar

treatment [15]. These data support the hypothesis that degenerative tears are the result, and not the source, of OA.

1.2.3 Surgical Treatment of Meniscal Tears

There are several surgical treatment options for meniscal tears, the most common of which is partial meniscectomy. Other alternatives include repair, which is limited to longitudinal tears in the periphery of the menisci, and transplantation. It remains unknown whether these alternative treatments are effective in preventing OA development [12, 16-17, 28]. Total meniscectomy, or the complete removal of the affected meniscus, was once the standard treatment for symptomatic meniscal tears. This procedure decreases tibiofemoral contact area by 50-70%, a change which significantly increases contact stress on the articular cartilage [1], and reduces its shock-absorbing capabilities [8-9]. The link between total meniscectomy and OA has been well-documented [29-31], and because this procedure has been linked to a high rate of OA development, it is now avoided [29-32]. In a cross-sectional study, Roos et al. reported a six-fold increase in the risk of OA following complete meniscectomy when compared to age- and sex-matched controls [31]. Thus, partial resection, in which the undamaged portion of the affected meniscus is preserved, is now routinely performed to eliminate symptoms while attempting to preserve articular cartilage integrity [15, 25, 29, 33-34].

Arthroscopic partial meniscectomy is the most common knee-related orthopaedic surgical procedure in the United States [17]. The American Academy of Orthopaedic Surgeons (AAOS) reported that 1.5 million arthroscopic knee procedures are performed in the United States each year, 850,000 of which are related to the meniscus [35]. The

cost of surgery alone is estimated at $2.5 billion. This estimate does not include the long-term costs associated with post-traumatic OA, which is likely to afflict many partial meniscectomy patients in the future. Because meniscal tears place the knee at risk for developing OA, a comprehensive understanding of the outcomes associated with current meniscal treatment options is paramount.

Partial meniscectomy does not eliminate the risk of OA due to an acute meniscal injury [15, 25, 28, 31, 33-34, 36-46]. Based on a 15-year follow-up study, Englund concluded that 50% of patients who underwent partial meniscectomy had radiographic evidence of OA, while an additional 20% had symptoms of OA without radiographic evidence [16]. Factors contributing to poor outcomes included degenerative tears, obesity, age, compartment, and sex [15, 25, 29, 33, 37, 43-44]. It should be noted that Englund found no difference in radiographic evidence of OA (grading joint space narrowing and osteophyte formation on a 4-point scale) between partial (<1/3) and subtotal (1/3-2/3) meniscectomies [25]. The size of each meniscectomy was subjectively assessed by each surgeon using an arthroscope. To date, no clinical studies have objectively measured the amount of meniscal tissue that can be removed following acute meniscal injury without placing the knee at risk of OA. In order to perform such a study it is necessary to accurately and reliably measure changes in meniscal and cartilage geometry after surgery and as OA progresses.

1.2.4 Osteoarthritis of the Tibiofemoral Joint

Osteoarthritis (OA) of the tibiofemoral joint is marked by distinct changes in cartilage volume and thickness [47-58]. *In vivo* methods that can accurately track these

initial volume and thickness changes are crucial for documenting the onset and progression of OA. The application of such methods to patients who have undergone partial meniscectomy for the treatment of an acute meniscal tear may help elucidate the mechanisms by which OA develops after partial meniscectomy.

Although the mechanisms of OA in the acutely injured knee are not known, altered joint contact mechanics are likely to contribute to OA development. When the meniscus is torn, the contact mechanics of the tibiofemoral joint are altered, which in turn disrupts the homeostasis of articular cartilage metabolism and places the knee at risk for the early development of OA. Other factors that may promote OA in the meniscal injured patient include joint inflammation [59-60] and impact damage sustained by the subchondral bone at the time of meniscal injury [6, 61]. Biomechanical studies have clearly shown that joint contact mechanics, specifically impact loading and contact area, are altered in both meniscectomized knees and knees which have undergone meniscal transplantation [2, 6, 20, 22-23, 62-63]. Cadaver and finite element models are valuable for assessment of the variables that effect joint contact, but the application of such models is limited because they do not incorporate the effects of joint inflammation and healing.

1.2.5 Meniscal Injury, Partial Meniscectomy, and Osteoarthritis

Although several clinical follow-up studies that evaluate outcome after partial meniscectomy have been performed, no cause-and-effect relationship between meniscal injury, partial meniscectomy, and OA development has been established. The long-term objective of the proposed work is to perform such a study. Most of the studies performed

to date were designed as retrospective studies and were based on radiographic evidence of OA progression and/or patient-oriented outcome measures [15, 25, 28, 31, 33-34, 36-37, 39-44]. These long-term clinical studies, particularly those which incorporated matched control groups [25, 28, 31, 34, 43], have provided valuable information related to general outcome, and have identified variables that are most likely associated with the development of OA following partial meniscectomy. However, they are not sufficient to evaluate the mechanism of OA in patients following partial meniscectomy, largely because they are retrospective studies that do not quantify the changes that occur within the joint over time. Recent developments in imaging, proteomics, and biochemical markers of articular cartilage metabolism have provided new methods to assess the initial response of cartilage to partial meniscectomy. Using the methods described and validated below, a long-term prospective study will be performed. This prospective study will employ these methods to test the hypotheses that isolated acute partial meniscectomy will affect the structure and metabolism of the articular cartilage, and that a change in joint contact mechanics is likely a mechanism for disease progression. One aim of the study will be to determine whether there is a critical volume of meniscal tissue that can be removed following acute meniscal injury without placing the knee at risk of OA. Before this long-term prospective study can be initiated, a method to quantify meniscal damage and the associated healing response must be developed. Therefore, an accurate and precise method for measuring the amount of meniscal tissue removed during partial meniscectomy, and for assessing articular cartilage volume and thickness following partial meniscectomy, is crucial for tracking patients' progression toward OA following this surgical procedure.

1.2.6 Quantitative Magnetic Resonance Imaging

Quantitative MRI is a promising technique for documenting the location and size of a meniscal resection. In an effort to develop a technique for sizing meniscal allografts, Stone et al. used an MR imaging approach to determine meniscal volume [64]. The imaging protocol included a 3-D MRI sequence (TR = 55 ms, TE = 15 ms, flip angle = 11^{o}, 16-18 cm FoV; 256 x 256 acquisition matrix); however, details regarding the segmentation process were not provided. The images were obtained on a 1.5T MRI scanner. The MRI measurements were performed six times prior to excising the menisci from the cadaver models used in the study. Once excised, the true meniscal volumes were measured by placing each meniscus in saline and measuring the volume of saline displaced. Stone et al. determined that the MRI technique was precise and repeatable, though it consistently underestimated the true meniscal volume by 20 and 44% for the medial and lateral menisci, respectively. Stone et al. concluded that the technique could be useful for measuring changes within a meniscus allograft over time with healing, but was not sufficient for sizing a meniscal allograft. The precision and repeatability values they reported provide credence to the approach. However with the use of high resolution MRI (3T) and improved segmentation techniques it may be possible to increase the accuracy and resolution of the method. By determining the size of a meniscus before and after surgery, it is possible to obtain a measurement of the amount of meniscus removed by subtracting the volumes obtained before and after surgery. It is also possible to recreate three-dimensional virtual models of the meniscus to assess regional changes in meniscal morphometry that occur with surgery and remodeling.

Quantitative MRI is also useful for documenting the volume and thickness of the articular cartilage of the tibiofemoral joint. Quantitative magnetic resonance imaging (qMRI) has been used to assess changes in cartilage morphometry, and it may prove to be a valuable measure for studying OA progression [48, 54-55]. Eckstein et al. performed a study to assess the accuracy of articular cartilage volume and thickness measurements made using 1.5T MRI [65]. The images were segmented in the sagittal plane using a two-step process, which included a region-growing algorithm. The volume and thickness measurements made using MRI were compared to similar measurements made using CT arthrography, which can be considered a gold standard for knee joint volume and thickness measurements. Eckstein et al. found the technique to be accurate and reproducible in both human and cadaver knees. High-resolution MRI (3T) and improved segmentation techniques increase the accuracy and repeatability of this technique. By using 3T quantitative MRI to examine articular cartilage thickness, it is possible to examine changes that may occur in these parameters in patients following partial meniscectomy.

The identification of regions of interest is necessary to track changes in articular cartilage thickness over time. Identifying specific regions of interest will allow the examination of changes in the weight-bearing regions of the tibiofemoral joint, and eliminate the variability associated with the cartilage at the edges of the joint. A coordinate system can be established based on the bone-cartilage interfaces of the femur and tibia that allows examination of the same areas of interest *in vivo* over time. While many studies have examined the use of quantitative MRI for tracking overall changes in cartilage volume and thickness [53, 58, 66-67], few have defined specific regions of

interest within the segmented cartilage plates for morphological evaluation [55, 68-69]. Specific regions of interest allow investigators to focus on changes in the primary load bearing regions, where they would be most significant, while excluding regions that are not affected and would dampen these differences. For longitudinal studies, regions of interest must be defined such that they can be reproducibly isolated at each time point. It is possible to use the three-dimensional models created by our segmentation technique to establish such coordinate systems for each subject examined.

1.3 Significance

Although it is generally accepted that total meniscectomy places the knee at significant risk for early OA, it remains unknown whether the extent of meniscal resection is predictive of outcome. The studies described in the following chapters provide the preliminary data necessary to develop and justify a long-term prospective controlled cohort study evaluating OA following partial meniscectomy. Such a study will influence the future care of patients undergoing surgical treatment for meniscus changes. This will be particularly important when a patient and his or her clinician must choose between partial meniscectomy and other more complicated, expensive treatment alternatives, which may include repair, allografts, xenografts, and tissue-engineered replacements, as they become available.

1.4 Specific Aims

Specific Aim 1: Refine and validate an image segmentation technique to quantify meniscal volume and articular cartilage thickness.

The objectives of the first aim were to refine an MR-based image segmentation and reconstruction technique to measure meniscal volume and tibiofemoral articular cartilage thickness. We used meniscal phantoms, cadaver models, and *in vivo* models to refine our segmentation technique. We then validated the segmentation method *in situ* using cadaver specimens and *in vivo* models. Our primary hypothesis for this aim was that meniscal volumes and articular cartilage thicknesses calculated using MR-based segmentation would be equal and reproducible compared to the meniscal volumes and articular cartilage thicknesses measured using water displacement and laser scanning techniques.

Specific Aim 2: Apply the segmentation technique to patients with acute meniscal tears.

The objective of the second aim was to perform a study using ten human subjects with meniscal tears who underwent partial meniscectomy. MR imaging of each subject's knees was performed just prior to surgery and one month after surgery. The segmentation technique refined and validated in Aim 1 was then applied to these MR images. We hypothesized that the segmentation technique would demonstrate a decrease in the

volume of the resected menisci after surgery, and that the meniscal volume and articular cartilage thickness measurements of each subject would be reproducible.

Specific Aim 3: Use the segmentation technique to evaluate outcomes of ACL transection and ACL reconstruction in a controlled animal model.

The objective of the third aim was to apply the segmentation technique validated in Aim 1 to ten Yucatan mini-pigs. The pigs were randomized into two groups of five. The first group underwent unilateral ACL transection, and the second group underwent unilateral ACL reconstruction with a bone-patellar tendon-bone allograft. The animals were allowed to heal for 15 weeks, and each hind limb was harvested after euthanasia. We obtained 3T MR images of each animal's hind limbs after harvest, and applied the articular cartilage segmentation technique to the images. We hypothesized that in both groups, the articular cartilage of the surgical limbs would exhibit signs of early OA development compared to the contralateral control limbs. We also expected that differences in articular cartilage thickness would be more pronounced in the ACL-transected limbs than the ACL-reconstructed limbs.

1.5 References

1. Ahmed, A.M. and D.L. Burke, *In-vitro measurement of static pressure distribution in synovial joints - Part I: Tibial surface of the knee.* J Biomech Engin, 1983. **105**: p. 216-225.
2. Haut Donahue, T.L., et al., *A finite element model of the human knee joint for the study of tibio-femoral contact.* Journal of Biomechanical Engineering, 2002. **124**(3): p. 273-280.
3. McKinley, T.O., D.K. English, and B.K. Bay, *Trabecular bone strain changes resulting from partial and complete meniscectomy.* Clinical Orthopaedics and Related Research, 2003. **407**: p. 259-267.
4. Pena, E., et al., *Finite element analysis of the effect of meniscal tears and meniscectomies on human knee biomechanics.* Clinical Biomechanics, 2005. **20**(5): p. 498-507.
5. Sekaran, S.V., M.L. Hull, and S.M. Howell, *Nonanatomic location of the posterior horn of a medial meniscal autograft implanted in a cadaveric knee adversely affects the pressure distribution on the tibial plateau.* American Journal of Sports Medicine, 2002. **30**(1): p. 74-82.
6. Wilson, W., et al., *Pathways of load-induced cartilage damage causing cartilage degeneration in the knee after meniscectomy.* Journal of Biomechanics, 2003. **36**(6): p. 845-851.

7. Fukuda, Y., et al., *Impact load transmission of the knee joint-influence of leg alignment and the role of meniscus and articular cartilage.* Clinical Biomechanics, 2000. **15**(7): p. 516-521.

8. Voloshin, A.S. and J. Wosk, *Shock absorption of meniscectomized and painful knees.* Journal of Biomedical Engineering, 1985. **5:**: p. 157-161.

9. McDermott, I.D. and A. A.A., *The consequences of meniscectomy.* J Bone Joint Surg Br, 2006. **88**(12): p. 1549-1556.

10. Levy, I.M., P.A. Torzilli, and J.D. Gould, *The effect of lateral meniscectomy on motion of the knee.* Journal of Bone and Joint Surgery, 1989. **71**: p. 401-406.

11. Levy, I.M., P.A. Torzilli, and R.F. Warren, *The effect of medial meniscectomy on anterior-posterior motion of the knee.* Journal of Bone and Joint Surgery, 1982. **64**(6): p. 883-888.

12. Arnoczky, S.P. and C.A. McDevitt, *The meniscus: Structure, Function, Repair, and Replacement*, in *Orthopaedic Basic Science*, J.A. Buckwalter, Editor. 2000, American Academy of Orthopaedic Surgeons: Illinois. p. 532-545.

13. Thijs, Y., et al., *A prospective study on knee proprioception after meniscal allograft transplantation.* Scand J Med Sci Sports, 2007. **17**: p. 223-229.

14. Nielsen, A.B. and J. Yde, *Epidemiology of acute knee injuries: a prospective hospital investigation.* Journal of Trauma, 1991. **31**(12): p. 1644-1648.

15. Englund, M., et al., *Patient-relevant outcomes fourteen years after meniscectomy: Influence of type of meniscal tear and size of resection.* Rheumatology, 2001. **40**: p. 631-639.

16. Englund, M., *Meniscal tear - a feature of osteoarthritis.* Acta Orthopaedica Scandinavica, 2004. **75**(Suppl 312): p. 8-45.

17. Ma, C.B. and S.A. Rodeo, *Meniscal Injuries,* in *Orthopaedic Knowledge Update: Sports Medicine 3*, J.G. Garrick, Editor. 2004, American Academy of Orthopaedic Surgeons: Rosemont. p. 199-212.

18. Baker, B.E., et al., *Review of meniscal injury and associated sports.* Am J Sports Med, 1985. **13**(1): p. 1-4.

19. Hede, A., et al., *Epidemiology of meniscal lesions in the knee. 1,215 open operations in Copenhagen 1982-84.* Acta Orthopaedica Scandinavica, 1990. **61**(5): p. 435-437.

20. Haut Donahue, T.L., et al., *The sensitivity of tibiofemoral contact pressure to the size and shape of the lateral and medial menisci.* Journal of Orthopaedic Research, 2004. **22**(4): p. 807-814.

21. Donahue, T.L.H., et al., *How the stiffness of meniscal attachments and meniscal material properties affect tibio-femoral contact pressure computed using a validated finite element model of the human knee joint.* Journal of biomechanics, 2003. **36**(1): p. 19-34.

22. Huang, A., et al., *Identification of cross-sectional parameters of lateral meniscal allografts that predict tibial contact pressure in human cadaveric knees.* Journal of Biomechanical Engineering, 2002. **124**(5): p. 481-489.

23. Huang, A., M.L. Hull, and S.M. Howell, *The level of compressive load affects conclusions from statistical analyses to determine whether a lateral meniscal*

autograft restores tibial contact pressure to normal: a study in human cadaveric knees. Journal of Orthopaedic Research, 2003. **21**(3): p. 459-464.

24. Fairbank, T.J., *Knee joint changes after meniscectomy.* Journal of Bone and Joint Surgery. British Volume, 1948. **30**: p. 664-670.
25. Englund, M., E.M. Roos, and L.S. Lohmander, *Impact of type of meniscal tear on radiographic and symptomatic knee osteoarthritis: A sixteen-year followup of meniscectomy with matched controls.* Arthritis and Rheumatism, 2003. **48**(8): p. 2178-2187.
26. Bhattacharyya, T., et al., *The clinical importance of meniscal tears demonstrated by magnetic resonance imaging in osteoarthritis of the knee.* J Bone Joint Surg Am, 2003. **85**(1): p. 4-9.
27. Berthiaume, M.J., et al., *Meniscal tear and extrusion are strongly associated with progression of symptomatic knee osteoarthritis as assessed by quantitative magnetic resonance imaging.* Ann Rheum Dis, 2005. **64**(4): p. 556-563.
28. Rockborn, P. and K. Messner, *Long term results of meniscus repair and meniscectomy: a 13-year functional and radiographic follow-up study.* Knee Surgery, Sports Traumatology, Arthroscopy, 2000. **8**: p. 2-9.
29. Englund, M. and L.S. Lohmander, *Risk factors for symptomatic knee osteoarthritis fifteen to twenty-two years after meniscectomy.* Arthritis & Rheumatism, 2004. **50**(9): p. 2811-2819.
30. McNicholas, M.J., et al., *Total meniscectomy in adolescence: a thirty year follow-up.* Journal of Bone and Joint Surgery - British Volume, 2000. **82**: p. 217 - 221.

31. Roos, H., et al., *Knee osteoarthritis after meniscectomy: prevalence of radiographic changes after twenty-one years, compared with matched controls.* Arthritis Rheum, 1998. **41**(4): p. 687-93.

32. Gopez, A.G. and E.C. Kavanagh, *MR imaging of the postoperative meniscus: repair, resection, and replacement.* Semin Musculoskelet Radiol, 2006. **10**(3): p. 229-40.

33. Chatain, F., et al., *The natural history of the knee following arthroscopic medial meniscectomy.* Knee Surgery, Sports Traumatology, Arthroscopy, 2001. **9**(1): p. 15-18.

34. Andersson-Molina, H., H. Karlsson, and P. Rockborn, *Arthroscopic partial and total meniscectomy: A long-term follow-up study with matched controls.* Arthroscopy, 2002. **18**(2): p. 183-189.

35. Ford, G.M., et al., *Associations of body mass index with meniscal tears.* American Journal of Preventive Medicine, 2005. **28**(4): p. 364-368.

36. Andersson, C. and J. Gillquist, *Instrumented testing for evaluation of sagittal plane laxity.* Clinical Orthopaedics and Related Research, 1990. **256**: p. 178-184.

37. Chatain, F., et al., *A comparative study of medial versus lateral arthroscopic meniscectomy on stable knees. 10-year minimum follow-up.* Arthroscopy, 2003. **19**(8): p. 842-849.

38. Cicuttini, F.M., et al., *Rate of knee cartilage loss after partial meniscectomy.* Journal of Rheumatology, 2002. **29**(9): p. 1954-1956.

39. Higuchi, H., et al., *Factors affecting long-term results after arthroscopic partial meniscectomy.* Clinical Orthopaedics and Related Research, 2000. **377**: p. 161-168.

40. Hoser, C., et al., *Long-term results of arthroscopic partial lateral meniscectomy in knees without associated damage.* Journal of Bone and Joint Surgery. British Volume, 2001. **83**(4): p. 513-516.

41. Hulet, C.H., et al., *Arthroscopic medial meniscectomy on stale knees - A 12-year follow-up.* Journal of Bone and Joint Surgery. British Volume, 2001. **83**(1): p. 29-32.

42. Rangger, C., et al., *Osteoarthritis after arthroscopic partial meniscectomy.* American Journal of Sports Medicine, 1995. **23**(2): p. 240-4.

43. Roos, E.M., et al., *Long-term outcome of meniscectomy: symptoms, function, and performance tests in patients with or without radiographic osteoarthritis compared to matched controls.* Osteoarthritis Cartilage, 2001. **9**(4): p. 316-324.

44. Roos, H., et al., *Osteoarthritis of the knee after injury to the anterior cruciate ligament or meniscus: The influence of time and age.* Osteoarthritis Cartilage, 1995. **3**(4): p. 261-7.

45. Hede, A., E. Larsen, and H. Sandberg, *The long term outcome of open total and partial meniscectomy related to the quantity and site of meniscus removed.* International Orthopaedics, 1992. **16**: p. 122-125.

46. Shelbourne, K.D. and J.F. Dickens, *Digital radiographic evaluation of medial joint space narrowing after partial meniscectomy of bucket-handle medial*

meniscus tears in anterior cruciate ligament-intact knees. Am J Sports Med, 2006. **34**(10): p. 1648-1655.

47. Cicuttini, F.M., A.E. Wluka, and S.L. Stuckey, *Tibial and femoral cartilage changes in knee osteoarthritis.* Ann Rheum Dis, 2001. **60**: p. 977-980.
48. Eckstein, F., D. Burstein, and T.M. Link, *Quantitative MRI of cartilage and bone: degenerative changes in osteoarthritis.* NMR Biomed, 2006. **19**(7): p. 822-854.
49. Amin, S., et al., *The relationship between cartilage loss on magnetic resonance imaging and radiographic progression in men and women with knee osteoarthritis.* Arthritis & Rheumatism, 2005. **52**(10): p. 3152-3159.
50. Jones, G., et al., *Early radiographic osteoarthritis is associated with substantial changes in cartilage volume and tibial bone surface area in both males and females.* Osteoarthritis and Cartilage, 2004. **12**(2): p. 169-174.
51. Graichen, H., et al., *Quantitative assessment of cartilage status in osteoarthritis by quantitative magnetic resonance imaging: technical validation for use in analysis of cartilage volume and further morphologic parameters.* Arthritis & Rheumatism, 2004. **50**(3): p. 811-816.
52. Cicuttini, F., et al., *Longitudinal study of the relationship between knee angle and tibiofemoral cartilage volume in subjects with knee osteoarthritis.* Rheumatology, 2004. **43**(3): p. 321-324.
53. Cicuttini, F.M., et al., *Longitudinal study of changes in tibial and femoral cartilage in knee osteoarthritis.* Arthritis & Rheumatism, 2004. **50**(1): p. 94-97.
54. Raynauld, J.P., et al., *Quantitative magnetic resonance imaging evaluation of knee osteoarthritis progression over two years and correlation with clinical*

symptoms and radiologic changes. Arthritis & Rheumatism, 2004. **50**(2): p. 476-487.

55. Raynauld, J.P., et al., *Reliability of a quantification imaging system using magnetic resonance images to measure cartilage thickness and volume in human normal and osteoarthritic knees.* Osteoarthritis and Cartilage, 2003. **11**(5): p. 351-360.

56. Glaser, C., et al., *Femoro-tibial cartilage metrics from coronal MR image data: Technique, test-retest reproducibility, and findings in osteoarthritis.* Magnetic Resonance in Medicine, 2003. **50**(6): p. 1229-1236.

57. Biswal, S., et al., *Risk factors for progressive cartilage loss in the knee: a longitudinal magnetic resonance imaging study in forty-three patients.* Arthritis Rheum, 2002. **46**(11): p. 2884-2892.

58. Wluka, A.E., et al., *The determinants of change in tibial cartilage volume in osteoarthritic knees.* Arthritis & Rheumatism, 2002. **46**(8): p. 2065-2072.

59. Jay, G.D., et al., *Lubricating ability of aspirated synovial fluid from emergency department patients with knee joint synovitis.* J Rheumatol, 2004. **31**(3): p. 557-64.

60. Kobayashi, M., et al., *Role of interleukin-1 and tumor necrosis factor alpha in matrix degradation of human osteoarthritic cartilage.* Arthritis Rheum, 2005. **52**(1): p. 128-135.

61. Carter, D.R., et al., *The mechanobiology of articular cartilage development and degeneration.* Clinical Orthopaedics and Related Research, 2004. **427**: p. S69-S77.

62. Donahue, T.L.H., et al., *A finite element model of the human knee joint for the study of tibio-femoral contact.* Journal of Biomechanical Engineering, 2002. **124**(3): p. 273-280.

63. Haut Donahue, T.L., et al., *How the stiffness of meniscal attachments and meniscal material properties affect tibio-femoral contact pressure computed using a validated finite element model of the human knee joint.* Journal of Biomechanics, 2003. **36**(1): p. 19-34.

64. Stone, K.R., et al., *3D MRI volume sizing of knee meniscus cartilage.* Arthroscopy, 1994. **10**(6): p. 641-644.

65. Eckstein, F., et al., *Accuracy of cartilage volume and thickness measurements with magnetic resonance imaging.* Clinical Orthopaedics & Related Research, 1998. **352**: p. 137-148.

66. Song, Y., et al., *Articular cartilage MR imaging and thickness mapping of a loaded knee joint before and after meniscectomy.* Osteoarthritis and Cartilage, 2006. **14**(8): p. 728-737.

67. Wluka, A.E., et al., *How does tibial cartilage volume relate to symptoms in subjects with knee osteoarthritis?* Annals of the Rheumatic Diseases, 2004. **63**(3): p. 264-268.

68. Koo, S., G.E. Gold, and T.P. Andriacchi, *Considerations in measuring cartilage thickness using MRI: factors influencing reproducibility and accuracy.* Osteoarthritis and Cartilage, 2005. **13**(9): p. 782-789.

69. Li, G., et al., *In vivo articular cartilage contact kinematics of the knee: an investigation using dual-orthogonal fluoroscopy and magnetic resonance image-*

based computer models. American Journal of Sports Medicine, 2005. **33**(1): p. 102-107.

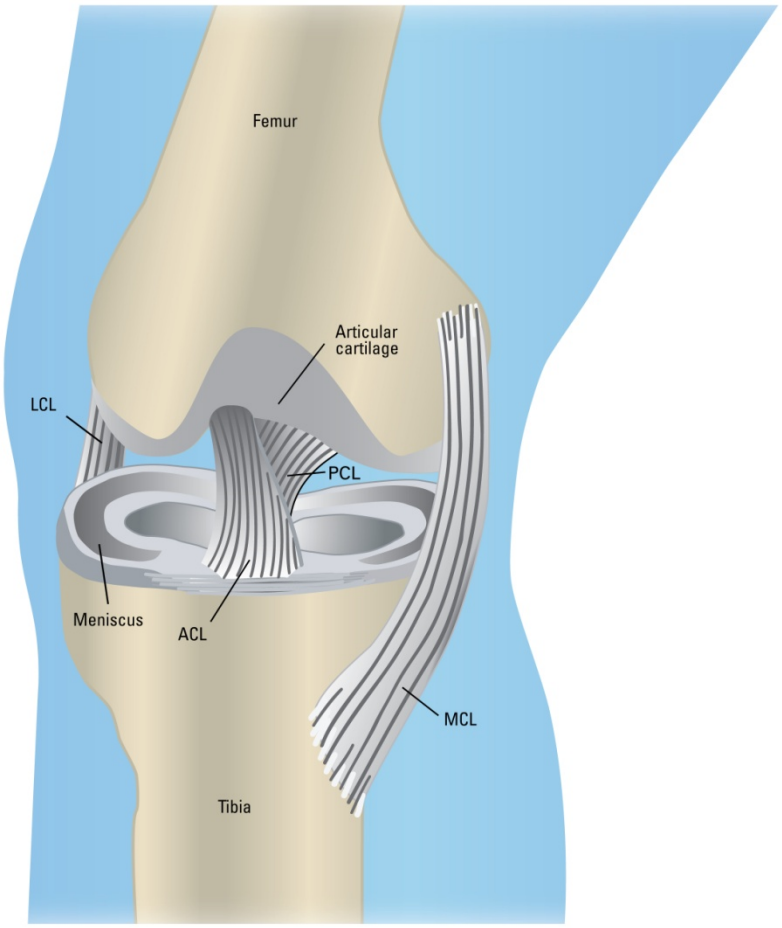

Figure 1.1: Schematic of the knee joint depicting the medial and lateral menisci, as well as the femur, tibia, articular cartilage, anterior cruciate ligament (ACL), posterior cruciate ligament (PCL), medial collateral ligament (MCL), and lateral collateral ligament (LCL). Figure by Patrick Bibbins.

Chapter 2

Quantification of Meniscal Volume by Segmentation of 3T Magnetic Resonance Images

Megan E. Bowers, Glenn A. Tung, Braden C. Fleming, Joseph J. Crisco, Jesus Rey

The following chapter was published in *Journal of Biomechanics*, 40: 2811-2815 (2007). (PMID: 17391677)

2.1 Abstract

Meniscal injuries place the knee at risk for early osteoarthritis (OA) because they disrupt their load-bearing capabilities. Partial resection is routinely performed to alleviate symptomatic meniscal tears. While the removal of meniscal tissue may not be the only factor associated with partial meniscectomy outcome, the amount removed certainly

contributes to functional loss. It is unknown, however, whether there is a critical amount of meniscal tissue that can be removed without diminishing the structure's chondroprotective role. In order to examine the existence of such a threshold, it is necessary to accurately quantify meniscal volume both before and after partial meniscectomy to determine the amount of meniscal tissue removed. Therefore, our goal was to develop and validate an MR-based method for assessing meniscal volume. The specific aims were: (1) to evaluate the feasibility of the MR-based segmentation method; (2) to determine the method's reliability for repeated measurements; and (3) to validate its accuracy in situ. MR images were obtained on a 3T magnet, and each scan was segmented using a biplanar approach. The MR-based volumes for each specimen were compared to those measured by water displacement. The results indicate that the biplanar approach of measuring meniscal volumes is accurate and reliable. The calculated volumes of the menisci were within 5% of the true values, the coefficients of variation were 4%, and the intraclass correlation coefficients were greater than 0.96. These data demonstrate that this method could be used to measure the amount of meniscal tissue excised during partial meniscectomy to within 125.7mm^3.

2.2 Introduction

The menisci of the knee are crescent-shaped fibrocartilagenous washers that protect articular cartilage by maximizing contact area and minimizing contact stress within the tibiofemoral joint. When a meniscus is torn, the contact mechanics of the tibiofemoral joint are altered, which disrupts the homeostasis of articular cartilage metabolism, placing the knee at risk for early osteoarthritis (OA). Biomechanical studies have clearly shown that joint contact mechanics are altered following meniscectomy and meniscal transplantation [1-7].

Total meniscectomy was once the standard treatment for symptomatic meniscal tears. This procedure decreases tibiofemoral contact area by 50-70%, a change which significantly increases contact stress on the articular cartilage [8] and reduces its shock-absorbing capabilities [9]. The link between meniscectomy and OA has been well-documented [10-12]. Thus, partial resection, in which the undamaged portion of the meniscus is preserved, is now routinely performed to eliminate symptoms while attempting to preserve cartilage integrity [10, 13-16]. However, partial meniscectomy may not eliminate the risk of early OA [12-26].

To date, no clinical studies have objectively measured the amount of meniscus that can be removed following acute meniscal injury without placing the knee at risk of OA. In order to examine whether a critical threshold exists, it is necessary to quantify the amount of meniscal tissue removed during surgery. Quantitative magnetic resonance imaging (MRI) has been used to assess dimensional changes of articular cartilage [27],

and could be used to construct models of the meniscus before and after partial meniscectomy; the difference between the two volumes would indicate the amount of tissue removed.

This study's objective was to validate an MR-based approach to document meniscal size and assess changes in meniscal volume following surgery. The specific aims were: (1) to evaluate the method's feasibility (phantom model); (2) to determine the technique's reliability (cadaver model); and (3) to validate the technique's accuracy *in situ* (cadaver model).

2.3 Methods

2.3.1 MR Imaging

Specimens were imaged on a 3T scanner (Siemens Trio, Erlangen, Germany) using a surface coil. The T2*-weighted 3D-CISS sequence [constructive interference in the steady state; TR/TE/FA, 14.5/7.3/35^{o}; FOV, 160mm; matrix, 512x512, slice length/gap, 1mm/0; avg, 1] was utilized. Preliminary testing determined that this sequence provided high contrast between meniscal tissue and adjacent structures.

2.3.2 Segmentation Technique

The phantom model and cadaver menisci were manually segmented from both sagittal and coronal plane image reconstructions using commercial software (Mimics 9.11; Materialise, Ann Arbor, MI). Three-dimensional voxel models were generated from the biplanar segmentations and wrapped with a triangular mesh to create a solid model of each structure. The solid models captured both meniscal volume and morphology **(Figure 2.1)**. Each model's volume was calculated by surface integration.

2.3.3 Water Volume Technique

The volume of each MR-based model was compared to its water displacement volume [28]. After imaging, the menisci were carefully dissected from the joint. Each meniscus was placed in a 25cc graduated cylinder containing 25cc of isotonic saline. The displaced saline was removed from the cylinder, using a micropipette, until the fluid level

was restored to 25cc. Each water volume measurement was repeated three times, and the values averaged. Previous testing determined that the coefficient of variation for repeated water displacement measurements was 1.5%.

2.3.4 Feasibility Study (Aim 1)

The feasibility of the segmentation method was evaluated using a plastic phantom model. A single intact fresh human cadaver knee with no evidence of knee pathology was imaged as described above. The menisci were segmented using MR-based biplanar segmentation, and 3-D models of the menisci were generated. Using rapid prototyping technology, plastic prototypes of these menisci were created. The volumes of the model menisci (medial = 4352.67mm^3; lateral = 3741.38mm^3) were confirmed by water displacement. The plastic models were then embedded within 1.7% agarose gel. The gel was created within a plastic cylinder (diameter 11cm, height 10cm) similar in size to a human knee cross-section. The phantom was imaged as described, and the plastic produced a contrast similar to that seen between menisci and surrounding tissues. The plastic menisci were segmented, and the MR-based volumes were compared with the known model volumes to establish a percent error in volume.

2.3.5 Reliability Study (Aim 2)

The reliability of the MR-based segmentation method for multiple scans was evaluated using a fresh human cadaver knee. The knee was scanned 7 times; the specimen was removed and repositioned within the coil between scans. After imaging, the cadaver menisci were carefully excised, and their water displacement volumes were

measured. After the menisci were segmented and reconstructed, the MR-based volumes were compared to the water displacement volumes. The coefficients of variation for both the medial and lateral menisci were calculated.

2.3.6 *In situ* Validation (Aim 3)

The MR-based segmentation method was then validated in situ. 10 fresh-frozen human cadaver knees (5 pairs; mean age=56; range=52-60) with no gross evidence of knee pathology were imaged, after which one knee from each pair underwent a partial medial meniscectomy. Partial meniscectomies were performed within the inner rim of the medial meniscus. Resection size was not standardized between specimens. All knees were then rescanned. The “pre-operative” and “post-operative” MR images of each knee were segmented, and the volumes of the medial and lateral menisci were calculated. The MR-based volume of meniscal tissue removed during each resection was determined by subtracting the post-operative volume from the pre-operative volume. This value was compared to the water displacement volume of the portion of meniscus removed. The post-operative scans of the medial meniscus of the contralateral knee and the lateral menisci from both knees served as “repeated standards” to assess reliability. Because these menisci did not undergo meniscectomy, no volume changes were expected between scans. Both menisci were then removed from all 10 knees, and their water displacement volumes were determined. Reliability was quantified by calculating intraclass correlation coefficients (ICCs) for the repeated standards. Accuracy was assessed by calculating the absolute error between the MR-based volume and water displacement volume for each

meniscus. Variation between right and left medial and lateral meniscal volumes was examined for these five pairs of cadaver specimens **(Figure 2.2)**.

2.4 Results

2.4.1 Feasibility Study (Aim 1)

When compared to the known volumes, the errors for the plastic medial and lateral menisci were 0.3% and 3.3%, respectively. The phantom MR-based volumes overestimated the intact model volumes for the medial and lateral menisci at 4363.8mm^3 (versus 4352. 7mm^3) and 3863.1mm^3 (versus 3741.4mm^3), respectively.

2.4.2 Reliability Study (Aim 2)

The mean absolute errors between MR-based and water displacement volumes of the medial and lateral menisci were 4.6% and 7.9%, respectively **(Table 2.1)**. The coefficients of variation were 4% for both compartments.

2.4.3 *In situ* Validation (Aim 3)

The ICCs for repeated standards were greater than 0.96, indicating that the technique was reliable. The mean absolute errors between MR-based and water displacement volumes across all specimens were less than 5.3% **(Figure 2.3)**. The average volumes of the resected pieces were 522 (range 330-880) mm^3 and 565 (range 325-1000) mm^3 for the MR-based segmentation and water displacement methods, respectively **(Figure 2.3)**. Excluding the volumes of the resected pieces, the mean absolute errors between MR-based volumes and water displacement volumes were 4.8% and 3.0% for the medial and lateral menisci, respectively **(Figure 2.2)**. The 95%

confidence interval of the difference between the calculated (MR) and actual (water displacement) volumes of the removed fragments was 125.7mm^3.

2.5 Discussion

The amount of meniscus that can be removed following an acute meniscal injury without placing the knee at risk of OA is unknown. In order to examine whether there is a critical threshold, it is necessary to quantify the amount of meniscal tissue removed during surgery. Such a method could be used to design a clinical study of partial meniscectomy for simple acute tears, in which each patient's partial meniscectomy and residual meniscal tissue could be quantified. Each patient could then be tracked, and the mechanisms of OA development following partial meniscectomy could be better understood. We have shown that this MR-based approach is accurate and reliable for tracking changes in meniscal volume. This method may also be useful for sizing meniscal allografts, because the MR-based segmentation technique results in a 3-D model in which both meniscal morphology and volume can be examined.

In developing a technique to size meniscal allografts, Stone et al. utilized a similar imaging approach [28]. They used a 3-D MR sequence on a 1.5T magnet. Images were segmented in the sagittal plane, and MR measurements were performed 6 times per cadaver specimen before the menisci were excised. The volumes of the menisci were then measured by water displacement. Stone reported that the MR technique was precise but consistently underestimated true meniscal volume by 20% and 44% for medial and lateral menisci, respectively.

Our MR-based segmentation approach has several improvements. Images were obtained on a 3T magnet using the T2*-weighted, 3D-CISS sequence. The protocol

provided high-resolution images and high contrast between meniscal tissue and adjacent structures. Because meniscal contours are best seen in orthogonal images, segmentations were performed using both sagittal and coronal views of the same volume to optimize the central and anterior/posterior boundaries of the menisci, respectively. The reliability study (Aim 2), in which coefficients of variation were less than 4% for both menisci, indicated that results were reproducible. The calculated volumes of the menisci for the in situ validation study were within 5% of their water displacement volumes, and the ICCs between methods were greater than 0.96. The method was accurate for detecting meniscal morphometry before and after partial meniscectomy to within 125.7mm^3.

Some limitations should be noted. The evaluations were performed using phantom (Aim 1) and cadaver specimens (Aims 2 and 3). Motion and blood flow artifacts were not present; thus, a clinical evaluation of reliability is needed. The segmentations were performed manually. To minimize variation, the images were segmented by a trained examiner under a musculoskeletal radiologist's direction. Since meniscal segmentations were performed independently, the results of the repeatability (Aim 2) and accuracy (Aim 3) studies minimize this concern. Although MRI is a reasonable means of detecting displaced meniscal fragments [29], the accuracy of this approach for more complicated tears (i.e. bucket handle tears) remains unknown. However, based on our results **(Figure 2.2)**, it would be possible to use the respective meniscus of the uninjured contralateral knee as a baseline, or check, for complex tears. Despite these limitations, the MR-based biplanar segmentation method provides an accurate and reliable way to document meniscal volumes from 3-D segmented models.

2.6 Acknowledgements

This work was funded by the National Institutes of Health (AR049199; AR047910; and AR047910S1). The authors gratefully acknowledge the technical support of Lynn Fanella and Theodore Trafton, and the statistical advice of Gary Badger (University of Vermont).

2.7 References

1. Haut Donahue, T.L., et al., *A finite element model of the human knee joint for the study of tibio-femoral contact.* Journal of Biomechanical Engineering, 2002. **124**(3): p. 273-280.
2. Donahue, T.L.H., et al., *How the stiffness of meniscal attachments and meniscal material properties affect tibio-femoral contact pressure computed using a validated finite element model of the human knee joint.* Journal of biomechanics, 2003. **36**(1): p. 19-34.
3. Haut Donahue, T.L., et al., *The sensitivity of tibiofemoral contact pressure to the size and shape of the lateral and medial menisci.* Journal of Orthopaedic Research, 2004. **22**(4): p. 807-814.
4. Huang, A., et al., *Identification of cross-sectional parameters of lateral meniscal allografts that predict tibial contact pressure in human cadaveric knees.* Journal of Biomechanical Engineering, 2002. **124**(5): p. 481-489.
5. Huang, A., M.L. Hull, and S.M. Howell, *The level of compressive load affects conclusions from statistical analyses to determine whether a lateral meniscal autograft restores tibial contact pressure to normal: a study in human cadaveric knees.* Journal of Orthopaedic Research, 2003. **21**(3): p. 459-464.
6. Wilson, W., et al., *Pathways of load-induced cartilage damage causing cartilage degeneration in the knee after meniscectomy*. Journal of Biomechanics, 2003. **36**(6): p. 845-851.

7. Fairbank, T.J., *Knee joint changes after meniscectomy.* Journal of Bone and Joint Surgery. British Volume, 1948. **30**: p. 664-670.

8. Ahmed, A.M. and D.L. Burke, *In-vitro measurement of static pressure distribution in synovial joints - Part I: Tibial surface of the knee.* J Biomech Engin, 1983. **105**: p. 216-225.

9. Voloshin, A.S. and J. Wosk, *Shock absorption of meniscectomized and painful knees.* Journal of Biomedical Engineering, 1985. **5:**: p. 157-161.

10. Englund, M. and L.S. Lohmander, *Risk factors for symptomatic knee osteoarthritis fifteen to twenty-two years after meniscectomy.* Arthritis & Rheumatism, 2004. **50**(9): p. 2811-2819.

11. McNicholas, M.J., et al., *Total meniscectomy in adolescence: a thirty year follow-up.* Journal of Bone and Joint Surgery - British Volume, 2000. **82**: p. 217 - 221.

12. Roos, H., et al., *Knee osteoarthritis after meniscectomy: prevalence of radiographic changes after twenty-one years, compared with matched controls.* Arthritis Rheum, 1998. **41**(4): p. 687-93.

13. Andersson-Molina, H., H. Karlsson, and P. Rockborn, *Arthroscopic partial and total meniscectomy: A long-term follow-up study with matched controls.* Arthroscopy, 2002. **18**(2): p. 183-189.

14. Chatain, F., et al., *The natural history of the knee following arthroscopic medial meniscectomy.* Knee Surgery, Sports Traumatology, Arthroscopy, 2001. **9**(1): p. 15-18.

15. Englund, M., et al., *Patient-relevant outcomes fourteen years after meniscectomy: Influence of type of meniscal tear and size of resection.* Rheumatology, 2001. **40**: p. 631-639.

16. Englund, M., E.M. Roos, and L.S. Lohmander, *Impact of type of meniscal tear on radiographic and symptomatic knee osteoarthritis: A sixteen-year followup of meniscectomy with matched controls.* Arthritis and Rheumatism, 2003. **48**(8): p. 2178-2187.

17. Andersson, C. and J. Gillquist, *Instrumented testing for evaluation of sagittal plane laxity.* Clinical Orthopaedics and Related Research, 1990. **256**: p. 178-184.

18. Chatain, F., et al., *A comparative study of medial versus lateral arthroscopic meniscectomy on stable knees. 10-year minimum follow-up.* Arthroscopy, 2003. **19**(8): p. 842-849.

19. Cicuttini, F.M., et al., *Rate of knee cartilage loss after partial meniscectomy.* Journal of Rheumatology, 2002. **29**(9): p. 1954-1956.

20. Higuchi, H., et al., *Factors affecting long-term results after arthroscopic partial meniscectomy.* Clinical Orthopaedics and Related Research, 2000. **377**: p. 161-168.

21. Hoser, C., et al., *Long-term results of arthroscopic partial lateral meniscectomy in knees without associated damage.* Journal of Bone and Joint Surgery. British Volume, 2001. **83**(4): p. 513-516.

22. Hulet, C.H., et al., *Arthroscopic medial meniscectomy on stale knees - A 12-year follow-up.* Journal of Bone and Joint Surgery. British Volume, 2001. **83**(1): p. 29-32.

23. Rangger, C., et al., *Osteoarthritis after arthroscopic partial meniscectomy.* American Journal of Sports Medicine, 1995. **23**(2): p. 240-4.

24. Rockborn, P. and K. Messner, *Long term results of meniscus repair and meniscectomy: a 13-year functional and radiographic follow-up study.* Knee Surgery, Sports Traumatology, Arthroscopy, 2000. **8**: p. 2-9.

25. Roos, H., et al., *Osteoarthritis of the knee after injury to the anterior cruciate ligament or meniscus: The influence of time and age.* Osteoarthritis Cartilage, 1995. **3**(4): p. 261-7.

26. Roos, E.M., et al., *Long-term outcome of meniscectomy: symptoms, function, and performance tests in patients with or without radiographic osteoarthritis compared to matched controls.* Osteoarthritis Cartilage, 2001. **9**(4): p. 316-324.

27. Eckstein, F. and C. Glaser, *Measuring cartilage morphology with quantitative magnetic resonance imaging.* Seminars in Musculoskeletal Radiology, 2004. **8**(4): p. 329-353.

28. Stone, K.R., et al., *3D MRI volume sizing of knee meniscus cartilage.* Arthroscopy, 1994. **10**(6): p. 641-644.

29. Wright, D.H., A.A. De Smet, and M. Norris, *Bucket-Handle Tears of the Medial and Lateral Menisci of the Knee: Value of MR Imaging in Detecting Displaced Fragments.* AJR. American Journal of Roentgenology, 1995. **165**: p. 621-625.

Meniscus	Water Vol. Mean (mm^3; n=3)	MR-Based Mean (mm^3; n=7)	%Error
Medial	3041 (±43)	2927 (±118)	4.6
Lateral	3067 (±71)	2801 (±112)	7.9

Table 2.1: Mean (± 1 standard deviation) MR-based and water displacement volumes of one cadaver knee scanned 7 times (Aim 2). Water volume measurements were repeated 3 times.

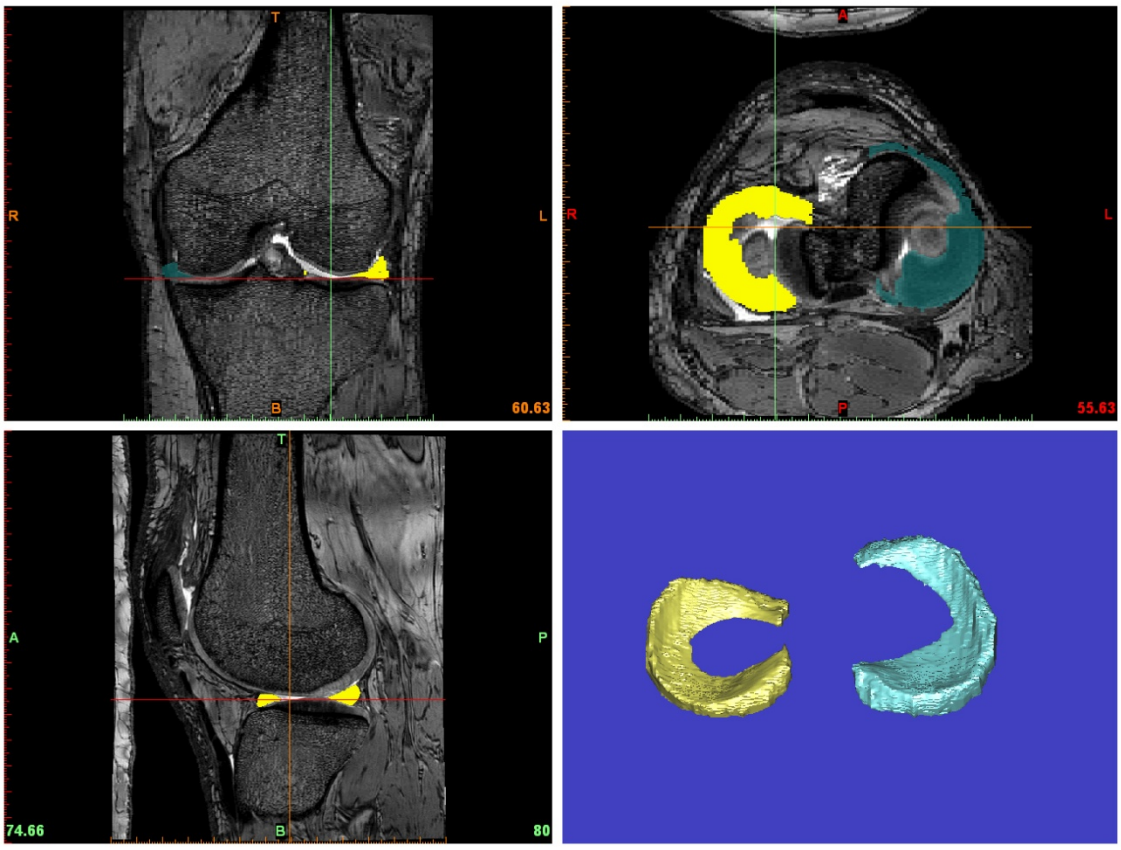

Figure 2.1: The user interface of the commercial segmentation software (Mimics 9.11; Materialise, Ann Arbor, MI) used for this study. The top panes show coronal (left) and axial (right) views; the bottom panes show the sagittal view (left) and 3-D meniscal reconstructions (right).

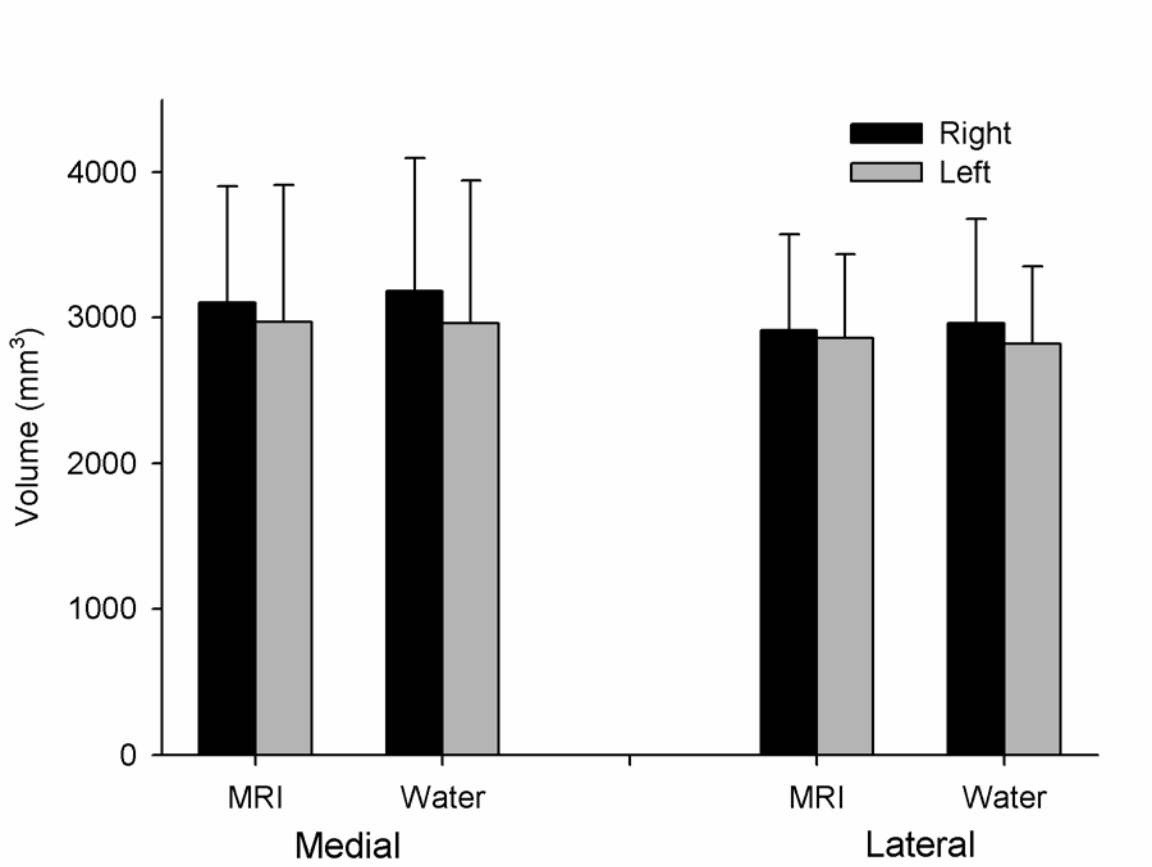

Figure 2.2: Mean (+1 standard deviation) MR-based and water displacement volumes for right and left medial and lateral menisci of specimens used in Aim 3. Water volumes of medial and lateral menisci for each pair of knees showed mean coefficients of variation (CV) of 5.78% and 4.95%, respectively. MR-based volumes of medial and lateral menisci for each pair showed mean CVs of 6.45% and 4.32%, respectively. Mean MR-based volumes of the medial menisci of the right and left knees were 3102mm^3 and 2969mm^3, respectively. Mean MR-based volumes of the lateral menisci of the right and left knees were 2913mm^3 and 2859mm^3, respectively.

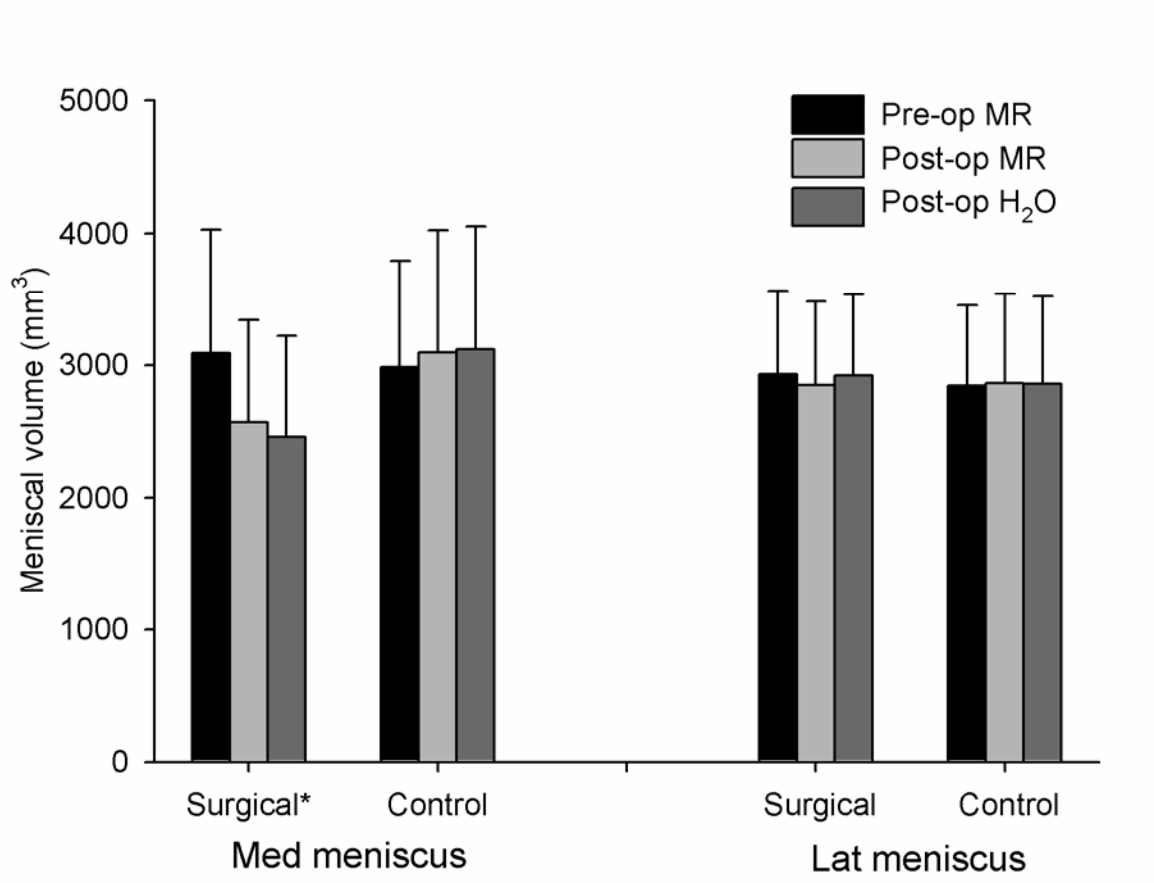

Figure 2.3: Mean (+1 standard deviation) meniscal volumes for surgical and contralateral control knees using MR-based segmentation and water displacement. 565mm^3 (range 325-1000mm^3; water displacement-based) were removed from the medial meniscus of the surgical* knee. The mean surgical* pre-op water volume was 3020±987mm^3 (the sum of the post-op water volume and the volume of meniscus removed during meniscectomy). Pre-op water displacement volume equaled post-op water volume for medial control and all lateral menisci.

Chapter 3

Effects of ACL Interference Screws on Articular Cartilage Volume and Thickness Measurements with 1.5T and 3T MRI

Megan E. Bowers, Glenn A. Tung, Nhon Trinh, Evan Leventhal, Joseph J. Crisco, Benjamin Kimia, Braden C. Fleming

The following chapter was published in *Osteoarthritis and Cartilage*, 16: 572-578 (2008). (PMID: 17933559)

3.1 Abstract

3.1.1 Objective

To assess the effects of interference screws, which are commonly used to surgically fix an anterior cruciate ligament (ACL) graft in the ACL-deficient knee, and magnetic field strength on cartilage volume and thickness measurements with quantitative MRI (qMRI).

3.1.2 Methods

Five cadaver knees were imaged using a cartilage-sensitive sequence (T1-weighted WE-3D FLASH) on 1.5T and 3T scanners with and without interference screws implanted. The tibiofemoral articular cartilage was segmented and reconstructed from the MR images, and volume and thickness measurements were made on the resulting three-dimensional models.

3.1.3 Results

Although several load-bearing regions showed significant differences in volume and thickness between magnet strengths, most showed no significant difference between screw conditions. The medial tibial cartilage showed a mean decrease in volume of 5.9% and 8.0% in the presence of interference screws at 3T and 1.5T, respectively. At 3T and 1.5T, the medial tibial cartilage showed a mean decrease in thickness of 7.0% and 12.0%, respectively, in the presence of interference screws.

3.1.4 Conclusions

Caution should be used when interpreting thickness and volume of cartilage at 3T in the presence of interference screws, particularly in the medial tibial compartment. Additionally, 3T and 1.5T qMRI should not be used interchangeably to assess structural changes in tibiofemoral articular cartilage during longitudinal studies.

3.2 Introduction

Patients who undergo anterior cruciate ligament (ACL) reconstruction may be at greater risk for early osteoarthritis (OA). Although many studies have evaluated the success of these procedures, few have attempted to examine the condition of the articular cartilage following surgery [1-5]. There is some evidence to suggest that ACL-reconstructed knees will exhibit signs of cartilage degeneration within five years of surgery using subjective radiographic grading techniques [1, 3, 6-7]. Objective methods that could quantify temporal changes in articular cartilage morphometry would be useful to document the natural history of OA in the ACL-injured knee, and to evaluate long-term outcomes in response to different treatment options.

Quantitative magnetic resonance imaging (qMRI) provides a way to directly assess the integrity and composition of the articular cartilage *in vivo* [8-11]. qMRI could provide insight into the mechanisms of OA in the ACL-injured and reconstructed knee by documenting temporal changes in articular cartilage volume and thickness associated with OA progression. With qMRI, three-dimensional virtual cartilage models are constructed from segmented MR images of articular cartilage using cartilage-sensitive pulse sequences. These models are then used to document changes in cartilage geometry over time [8-9, 12]. The precision of MRI-based cartilage volume measurements has been reported to range between 1-4% [11, 13-15]. High degrees of reliability (interclass correlation coefficients greater than 0.92) have also been published [8]. Using qMRI, the cartilage volume of the tibiofemoral joint has been shown to decrease 0.3-0.5% per year

with natural aging [11], as compared to 4-6.5% per year in patients with radiographic evidence of OA [11, 16-18].

In one method commonly used to reconstruct the torn ACL, the proximal and distal bone blocks of the bone-patellar tendon-bone graft are typically fixed using titanium interference screws; one is placed in the femoral bone tunnel, and the other in the tibial bone tunnel. The screws, however, produce artifacts on MR images from magnetic susceptibility, or local distortions in the uniformity of the magnetic field lines, which could potentially affect the reliability of cartilage volume and thickness measurements. These artifacts are seen on MR images at the interface between materials of different magnetic susceptibility, such as metallic implants and surrounding tissues. Ferromagnetic metals, such as nickel, iron, and cobalt, exhibit large magnetic susceptibility and produce significant artifacts, while non-ferrous metals, such as titanium, show lower magnetic susceptibility, and therefore less artifact [19]. Artifacts, which generally appear in the image as a signal void in the region around the implant **(Figure 3.1)**, are directly proportional to the magnetic field strength, and are inversely proportional to the readout gradient strength and voxel size [19-22]. The pulse sequence selected for MR imaging also influences image degradation. Susceptibility artifacts are greater for gradient-echo pulse sequences and are less conspicuous using turbo or fast spin-echo pulse sequences when compared to conventional spin-echo sequences [20, 23].

MR imaging at 3T rather than 1.5T has recently been recommended for qMRI because the higher magnetic field strength provides greater resolution and a higher signal-to-noise ratio for detecting early changes in cartilage morphometry [13, 24]. However, magnetic susceptibility artifacts could be amplified at 3T because of the higher

field strength, or they may be less conspicuous because of the smaller voxel size.

The effect of magnetic susceptibility artifacts on images obtained from knees containing titanium interference screws is not known. Thus, it is necessary to evaluate any errors the screws may introduce before qMRI can be used to document the progression of OA in the ACL-reconstructed patient. The objectives of this study were to assess the effect of tibial and femoral interference screws on articular cartilage volume and thickness measurements from segmented images obtained on both 1.5T and 3T scanners. We hypothesized that: 1) there would be no significant difference in the tibial and femoral cartilage volume and thickness measurements with and without interference screws placed in the knee; and 2) the cartilage volume and thickness measurements reconstructed from 1.5T and 3T images would be equivalent.

3.3 Materials and Methods

3.3.1 Specimens

Five fresh frozen, intact, right human cadaver knees (3 female, 2 male) were acquired for this study. The mean age of the subjects from whom the specimens were obtained was 56 (range, 51-59) years. The specimens had no evidence of ligament or meniscal tears. Three of the specimens had signs of articular cartilage surface wear (2 mild, 1 moderate) by visual inspection.

3.3.2 MR Imaging

All knees were imaged on 1.5T and 3T magnets (Siemens Symphony and Trio, respectively; Erlangen Germany), using commercially available polarized knee coils. The manufacturers of the quadrature knee coils were Siemens Medical Systems (Erlangen, Germany) and USA Instruments, Inc. (Aurora, OH) for the 1.5T and 3T magnets, respectively. In a preliminary evaluation of several pulse sequences frequently used for quantitative cartilage segmentation, we found that the T1-weighted, water-excitation, three-dimensional fast low-angle shot (WE-3D FLASH) sequence on the 3T scanner minimized image distortion from magnetic susceptibility artifacts and maximized cartilage-bone contrast compared to fat-saturated, intermediate-weighted spin echo pulse sequences **(Table 3.1)**. A similar WE-3D FLASH sequence was adopted for use on the 1.5T magnet **(Table 3.1)**.

3.3.3 ACL Interference Screws

Two 9x20mm titanium interference screws (Arthrex, Inc; Naples FL) were placed in the tibia and femur with the aid of an arthroscope and a commercial drill guide system for ACL reconstruction (Arthrex, Inc; Naples FL). The screw locations were selected to duplicate those typically used to affix an ACL allograft during surgery. Complete ACL reconstruction was not performed.

3.3.4 Test Protocol

After thawing, the specimens were wrapped in plastic bags to protect the scanning equipment from biohazard contamination. Each knee was placed in full extension and positioned within a transmit-receive knee surface coil and the magnet following the manufacturer-recommended protocol for positioning a patient for a knee evaluation. All scans were performed by certified MR technologists.

Each knee was scanned on the 1.5T and 3T scanners, both with and without the interference screws implanted. To minimize bias, test order was determined using a block randomization procedure. Specimens were first randomized by screw condition (screws implanted versus no screws implanted), and then within each screw condition, they were randomized by magnetic field strength (1.5T versus 3T). A total of 20 volumetric scans were performed (2 screw conditions x 2 magnetic field strengths x 5 specimens) using the T1-weighted WE-3D FLASH sequence.

3.3.5 Segmentation Technique

The femoral and tibial articular cartilage structures of each specimen were

manually segmented in the sagittal plane and reconstructed using commercial software (Mimics 9.11; Materialise, Ann Arbor, MI). Three-dimensional voxel models were generated and wrapped with a triangular mesh to create a virtual solid model of each cartilage structure. The solid models captured both articular cartilage volume and morphology.

3.3.6 Tibiofemoral Articular Cartilage Volume

The three-dimensional femoral articular cartilage model was cropped in order to isolate the tibiofemoral joint. Cropping was performed along the anterior-posterior axis such that the posterior half of the distal femur was selected. The volume was then further separated into those of the medial and lateral femoral condyles for each screw and magnet condition. The volume of each three-dimensional model of the articular cartilage structures was determined by surface integration. Preliminary data showed coefficients of variation (CVs) of 1.8% and 2.8% for the femoral and tibial cartilage volumes, respectively (n = 7), indicating that these measurements are repeatable.

3.3.7 Cartilage Thickness

We focused our thickness measurements on specific load-bearing regions of interest (ROIs). A cylinder was fit to the bone-cartilage interface of the femoral cartilage model of the tibiofemoral joint **(Figure 3.2)**. The notch marking the junction between the tibiofemoral and patellofemoral joints on the lateral condyle was identified on one sagittal MR image. A line was drawn from the notch (0^o) to the center of the cylinder. Each condyle of the tibiofemoral joint was then divided at 40^o, 70^o, 100^o, and 130^o from

the notch point (anterior) toward the posterior aspect of the condyle to create 6 patches of cartilage (3 medial, 3 lateral); the medial-lateral width of each patch was 20% of the overall medial-lateral width of the femoral cartilage and centered about the midline of each condyle.

Two regions on the tibial cartilage (1 medial, 1 lateral) were defined by calculating the centroids of each segmented cartilage region (compartment) using MATLAB (The Mathworks, Inc., Natick, MA). The inertial axes of the medial compartment were also determined using MATLAB, and axes of the same orientation were centered about the centroids of both the medial and lateral tibial compartments. The ROI for each compartment was then defined as the area ±20% of the overall anterior-posterior depth and ±15% of the overall medial-lateral width from the centroid **(Figure 3.3)**. The average thickness of each patch was calculated by a closest point algorithm using MATLAB.

Preliminary data showed mean coefficients of variation (CVs) of 4.7% and 2.7% for the thicknesses of the femoral and tibial ROIs, respectively (n = 7), indicating that both the coordinate system and the ROI thickness determination are repeatable.

3.3.8 Statistical Analysis

Based on preliminary data, the sample size for this study was derived to have sufficient power (80%) to detect a 10% difference in tibial articular cartilage volume between experimental conditions. A two-way repeated measures analysis of variance was performed to compare (1) the cartilage volumes of the proximal tibia and distal femur in response to screw condition (screws versus no screws) and magnetic field strength (1.5T

versus 3T), and (2) the cartilage thickness of each ROI in response to screw condition and magnetic field strength. Fisher's least significant difference test was used to make pair-wise comparisons between conditions. Statistical significance was set at $p<0.05$.

3.4 Results

3.4.1 Tibiofemoral Articular Cartilage Volume

There were no significant differences in the medial femoral cartilage volumes between magnet (12% reduction at 1.5T, p=0.07) or screw (1.0% reduction in the presence of screws, p=0.85) conditions **(Table 3.2)**. For the lateral femoral cartilage volumes, there was a significant difference between magnet strengths (12.5% reduction at 1.5T, p=0.006), but not screw conditions (4.2% reduction in the presence of screws, p=0.16) **(Table 3.2)**. No significant interaction was found between the screws and magnetic field strength conditions for either compartment (p>0.46).

For the medial tibial cartilage volume, there was no significant difference between magnet strengths (5.9% reduction at 1.5T, p=0.46) **(Table 3.2)**. There was, however, a trend for a screw effect (p=0.08). The mean decrease in cartilage volume due in the presence of the interference screws was less than 9% for this compartment. No significant interaction was found between screw condition and magnetic field strength (p=0.75). For the lateral tibial cartilage volumes, there was no significant difference between screw conditions (4.1% reduction in the presence of screws, p=0.30), but there was a significant difference between magnet strengths (p=0.03) **(Table 3.2)**. The mean increase in the lateral tibial cartilage volume at 3T compared to 1.5T was 9.1%. No significant interaction was found between screw condition and magnetic field strength (p=0.19).

3.4.2 Cartilage Thickness

For the most anterior ROI on the medial femoral condyle (40-70^{o}; Region 1 in **Figure 3.2c**), there was no significant difference in the mean thickness values between magnet strengths (8.8% reduction at 1.5T, p=0.09) or screw conditions (3.5% reduction in the presence of screws, p=0.39). For the central ROI on the medial femoral condyle (70-100^{o}; Region 2 in **Figure 3.2c**), there was no significant difference in thickness between magnet strengths (3.4% reduction at 1.5T, p=0.46) or screw conditions (0.0% change in the presence of screws, p=0.99). For the posterior ROI on the medial femoral condyle (100-130^{o}; Region 3 in **Figure 3.2c**), there was no significant difference in thickness between magnet strengths (1.8% increase at 1.5T, p=0.60) or screw conditions (1.3% increase in the presence of screws, p=0.81). No significant interactions were found between the screws and magnetic field strength conditions for any ROI (p>0.51) **(Figure 3.4)**.

For the most anterior ROI on the lateral femoral condyle (40-70^{o}) there was no significant difference in thickness between magnet strengths (0.1% increase at 3T, p=0.72) or screw conditions (0.9% decrease in the presence of screws, p=0.79). For the central ROI on the lateral femoral condyle (70-100^{o}), there was no significant difference in thickness between screw conditions (0.0% decrease in the presence of screws, p=0.998), but there was a strong trend for an interaction between magnet strength and the presence of the screw, suggesting that the screw effect was magnet-dependent (p=0.053). For this ROI, there was a 1.5% mean difference in thickness between screw conditions at 3T, but only a 0.5% mean difference in thickness at 1.5T. In both cases, the thickness was greater in the presence of interference screws than without the screws. For the posterior

ROI on the lateral femoral condyle (100-130^{o}), there was no significant difference in thickness between magnet strengths (2.3% decrease at 1.5T, p=0.83) or screw conditions (4.9% decrease in the presence of screws, p=0.09) **(Figure 3.5)**.

For the medial tibial ROI, there was no significant difference in thickness between magnet strengths (8.2% decrease at 1.5T, p=0.35), but there was a significant decrease in thickness in the presence of interference screws (p=0.03). The mean difference in thickness between screw conditions for this ROI was 11.5%. For the lateral tibial ROI, however, there was a significant increase in thickness at 3T compared to 1.5T (6.7% increase, p=0.004), but there was no significant difference in thickness between screw conditions (1.2% reduction in the presence of screws, p=0.57). No significant interaction was found between screw condition and magnetic field strength for any tibial ROI (p>0.11) **(Figure 3.5)**.

3.5 Discussion

There is clinical evidence to suggest that patients who undergo ACL reconstruction continue to exhibit progressive articular cartilage damage in the reconstructed knee [1-3, 5, 25-28]. However, there are many factors that may affect cartilage degeneration in the ACL-injured and reconstructed knee (i.e. initial subchondral trauma, concomitant injuries of the meniscus, general inflammation, altered joint motion and abnormal joint contact stresses) [29-30]. A quantitative method that is sensitive to early changes in articular cartilage structure, and that could be applied to patients who have undergone ACL reconstruction with titanium interference screws, would enable researchers to evaluate potential mechanisms of OA progression in this patient population. qMRI with cartilage-sensitive pulse sequences meets these requirements within certain constraints.

The T1-weighted WE-3D FLASH sequence is effective in tracking structural changes in articular cartilage for patients with OA [9]. Bauer et al concluded that based on signal-to-noise and contrast-to-noise ratios, the water-excitation gradient-echo sequence at 3T is superior to both the fat-saturated gradient-echo sequence at 3T or 1.5T and to the turbo spin-echo sequence for volumetric cartilage calculations [31]. The article did not investigate the water-excitation gradient-echo sequence at 1.5T. Our investigation used the water-excitation gradient-echo sequence on both the 3T and 1.5T magnets. Our study showed a slight increase in both SNR and the effective SNR (SNRe) in the presence of interference screws **(Table 3.1)**. As expected, there was also a notable

increase in both SNR and SNRe at 3T compared to 1.5T. To minimize the expected magnetic susceptibility artifacts on the gradient echo sequence, we selected MR imaging parameters to minimize voxel size. Our data demonstrate that measurements of tibiofemoral cartilage volume and thickness were largely unaffected by the presence of titanium interference screws, and that the lack of the screw effect was independent of magnetic field strength. Although most ROIs showed no differences in volume and thickness between screws or magnet strength, some differences were noted. The medial tibial cartilage volume showed a trend for a 9% reduction in cartilage volume when the screws were present. Similarly, the medial tibial ROI showed a significant decrease of 11.5% in the mean thickness value when the screw was present ($p=0.03$). The sensitivity of the medial tibial compartment to the presence of the screw is not surprising, because the screw is located just proximal to this compartment. Therefore, caution must be used when interpreting qMRI volume and thickness measurements in the medial compartment of the tibia in the presence of metallic interference screws. Although this does not exclude the use of qMRI for tracking changes in the other regions of the tibiofemoral joint, any changes in thickness less than approximately 0.30mm (11.5%) in the medial tibial compartment may be due to artifact and not cartilage degeneration. In contrast, the lateral femoral interference screw is farther away from the lateral femoral articular cartilage.

Kornaat et al. imaged knees of ten healthy volunteers on both 1.5T and 3T scanners using a sagittal fat-suppressed 3D-steady-state-free-precession (SSFP) sequence, a sagittal Dixon 3D-SSFP sequence, and a 3D spoiled gradient recall echo sequence to measure cartilage thickness of the distal femur from each sequence [24]. Although

improvements were seen with respect to the signal-to-noise and contrast-to-noise ratios with the 3T scanner, no significant differences in cartilage thickness were reported between scanners or sequences [24]. The thickness of the tibial cartilage was not evaluated [24]. Eckstein et al also evaluated the precision of qMRI when performed on 1.5T and 3T magnets [13]. They determined that cartilage volume and thickness measurements decreased with reductions in slice thickness, and that these measurements from the 1.5T and 3T MR images were highly correlated [13]. When the qMRI data of these investigations are considered in conjunction with those of the present study, the potential benefits for using 3T are highlighted. These results suggest, at the very least, that it is prudent to use the same magnetic field strength when tracking longitudinal changes in cartilage volume within a patient.

There are several limitations of this study. First, the findings apply directly to articular cartilage segmentation based on the T1-weighted WE-3D FLASH sequence. The results of other cartilage-sensitive pulse sequences may be different. Prior to this study, we evaluated another cartilage-sensitive pulse sequence, the frequency selective fat-saturation turbo spin-echo intermediate-weighted sequence. Counterintuitively, we found that the T1-weighted WE-3D FLASH sequence minimized image distortion in the vicinity of the interference screws **(Figure 3.1)** while the fat-saturation turbo spin-echo intermediate-weighted sequence tended to increase magnetic susceptibility artifact. The T1-weighted 3D gradient echo sequence was superior to the turbo spin echo sequence with respect to both signal-to-noise and contrast-to-noise ratios for articular cartilage imaging [31]. Thus, the T1-weighted WE-3D FLASH sequence was selected for this study.

The images used in this study were acquired from cadaver specimens, and were not compromised by either knee motion or blood flow artifacts. It is possible that the errors would be greater if the images were acquired *in vivo* [13]. Nonetheless, the cadaver model was beneficial because it allowed us to systematically measure the effects of interference screws and magnetic field strength, using each specimen as its own control.

The articular cartilage segmentations in this study were performed manually using commercial software (Mimics 9.11). Semi-automated techniques have been developed to increase the accuracy and efficiency of segmentation [8, 24, 32-33]. To reduce potential sources of error and to minimize this concern, the cartilage segmentations in the present study were performed by a single trained examiner under the direction of a musculoskeletal radiologist.

Additionally, segmentations were not compared to a true gold standard in the present study. Preliminary data did, however, show mean CVs of 4.7% and 2.7% for the thicknesses of the femoral and tibial ROIs, respectively, and 1.8% and 2.8% for the femoral and tibial cartilage volumes, respectively, indicating that these measurements are repeatable.

Standard size (9 x 20mm) titanium interference screws were used in this study. We cannot determine from the present study whether larger or smaller interference screws would influence the results of qMRI differently. In general, one would expect that a larger interference screw would cause some increase in the size of the magnetic susceptibility artifact, though the relationship is not linear. The extent of the artifact also depends on the position and composition of the interference screw, as well as the selected

pulse sequence parameters. However, because standard size screws were used in this study, the results apply to the majority of screws used for ACL reconstruction.

Complete ACL reconstructions were not performed on the cadavers imaged in this study. While it cannot be determined from our results whether the outcome would change if a complete ACL reconstruction were performed, we would not expect to see a chance in outcome with complete reconstruction because the interference screws would still be placed in the same locations, and other changes would involve only soft tissues. Since the ACL autograft courses through the intercondylar notch, and is not proximal to the femoral or tibial articular cartilage, one would not expect a major impact of the graft on imaging of the femoral or tibial articular cartilage, and therefore on volume and thickness measurements of this cartilage.

Freeze-thaw cycles and surgical intervention have the potential to introduce air artifacts into cadaver specimens. Although air and articular cartilage have vastly different intensities on MR images, these artifacts cannot be entirely eliminated. In the present study, segmentation in post-operative limbs was conducted by interpolating over air artifacts when present. This interpolation was performed to minimize the effects of any air artifacts. In future studies, saline could be injected into the joints post-operatively to attempt to eliminate air artifacts.

Although the data suggest that the medial tibial cartilage volume is affected by magnetic field strength, we did not determine which field strength provides the most accurate measurement. We assume that the 3T images are more accurate because more slices are used to reconstruct the 3-D models. The slice thickness was 1.5mm for the 3T magnet and 2.0mm for the 1.5T magnet. The slice thickness for each magnet was selected

to keep the sequence acquisition time under 10 minutes, which is practical when imaging subjects. Therefore, less interpolation was required when the 3-D voxel models were created from the segmented 3T MR images. A comparison to a known standard would be required in order to evaluate the accuracy of segmented volumes based on MR imaging at different field strengths.

Finally, the effect of magnetic field strength on medial tibial cartilage volume was marked by a strong trend, but it was not statistically significant ($p=0.08$). This study was 80% powered to detect a 10% difference in cartilage volume based on our sample size. The mean difference in medial tibial cartilage volume was less than 6% between magnetic field strengths.

The results of the present study suggest that caution should be used when interpreting thickness and volume of the medial tibial cartilage at 3T in the presence of interference screws. Additionally, 3T and 1.5T qMRI should not be used interchangeably to assess structural changes in articular cartilage during longitudinal studies.

3.6 Acknowledgements

The authors gratefully acknowledge the support of Dr. Charles B. Eaton (NIH Osteoarthritis Initiative) for providing us access to the 3T MR system at Memorial Hospital (Pawtucket, RI), and the technical expertise of Dan Arcuri, Lynn Fanella and Theodore Trafton. The statistical analyses were performed by Gary Badger from the Department of Medical Biostatistics at the University of Vermont.

The project was supported by grants from the National Institutes of Health (AR047910, AR047910S1), the Department of Diagnostic Imaging at Rhode Island Hospital, and the RIH Orthopaedic Foundation, Inc. The interference screws were donated by Arthrex, Inc (Naples FL).

3.7 References

1. Daniel, D.M., et al., *Fate of the ACL-injured patient: A prospective outcome study.* Am J Sports Med, 1994. **22**: p. 632-644.
2. Fink, C., C. Hoser, and K.P. Benedetto, *Development of arthrosis after rupture of the anterior cruciate ligament. A comparison of surgical and conservative therapy.* Unfallchirurg, 1994. **97**: p. 357-361.
3. Howe, J.G., et al., *Anterior cruciate ligament reconstruction using quadriceps patellar tendon graft. Part I. Long-term followup.* Am J Sports Med, 1991. **19**(5): p. 447-462.
4. Johma, N.M., et al., *Long term osteoarthritic changes in anterior cruciate ligament reconstructed knees.* Clin Orthop Relat Res, 1999. **358**: p. 188-193.
5. Lohmander, L.S. and H. Roos, *Knee ligament injury, surgery and osteoarthrosis. Truth or consequences?* Acta Orthopaedica Scandinavica, 1994. **65**(6): p. 605-9.
6. Kannus, P., M. Jarvinen, and T. Paakkala, *A radiological scoring scale for evaluation of post-traumatic osteoarthritis after knee ligament injuries.* International Orthopaedics, 1988. **12**(4): p. 291-297.
7. Kellgren, J.K. and J.S. Lawrence, *Radiological assessment of osteoarthritis.* Ann Rheum Dis, 1957. **15**: p. 494-501.
8. Eckstein, F. and C. Glaser, *Measuring cartilage morphology with quantitative magnetic resonance imaging.* Seminars in Musculoskeletal Radiology, 2004. **8**(4): p. 329-353.

9. Eckstein, F., *Noninvasive study of human cartilage structure by MRI.* Methods in Molecular Medicine, 2004. **101**: p. 191-218.

10. Burstein, D. and M. Gray, *New MRI techniques for imaging cartilage.* J Bone Joint Surg Am, 2003. **85**(Suppl 2): p. 70-77.

11. Gray, M.L., et al., *Toward imaging biomarkers for osteoarthritis.* Clinical Orthopaedics and Related Research, 2004. **427**(Suppl): p. S175-S181.

12. Koo, S., G.E. Gold, and T.P. Andriacchi, *Considerations in measuring cartilage thickness using MRI: factors influencing reproducibility and accuracy.* Osteoarthritis and Cartilage, 2005. **13**(9): p. 782-789.

13. Eckstein, F., et al., *Accuracy and precision of quantitative assessment of cartilage morphometry by magnetic resonance imaging at 3.0 T.* Arthritis & Rheumatism, 2005. **52**(10): p. 3132-3136.

14. Eckstein, F., et al., *Long-term and resegmentation precision of quantitative cartilage MR imaging (qMRI).* Osteoarthritis and Cartilage, 2002. **10**(12): p. 922-928.

15. Glaser, C., et al., *Femoro-tibial cartilage metrics from coronal MR image data: Technique, test-retest reproducibility, and findings in osteoarthritis.* Magnetic Resonance in Medicine, 2003. **50**(6): p. 1229-1236.

16. Cicuttini, F.M., et al., *Rate of knee cartilage loss after partial meniscectomy.* Journal of Rheumatology, 2002. **29**(9): p. 1954-1956.

17. Cicuttini, F.M., et al., *Longitudinal study of changes in tibial and femoral cartilage in knee osteoarthritis.* Arthritis & Rheumatism, 2004. **50**(1): p. 94-97.

18. Wluka, A.E., et al., *The determinants of change in tibial cartilage volume in osteoarthritic knees.* Arthritis & Rheumatism, 2002. **46**(8): p. 2065-2072.

19. Suh, J.S., et al., *Minimizing artifacts caused by metallic implants at MR imaging: experimental and clinical studies.* American Journal of Roentgenology, 1998. **171**(5): p. 1207-1213.

20. Czervionke, L.F., et al., *Magnetic susceptibility artifacts in gradient-recalled echo MR imaging.* American Journal of Neuroradiology, 1988. **9**(6): p. 1149-1155.

21. Farhani, K., et al., *Effect of field strength on susceptibility artifacts in magnetic resonance imaging.* Comput Med Imaging Graph 1990. **14**: p. 409-413.

22. Petersilge, C.A., et al., *Optimizing imaging parameters for MR evaluation of the spine with titanium pedicle screws.* American Journal of Roentgenology, 1996. **166**(5): p. 1213-1218.

23. Tartaglino, L.M., et al., *Metallic artifacts on MR images of the postoperative spine: reduction with fast spin-echo techniques.* Radiology, 1994. **190**(2): p. 565-569.

24. Kornaat, P.R., et al., *MR imaging of articular cartilage at 1.5T and 3.0T: Comparison of SPGR and SSFP sequences.* Osteoarthritis and Cartilage, 2005. **13**(4): p. 338-344.

25. DeVita, P., T. Hortobagyi, and J. Barrier, *Gait biomechanics are not normal after anterior cruciate ligament reconstruction and accelerated rehabilitation.* Med Sci Sports Exerc, 1998. **30**(10): p. 1481-1488.

26. Johnson, R.J., et al., *Five- to ten-year follow-up evaluation after reconstruction of the anterior cruciate ligament.* Clin Orthop Relat Res, 1984. **183**(183): p. 122-140.

27. Von Porat, A., E.M. Roos, and H. Roos, *High prevalence of osteoarthritis 14 years after an anterior cruciate ligament tear in male soccer players: a study of radiographic and patient relevant outcomes.* Ann Rheum Dis, 2004. **63**(3): p. 269-273.

28. Fithian, D.C., et al., *Prospective trial of a treatment algorithm for the management of the anterior cruciate ligament–injured knee.* Am J Sports Med, 2005. **33**(3): p. 335-346.

29. Andriacchi, T.P., et al., *A framework for the in vivo pathomechanics of osteoarthritis at the knee.* Ann Biomed Engin, 2004. **33**(3): p. 447-457.

30. Fleming, B.C., et al., *Ligament injury, reconstruction, and osteoarthritis.* Curr Opin Orthop, 2005. **16**(5): p. 354-362.

31. Bauer, J., et al., *Volumetric Cartilage Measurements of Porcine Knee at 1.5-T and 3.0-T MR Imaging: Evaluation of Precision and Accuracy.* Radiology, 2006. **241**(2): p. 399-406.

32. Stammberger, T., et al., *Determination of 3D cartilage thickness data from MR imaging: computational method and reproducibility in the living.* Magnetic Resonance in Medicine, 1999. **41**(3): p. 529-536.

33. Gougoutas, A.J., et al., *Cartilage volume quantification via Live Wire segmentation.* Academic Radiology, 2004. **11**(12): p. 1389-1395.

	3 Tesla	1.5 Tesla
qMRI	T1-weighted water-excitation three-dimensional fast low-angle shot (WE-3D FLASH): 20/7.6 [TR(ms)/ TE(ms)]; 12° [flip angle]; 160mm [field of view]; 0.3125mm/1.5mm/0mm [in-plane resolution/slice thickness/interslice gap]; 80 slices per slab; 130 hz/pixel [bandwidth]; 512x512 [matrix]; right/left [phase encoding direction]; one average of two excitations. (With screws: SNR = 72.9, SNRe = $3.6sec^{-1/2}$; without screws: SNR = 41.3, SNRe = $2.1sec^{-1/2}$).	T1-weighted WE-3D FLASH: 17.2/7.3; 30^{o}; 160mm; 0.3125mm/2mm/0mm [in-plane resolution/slice thickness/interslice gap]; 52 slices per slab; 160 hz/pixel; 512x512; anterior-posterior; one average. (With screws: SNR = 25.6, SNRe = $1.2sec^{-1/2}$; without screws: SNR = 19.2, SNRe = $0.9sec^{-1/2}$).

Table 3.1: Pulse sequences employed on the 3T and 1.5T scanners.

Magnet	Screw	Femoral Volume (mm^3)		Tibial Volume (mm^3)	
		Medial	Lateral	Medial	Lateral
3T	**No**	2896 (±1142)	3711 (±1502)	2265 (±898)	3193 (±1205)
3T	**Yes**	2978 (±1409)	3611 (±1534)	2043 (±902)	2915 (±1233)
1.5T	**No**	2722 (±1090)	3429 (±1370)	2159 (±796)	2754 (±1046)
1.5T	**Yes**	2583 (±1188)	3230 (±1326)	1999 (±658)	2790 (±1052)

Table 3.2: Mean (±1 standard deviation) tibiofemoral cartilage volumes for each magnet and screw condition.

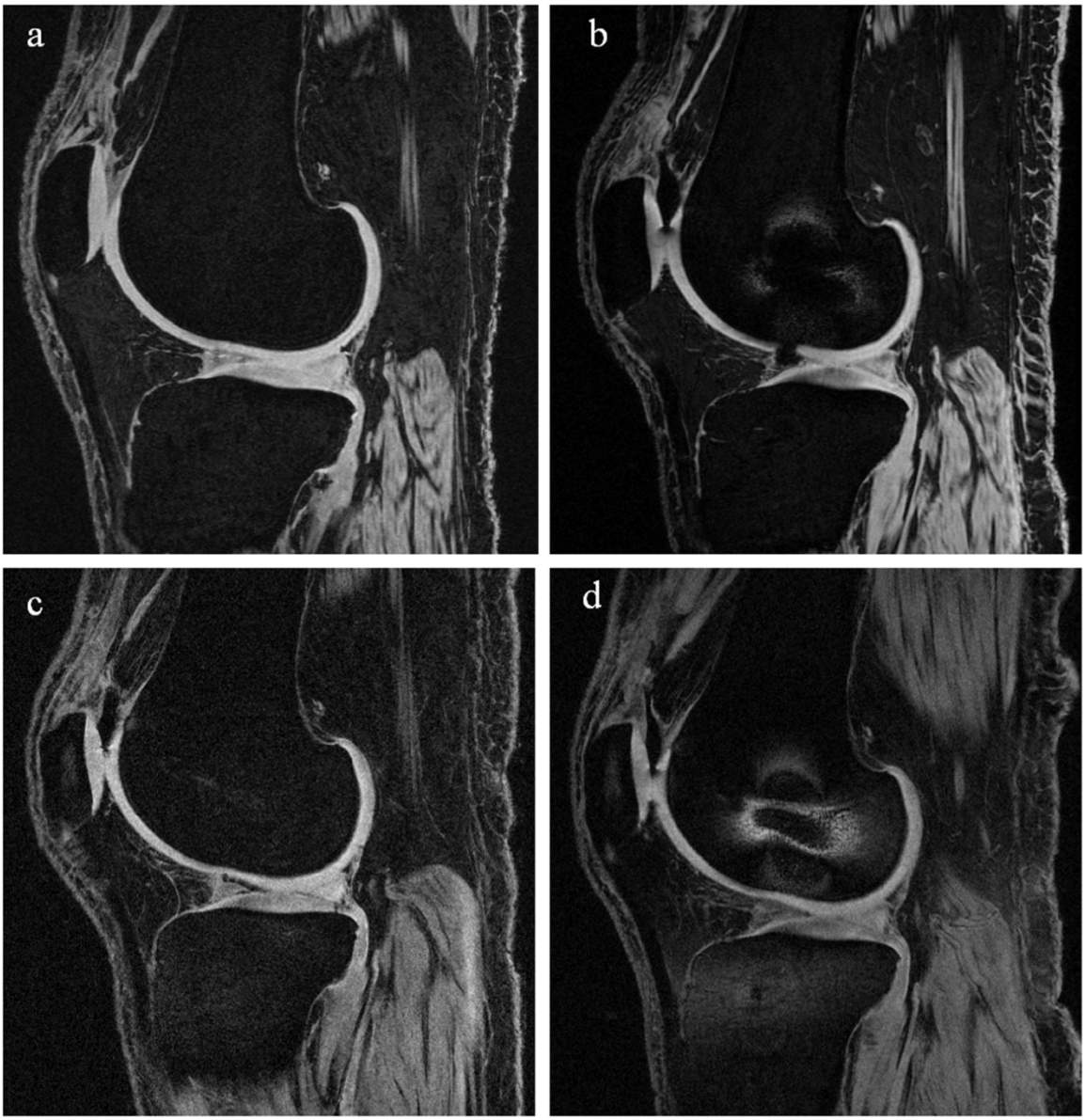

Figure 3.1: Representative sagittal-plane images of a single cadaver specimen imaged using the T1-weighted WE-3D FLASH sequence (a) at 3T without interference screws, (b) at 3T with interference screws, (c) at 1.5T without interference screws, and (d) at 1.5T with interference screws. These slices capture the lateral femoral condyle, so only the femoral interference screw is visible. It can be seen that the distortion is relatively localized around the femoral screw, and did not affect the overall cartilage segmentations of the tibiofemoral joint. Image (b) shows an air artifact near the anterior portion of the meniscus. Segmentation was interpolated over air artifacts.

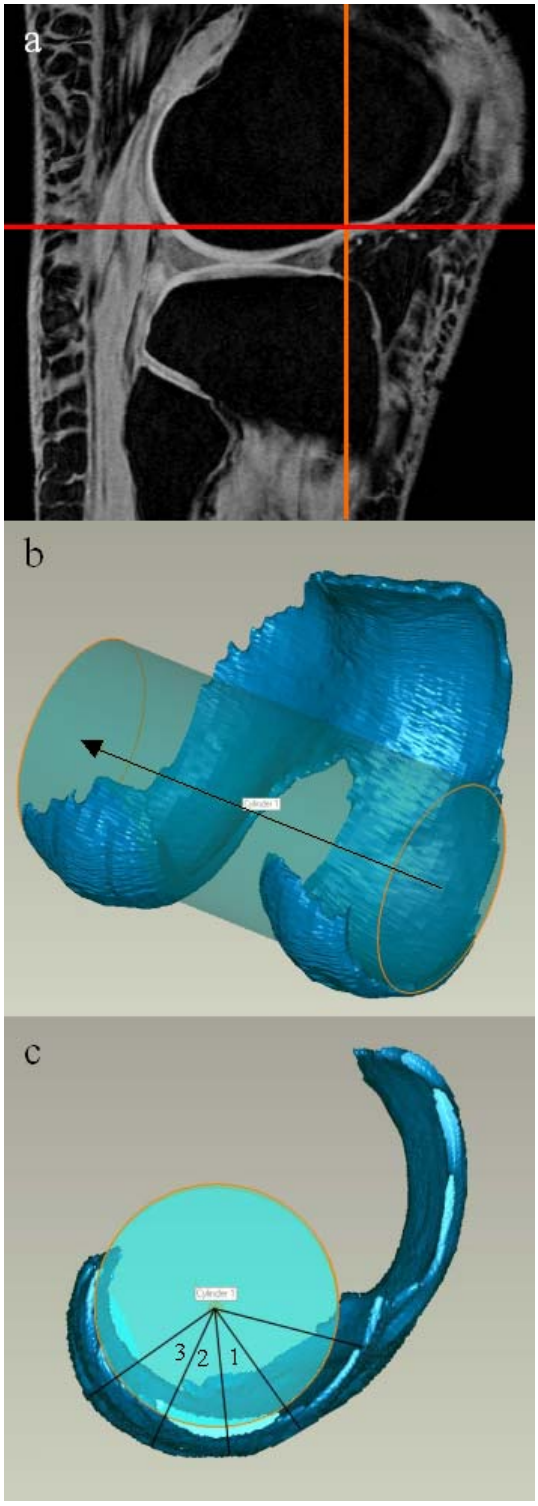

Figure 3.2: (A) The "notch" is marked by crosshairs on the lateral side of the TF joint, seen in the sagittal plane. (B) A cylinder was fit to the femoral condyles. (C) A line was drawn from the notch to the cylinder axis. The location of each ROI in the sagittal plane of the femur is shown.

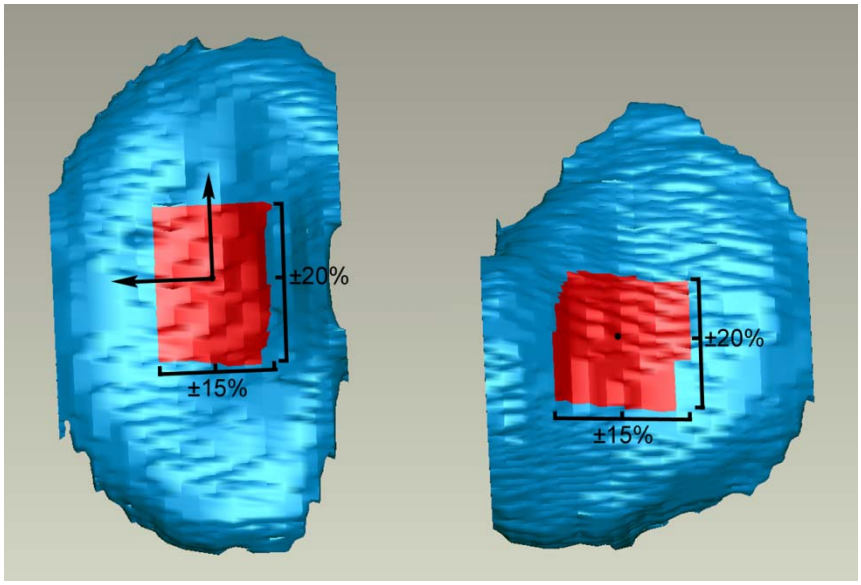

Figure 3.3: The ROIs for the tibial compartments are shown. Axes with the same orientation as those from the medial compartment were centered about the centroid of the lateral compartment to establish the coordinate system in that ROI. The orthogonal was oriented out of the page.

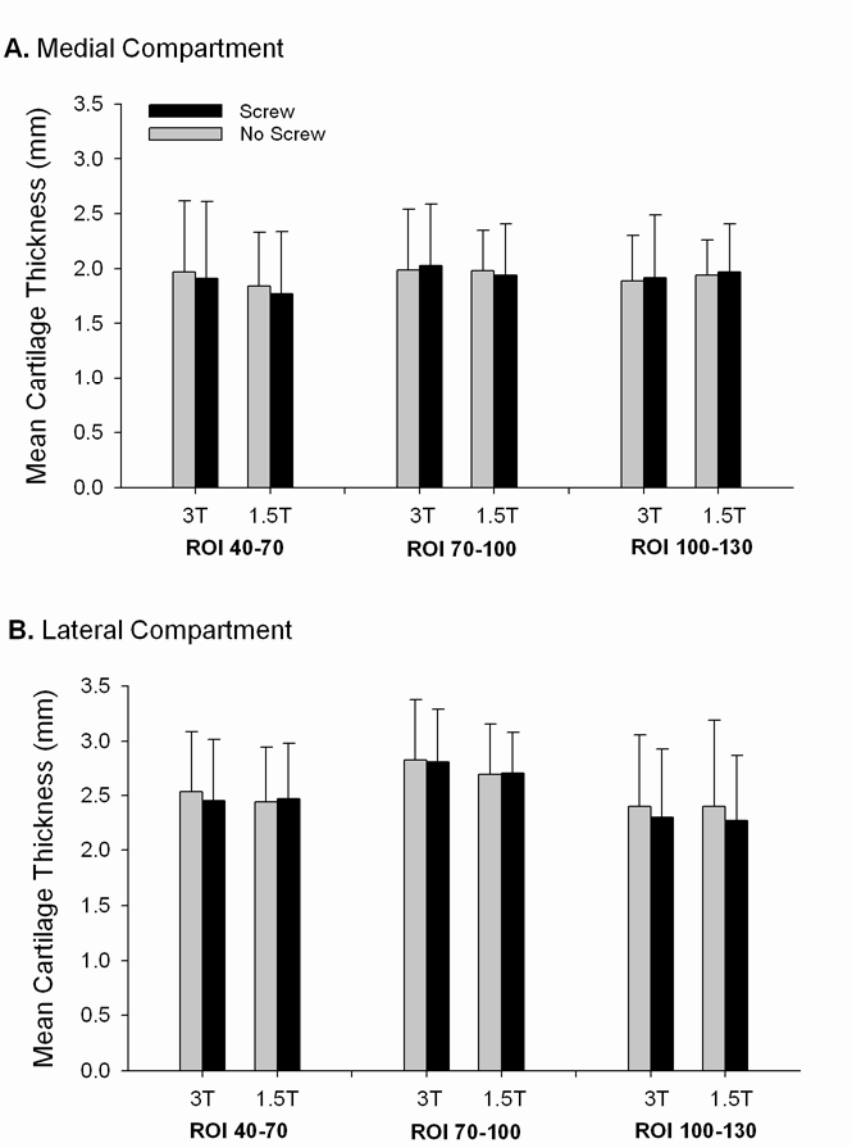

Figure 3.4: The mean femoral cartilage thicknesses for both screw condition and magnetic field strengths (error bars represent 1 standard deviation). (A) On the medial femoral condyle, there were no significant differences in thickness between magnet strengths or screw conditions for any ROI. (B) On the lateral femoral condyle, the 70-100^{o} ROI showed a strong trend for interaction between magnet strengths (p=0.053). No other ROI on the lateral femoral condyle showed any significant differences in thickness between magnet strengths or screw conditions.

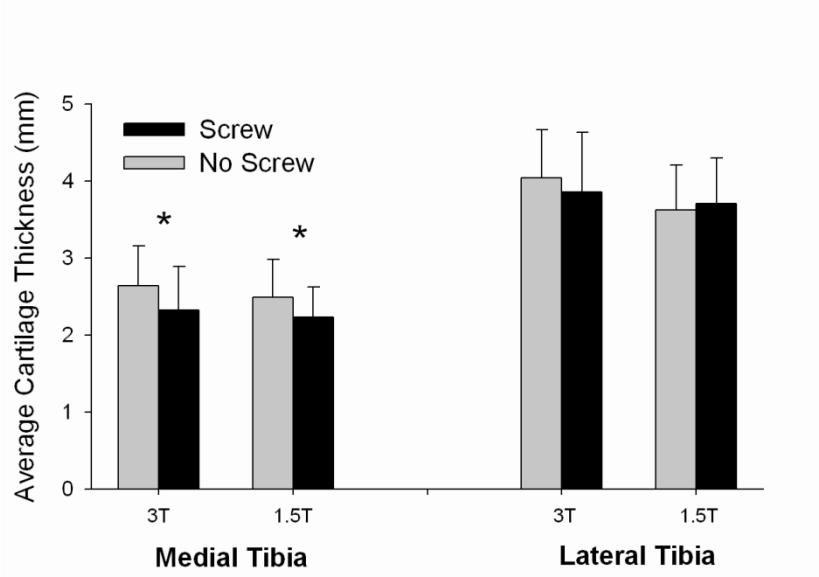

Figure 3.5: Average medial and lateral tibial cartilage thicknesses for both screw conditions and magnetic field strengths (error bars represent 1 standard deviation). For the medial tibial ROI, there was no significant difference in thickness between magnet strengths ($p=0.35$), but there was a significant difference in thickness between screw conditions ($p=0.03$). For the lateral tibial ROI, however, there was a significant difference in thickness between magnet strengths ($p=0.004$), but not screw conditions ($p=0.57$). No significant interaction was found between screw condition and magnetic field strength for any tibial ROI ($p>0.11$).

Chapter 4

Quantitative MR Imaging using "LiveWire" to Measure Tibiofemoral Articular Cartilage Thickness

Megan E. Bowers, Nhon Trinh, Glenn A. Tung, Joseph J. Crisco, Benjamin B. Kimia, Braden C. Fleming

The following chapter was published in *Osteoarthritis and Cartilage*, 16: 1167-1173 (2008). (PMID: 18407529)

4.1 Abstract

4.1.1 Objective

To assess the reliability and accuracy of manual and semi-automated segmentation methods for quantifying knee cartilage thickness. This study employed both manual and LiveWire-based semi-automated segmentation methods, *ex vivo* and *in vivo*, to measure tibiofemoral cartilage thickness.

4.1.2 Methods

The articular cartilage of a cadaver knee and a healthy volunteer's knee were segmented manually and with LiveWire from multiple 3T MR images. The cadaver specimen's cartilage thickness was also evaluated with a 3D laser scanner, which was assumed to be the gold standard. Thickness measurements were made within specific cartilage regions. The reliability of each segmentation method was assessed both *ex vivo* and *in vivo*, and accuracy was assessed *ex vivo* by comparing segmentation results to those obtained with laser scanning.

4.1.3 Results

The cadaver specimen thickness measurements showed mean coefficients of variation (CVs) of 4.16%, 3.02%, and 1.59%, when evaluated with manual segmentation, LiveWire segmentation, and laser scanning, respectively. The cadaver specimen showed mean absolute errors versus laser scanning of 4.07% and 7.46% for manual and LiveWire segmentation, respectively. *In vivo* thickness measurements showed mean CVs of 2.71% and 3.65% when segmented manually and with LiveWire, respectively.

4.1.4 Conclusions

Manual segmentation, LiveWire segmentation, and laser scanning are repeatable methods for quantifying knee cartilage thickness; however, the measurements are technique-dependent. *Ex vivo*, the manual segmentation error was distributed around the laser scanning mean, while LiveWire consistently underestimated laser scanning by

8.9%. Although LiveWire offers repeatability and decreased segmentation time, manual segmentation more closely approximates true cartilage thickness, particularly in cartilage contact regions.

4.2 Introduction

Osteoarthritis (OA) of the tibiofemoral (TF) joint is marked by distinct changes in cartilage volume and thickness [1-13]. *In vivo* methods that accurately track these initial changes are crucial for documenting the onset and progression of OA. Quantitative magnetic resonance imaging (qMRI) has shown promise for assessing changes in cartilage morphometry, and may prove to be a valuable measure for OA progression [2, 7, 9, 14-16].

Quantitative MRI requires accurate, reliable, and efficient cartilage segmentation techniques. Both manual and semi-automated segmentation approaches have been developed [2, 17-23]. While manual segmentation allows full user control, it is user-dependent, tedious, and time-consuming. Semi-automated approaches, while generally faster, are also prone to segmentation errors because they may miss localized features of cartilage damage, and do not function well in regions of poor contrast. Some studies have shown semi-automated segmentation techniques to be more reliable than manual methods [21]; despite these findings, some commercial segmentation companies, including Chondrometrics GmbH, have returned from semi-automated methods to manual segmentation [2, 24-27]. Despite recent attempts [28] and the use of cartilage-sensitive MRI sequences, a fully automated cartilage segmentation technique remains elusive due to the limited contrast between the cartilage and adjacent tissues. Various pulse sequences, such as the double-echo steady state (DESS), and the use of contrast agents have been added to scanning protocols in an effort to improve cartilage contrast. Each

method has theoretical and practical trade-offs [29-30], and no sequence or protocol has shown unequivocal superiority.

There are several semi-automated segmentation algorithms, the most common of which uses active contours, or “snakes” [20-21, 31-33]. With this method, the user plants “seed points” near cartilage interfaces, and cartilage boundaries are fit to those surfaces based on image contrast differences. Because active contours rely upon gradient descents, they are prone to instabilities, errors, and selection of local minima, particularly in regions of low contrast and local defects [34-35]. Because of these limitations, an approach that directly follows cartilage edges may be advantageous. One such approach is “LiveWire,” which uses localized image intensity to directly map cartilage boundaries [23, 36-37]. With this approach, the user initiates a contour with the cursor, which then “snaps” to the optimal boundary closest to the current cursor position. To continue the segmentation, the user merely moves the cursor in the general vicinity of the cartilage boundary, and the LiveWire algorithm selects the appropriate edge. Although semi-automated, it is less likely to get trapped in local minima than active snakes or other approaches. In a cadaver study of the patellofemoral (PF) joint, the accuracy of a LiveWire segmentation approach for measuring cartilage volume was within 97.8% of the true volume, with inter- and intra-operator coefficients of variation of 3.0% and 0.4%, respectively [23]. For the present study, the LiveWire algorithm was adapted for segmentation of the TF joint.

While many studies have examined the use of qMRI for tracking overall changes in cartilage volume and thickness [8, 12, 38-39], only a few have defined specific regions of interest (ROIs) within segmented cartilage for morphological evaluation [9, 31, 40-41].

The identification of specific ROIs allows investigators to focus on primary load-bearing regions, where thickness changes are most significant, while excluding regions that are not affected and may mitigate these changes. For longitudinal studies, ROIs must be defined such that they can be reproducibly identified at each time point.

The objectives of this study were to develop and implement a LiveWire-based segmentation method to quantify TF articular cartilage thickness, and to compare measurements to those obtained with manual segmentation. The specific aims were: (1) to evaluate the reliability of TF cartilage thickness measurements using the LiveWire and manual segmentation approaches both *ex vivo* and *in vivo*, and (2) to assess the accuracy of TF cartilage thickness measurements *ex vivo* by comparing LiveWire and manual segmentation approaches to laser scanning, a reference standard.

4.3 Materials and Methods

4.3.1 MR Imaging

All images (fourteen total scans: seven of one cadaver, and seven of one subject) were acquired on a 3T system (Siemens Trio; Erlangen, Germany) using a commercially available polarized knee coil. MR images were acquired using the T1-weighted water-excitation three-dimensional fast low-angle shot (WE-3D FLASH) sequence: repetition time, 20ms; echo time, 7.6ms; flip angle, 12°; field of view, 160mm; in-plane resolution, 0.3125mm; slice thickness/interslice gap, 1.5mm/0mm; slices per slab, 80; matrix, 512 x 512; phase-encoding, right-to-left; number of averages, one.

4.3.2 Manual Segmentation

The femoral and tibial articular cartilage structures of each specimen were manually segmented in the sagittal plane by a single experienced investigator, and reconstructed using commercial software (Mimics 9.11; Materialise, Ann Arbor, MI, USA). 3D voxel models were generated and wrapped with a triangular mesh to create a virtual solid model of each cartilage structure. The solid models captured both articular cartilage volume and morphology.

4.3.3 LiveWire Segmentation

The femoral and tibial cartilage structures from each scan of each knee were also segmented using LiveWire. For this application, the LiveWire algorithm was adapted to

work in concert with manual segmentation, such that the user could override the semi-automated method in regions where cartilage boundaries were not clear. The resulting contours were exported as point clouds that were used to generate closed-surface (solid) models for each structure. The solid models were constructed by wrapping a triangular surface mesh to the 3D point cloud [42].

Both the manual and LiveWire segmentations were completed independently by an experienced user who was trained by a musculoskeletal radiologist. The resulting 3D models were used to make cartilage thickness measurements.

4.3.4 Laser Scanning

The accuracy of each segmentation technique was assessed on a cadaver specimen using a 3D laser scanner to obtain the true cartilage morphometry (ShapeGrabber PLM Series; Vitana Corp, Ottawa, Ont). The laser scanner employed a high-resolution scan head (SG-1000). The resolution along the scanning direction was 100μm, and the depth resolution was 5μm. For each bone that was scanned, all soft tissues, except the articular cartilage, were first removed. Laser scans from twenty different views of each bone were taken to fully image the cartilage surfaces, with sufficient overlap for subsequent reconstruction **(Figure 4.1)**. Six dry wall screws were inserted into each bone to provide additional reference landmarks to facilitate the registration of different views. The articulating end of each bone was regularly bathed in physiological saline to prevent soft tissues from drying. After one set of scans was completed, the cartilage was dissolved from the bone by immersing the articulating surface in 5.25% sodium hypochlorite solution (Clorox© bleach) for four hours. The bone

was then rescanned using the same protocol. After scanning, the laser data were smoothed by treating each scan as a two-dimensional function (horizontal and vertical directions as the x- and y- axes; depth as the z-axis), and smoothing the function using a two-dimensional Gaussian kernel. The twenty scans were then merged to construct the contours of the cartilage and bone surfaces [31]. The two surfaces were then superimposed to obtain a laser scan model of each cartilage structure. The reliability of the laser scanning method was determined to create a baseline for comparison of the previously described segmentation techniques. For the purpose of this study, the resulting 3D models were considered the gold standard for comparison to the 3D models generated from the cartilage segmentation algorithms.

4.3.5 Cartilage Thickness

TF cartilage thickness measurements were performed on specific load-bearing ROIs [31, 41]. A distinct notch marking the junction between the TF and PF joints on the lateral femoral condyle was identified on the first sagittal MR image in which it appeared **(Figure 4.2a)**. The bone-cartilage interface of the 3D femoral cartilage model was fit with a cylinder **(Figure 4.2b)**. A line was drawn from the notch (0^o) to the center of the cylinder. Each femoral condyle was then divided at 40^o, 70^o, 100^o, and 130^o from the notch point toward the posterior aspect of the femur to create six femoral ROIs [three medial (M1: 40-70^o), (M2: 70-100^o), (M3: 100-130^o); and three lateral: (L1: 40-70^o), (L2: 70-100^o), (L3: 100-130^o)] **(Figure 4.2b, c)**. Each ROI's medial-lateral width was 20% of the overall medial-lateral width of the femoral cartilage, and each ROI was centered about the midline of its respective condyle **(Figure 4.2c)**.

Two tibial ROIs [one medial (MT) and one lateral (LT)] were defined on the cartilage regions of the 3D model resulting from segmentation. The centroid of each compartment was calculated with MATLAB (The Mathworks, Inc., Natick MA, USA). The inertial axes of the medial compartment were also determined using MATLAB, and axes of the same orientation were projected onto the centroids of both the medial and lateral tibial compartments. The ROI of each compartment was then defined as the area ±20% of the overall anterior-posterior length and ±15% of the overall medial-lateral width from the centroid **(Figure 4.2d)**. The mean thickness of each cartilage patch was calculated with a closest point algorithm using MATLAB.

The same procedures were used to identify the corresponding ROIs on the tibial and femoral cartilage models obtained from the laser scanning process described above.

4.3.6 *Ex vivo* Assessment

One fresh-frozen human cadaver knee (54-year-old female) was used to evaluate both the accuracy and reliability of the manual and LiveWire segmentation methods. The specimen showed no evidence of knee injury or cartilage damage upon visual inspection. It was imaged seven times using the T1-weighted WE-3D FLASH sequence. Between each scan, the knee was removed from the coil, flexed and extended twenty times, and reinserted into the coil. The resulting images were segmented and reconstructed using both methods described above. After MR imaging was complete, the joint was disarticulated, and the distal femur and proximal tibia were assessed using the described 3D laser scanning method.

4.3.7 *In vivo* Assessment

The knee of a healthy volunteer (23-year-old female) was also scanned seven times. Between each scan, the subject exited the scanner, walked around the facility for five minutes, and then re-entered the scanner for the next scan. The MR scans were segmented and reconstructed using both methods described above.

4.3.8 Statistical Analysis

The reliability of each technique (Aim 1) was established by calculating the coefficients of variation (CVs) for the *ex vivo* and *in vivo* experiments. To assess the accuracy of both segmentation methods, two-way analyses of variance (factors: method and trials) were performed to compare the mean thickness values of the two segmentation methods with those obtained from the laser scanner, and with each other. Each ROI was analyzed in a separate ANOVA.

4.4 Results

4.4.1 Reliability (Aim 1)

The reliability of both segmentation methods was assessed both *ex vivo* and *in vivo* by determining the CV(%) for each ROI (M1-3, L1-3, MT, and LT) over the seven repeated MR scans **(Table 4.1)**. The cadaver specimen showed mean CVs across all ROIs of 4.16%, 3.02%, and 1.59% for manual segmentation, LiveWire segmentation, and laser scanning, respectively.

In vivo, the mean CVs across all ROIs were 2.71% and 3.65% for manual and LiveWire segmentation, respectively **(Table 4.1)**.

4.4.2 Accuracy (Aim 2)

The accuracy of both segmentation methods was assessed *ex vivo* by the comparison of mean ROI thicknesses to laser scanning results **(Figure 4.3)**. The mean absolute error across all ROIs between manual segmentation and laser scanning was 4.07% (5.35% over six femoral ROIs; 0.22% over two tibial ROIs), while this error between LiveWire segmentation and laser scanning was 7.46% (8.93% over six femoral ROIs; 3.06% over two tibial ROIs). With the exception of MT, there were significant differences in thickness values in each ROI measured *ex vivo* between LiveWire and manual segmentation ($p<0.02$). Thickness values obtained from LiveWire segmentation consistently underestimated those obtained by manual segmentation and laser scanning **(Figure 4.3)**. The region MT showed no significant differences between manual

segmentation, LiveWire segmentation, or laser scanning ($p=0.11$). The regions M1, M2, and L1 showed significant differences in thickness measurements between LiveWire segmentation and laser scanning ($p<0.001$), whereas regions M3, L2, L3, and LT did not ($p>0.08$). Similarly, the regions M2, M3, and L2 showed significant differences in thickness measurements between manual segmentation and laser scanning ($p<0.025$), whereas regions M1, L1, L3, and LT did not ($p>0.11$).

In vivo, each ROI over seven trials showed significantly different thickness measurements between the two segmentation methods ($p<0.011$). LiveWire segmentation consistently underestimated manual segmentation. When pooled across the femoral ROIs, manual and LiveWire segmentations produced mean thickness values of 2.33(±0.024)mm and 2.04(±0.034)mm, respectively. Similarly, when pooled across the tibial ROIs, the manual and LiveWire segmentations produced mean values of 2.81(±0.061)mm and 2.47(±0.041)mm, respectively.

4.5 Discussion

Both the LiveWire and manual segmentation techniques were repeatable for analyzing TF articular cartilage thickness. The segmentation-based thickness measurements each had mean CVs of less than 4.17%, both *ex vivo* and *in vivo*, in the defined ROIs over seven trials (Aim 1). Similarly, laser scanning thickness measurements had a mean CV of 1.59% over seven trials, suggesting that this method is an acceptable gold standard for the evaluation of segmentation-based cartilage thickness measurements. *In vivo*, the mean CVs across all ROIs were 2.71% and 3.65% for manual and LiveWire segmentation, respectively. When the accuracy of each segmentation technique was assessed, the mean absolute error between manual segmentation and laser scanning was 4.07% (5.35% over the femoral ROIs; 0.22% over the tibial ROIs), while the mean absolute error between LiveWire segmentation and laser scanning was 7.46% (8.93% over the femoral ROIs; 3.06% over the tibial ROIs) (Aim 2). These results indicate that although each method is repeatable, TF cartilage thickness measurements based upon manual segmentation more closely approximate true cartilage thicknesses than do those based upon LiveWire segmentation.

While there are several possible explanations for the generally lower CVs seen *in vivo*, it is likely that a living knee has higher water content than does a cadaver knee, and therefore provides greater articular cartilage contrast on MRI. Differences in age and tissue fixation between the cadaveric and living specimens may also explain the noted results. Similarly, there are several possible explanations for the much lower absolute

errors seen in the tibial ROIs when compared to the femoral ROIs. The femoral cartilage is curved, and therefore is not consistently orthogonal to the long axis of the magnetic field when compared to the relatively flat tibia. The curved femoral cartilage is prone to more error due to partial volume effects, as well as other MRI and voxel reconstruction phenomena. In addition, tibial cartilage, in both compartments, is generally thicker than femoral cartilage. Because the mean tibial thickness is greater, the error value will translate to a smaller percent error than in the femur. When combined, these explanations may account for the lower absolute errors seen in the tibia.

LiveWire thickness measurements consistently underestimated those made with manual segmentation and laser scanning. This underestimation suggests a systematic error in the calculation of cartilage thickness with LiveWire. It is feasible, therefore, that this error may be reduced by systematically adjusting the cartilage thickness values obtained from LiveWire segmentation, thereby improving the accuracy of LiveWire-based cartilage thickness measurements. There are many possible explanations for this segmentation bias; one is that each method uses a slightly different interpolation algorithm when creating segmentation-based 3D models. Second, the process of reconstructing a 3D model from LiveWire segmentation requires several steps of manual user input, including the repair of any errors associated with the “wrapping” of the triangular mesh, and therefore allows some room for variability. The 3D model reconstruction process associated with manual segmentation, however, is automated. Therefore, the source of error may be in the reconstruction process, rather than in segmentation. Although this represents a limitation of the LiveWire method in its current form, its 3D modeling process could be adjusted and streamlined in the future.

Despite the apparently systematic error associated with LiveWire, the method has several inherent advantages over manual segmentation. LiveWire segmentation is faster than manual segmentation, which is tedious and time-consuming; manual segmentation of one set of images may take up to two hours. Because LiveWire employs an algorithm with smaller bounding boxes than traditional semi-automated segmentation techniques, it is less likely to become trapped in local minima. As previously mentioned, LiveWire was programmed for our purposes to work in concert with manual segmentation when a local defect was encountered in which the segmentation was not clear. This feature was employed only when LiveWire could not find an appropriate boundary. Thus, the option to switch to manual segmentation when necessary allowed the user to capture features of the articular cartilage that the primary semi-automated segmentation approach might have excluded, while still decreasing segmentation time. Although it is not certain whether this feature would be an advantage for segmenting of knees with generalized chondral defects, we would hypothesize that the addition of the manual segmentation option to the semi-automated algorithm would remain an advantage for such knees, especially since these knees are often more challenging to segment than healthy knees.

After examining the results of the present study, we qualitatively evaluated the differences between manual and LiveWire segmentation by overlaying representative contours of each method onto their respective MR image slices. We saw that while LiveWire seemed to more closely approximate cartilage boundaries toward the extreme edges of the tibial and femoral cartilage, manual segmentation appeared to provide a closer approximation in regions of low contrast and cartilage contact. Manual segmentation results may have appeared more favorable in the present study because the

ROIs examined were focused upon load-bearing cartilage areas, rather than the edges of the cartilage structures. Additionally, it may be possible that the differences in thickness seen in the varying weight-bearing regions may have been due simply to the fact that some regions have greater average thickness values than others. In regions with greater average thickness, such as L2 and LT, a small difference in thickness between segmentation methods, although valid, may not be statistically significant, because the percent difference is relatively small. Similarly, in regions with small average thickness values, such as M1 and L1, a small difference in thickness may be statistically significant because the percent difference is relatively large. Because LiveWire appears to be more effective in some areas of the knee joint, while manual segmentation is better in others, some efficient combination of both methods, similar to the program employed in this study, may provide the best results while still offering decreased segmentation time.

The ROIs examined in the present study were chosen to represent the weight-bearing regions of the femur and tibia. Because qMRI is useful for tracking the onset and progression of early OA, it seems practical to focus on thickness changes in weight-bearing regions.

A “fully” automated segmentation technique has recently been reported [13, 28, 43]. This method, however, requires the use of manual segmentation to “teach” the software to properly segment cartilage. These methods have, thus far, only been applied to healthy joints; their success on joints with varying degrees of OA progression remains unknown, and the evaluations have only been performed using low-field (0.18T) MRI.

In 2005, Koo et al. published a study evaluating knee cartilage thickness with segmented MR images [31]. In that study, Koo et al. used a semi-automated B-Spline snake segmentation method to measure cartilage thickness in six femoral ROIs *ex vivo* and *in vivo*. The *ex vivo* specimens were porcine, and were evaluated with both MRI segmentation and 3D laser scanning, similar to the evaluation described in the present study. Koo et al. reported *in vivo* intra-observer femoral thickness measurement CVs of 2-3%, which are comparable to the values reported in the current study. For one *in vivo* specimen that was scanned twice, Koo reported variability of approximately 4% of the total cartilage thickness in weight-bearing regions. Although the ROIs defined by Koo et al. were slightly different than those described in the present study, the results were comparable in terms of accuracy and reliability. Although Koo et al. reported some tibial thickness data, the details concerning these measurements were not specified.

The present study has some limitations. The accuracy assessment (Aim 2) of MR imaging-based cartilage thickness measurements assumes that laser scanning is the gold standard. A preliminary validation study showed laser scanning thickness measurements of phantom articular cartilage to be within 4.5% and 3.6% of caliper-based thickness measurements for the femoral and tibial cartilage, respectively. Although it is difficult to determine the true cartilage thickness of a cadaver specimen, our laser scanning method showed a mean CV of 1.59% for all ROIs over seven trials, indicating that the method was reliable. The use of laser scanning also prevented the assessment of accuracy *in vivo*, a problem that was offset in the present study by the addition of an *ex vivo* component. Additionally, the *ex vivo* MR images used within this study were not affected by motion or blood flow artifacts; for this reason, we also tested both segmentation methods *in vivo*.

Finally, due largely to the amount of time required for acquiring and processing the laser scan data, this study includes a limited number of samples (two knees—one cadaver, one volunteer—each scanned seven times). Even with this number of samples, however, we were able to detect statistically significant differences in articular cartilage thickness measurements between methods. It is important to note that the purpose of this study was to compare the reliability of two separate methods of articular cartilage segmentation; therefore, knees of different stages of OA, focal and generalized chondral defects, and different ages and genders were not evaluated. The *ex vivo* and *in vivo* specimens scanned multiple times allowed for evaluation of variability due to each segmentation method, without the complication of examining knees in various conditions.

In conclusion, manual segmentation, LiveWire segmentation, and laser scanning are repeatable methods for quantifying tibiofemoral articular cartilage thickness. However, the thickness measurements appear to be technique-dependent. Assuming that the laser scanning method is an appropriate standard for comparison, manual segmentation provided a more accurate measurement of cartilage thickness in load-bearing regions of the tibiofemoral joint.

4.6 Acknowledgements

This project was funded by the National Institutes of Health (AR047910; AR047910S1).

4.7 References

1. Cicuttini, F.M., A.E. Wluka, and S.L. Stuckey, *Tibial and femoral cartilage changes in knee osteoarthritis.* Ann Rheum Dis, 2001. **60**: p. 977-980.
2. Eckstein, F., D. Burstein, and T.M. Link, *Quantitative MRI of cartilage and bone: degenerative changes in osteoarthritis.* NMR Biomed, 2006. **19**(7): p. 822-854.
3. Amin, S., et al., *The relationship between cartilage loss on magnetic resonance imaging and radiographic progression in men and women with knee osteoarthritis.* Arthritis & Rheumatism, 2005. **52**(10): p. 3152-3159.
4. Jones, G., et al., *Early radiographic osteoarthritis is associated with substantial changes in cartilage volume and tibial bone surface area in both males and females.* Osteoarthritis and Cartilage, 2004. **12**(2): p. 169-174.
5. Graichen, H., et al., *Quantitative assessment of cartilage status in osteoarthritis by quantitative magnetic resonance imaging: technical validation for use in analysis of cartilage volume and further morphologic parameters.* Arthritis & Rheumatism, 2004. **50**(3): p. 811-816.
6. Cicuttini, F., et al., *Longitudinal study of the relationship between knee angle and tibiofemoral cartilage volume in subjects with knee osteoarthritis.* Rheumatology, 2004. **43**(3): p. 321-324.
7. Raynauld, J.P., et al., *Quantitative magnetic resonance imaging evaluation of knee osteoarthritis progression over two years and correlation with clinical*

symptoms and radiologic changes. Arthritis & Rheumatism, 2004. **50**(2): p. 476-487.

8. Cicuttini, F.M., et al., *Longitudinal study of changes in tibial and femoral cartilage in knee osteoarthritis.* Arthritis & Rheumatism, 2004. **50**(1): p. 94-97.
9. Raynauld, J.P., et al., *Reliability of a quantification imaging system using magnetic resonance images to measure cartilage thickness and volume in human normal and osteoarthritic knees.* Osteoarthritis and Cartilage, 2003. **11**(5): p. 351-360.
10. Glaser, C., et al., *Femoro-tibial cartilage metrics from coronal MR image data: Technique, test-retest reproducibility, and findings in osteoarthritis.* Magnetic Resonance in Medicine, 2003. **50**(6): p. 1229-1236.
11. Biswal, S., et al., *Risk factors for progressive cartilage loss in the knee: a longitudinal magnetic resonance imaging study in forty-three patients.* Arthritis Rheum, 2002. **46**(11): p. 2884-2892.
12. Wluka, A.E., et al., *The determinants of change in tibial cartilage volume in osteoarthritic knees.* Arthritis & Rheumatism, 2002. **46**(8): p. 2065-2072.
13. Qazi, A.A., et al., *Separation of healthy and early osteoarthritis by automatic quantification of cartilage homogeneity.* Osteoarthritis and Cartilage, 2007. **15**(10): p. 1199-206.
14. Bauer, J., et al., *Volumetric Cartilage Measurements of Porcine Knee at 1.5-T and 3.0-T MR Imaging: Evaluation of Precision and Accuracy.* Radiology, 2006. **241**(2): p. 399-406.

15. Bolbos, R., et al., *Knee cartilage thickness measurements using MRI: a 4 1/2-month longitudinal study in the meniscectomized guinea pig model of OA.* Osteoarthritis Cartilage, 2007. **15**(6): p. 656-65.

16. Bolbos, R., et al., *Measurement of knee cartilage thickness using MRI: a reproducibility study in a meniscectomized guinea pig model of osteoarthritis.* NMR in Biomedicine, 2007. EPub.

17. Eckstein, F., et al., *Accuracy of cartilage volume and thickness measurements with magnetic resonance imaging.* Clinical Orthopaedics & Related Research, 1998. **352**: p. 137-148.

18. Solloway, S., et al., *The use of active shape models for making thickness measurements of articular cartilage from MR images.* Magnetic Resonance in Medicine, 1997. **37**(6): p. 943-952.

19. Kshirsagar, A.A., et al., *Measurement of localized cartilage volume and thickness of human knee joints by computer analysis of three-dimensional magnetic resonance images.* Investigative Radiology, 1998. **33**(5): p. 289-299.

20. Kauffmann, C., et al., *Computer-aided method for quantification of cartilage thickness and volume changes using MRI: Validation method using a synthetic model.* IEEE Transactions on Biomedical Engineering, 2003. **50**: p. 978-988.

21. Stammberger, T., et al., *Interobserver reproducibility of quantitative cartilage measurements: comparison of B-spline snakes and manual segmentation.* Magnetic Resonance Imaging, 1999. **17**(7): p. 1033-1042.

22. Stammberger, T., et al., *Determination of 3D cartilage thickness data from MR imaging: computational method and reproducibility in the living.* Magnetic Resonance in Medicine, 1999. **41**(3): p. 529-536.

23. Gougoutas, A.J., et al., *Cartilage volume quantification via Live Wire segmentation.* Academic Radiology, 2004. **11**(12): p. 1389-1395.

24. Eckstein, F., et al., *Brief report: Two year longitudinal change and test--retest-precision of knee cartilage morphology in a pilot study for the osteoarthritis initiative.* Osteoarthritis and Cartilage, 2007. **15**: p. 1326-1332.

25. Eckstein, F., et al., *Quantitative Imaging of Cartilage Morphology at 3.0 Tesla in the Presence of Gadopentate Dimeglumine (Gd-DTPA).* Magnetic Resonance in Medicine, 2007. **58**: p. 402-406.

26. Eckstein, F., et al., *Impact of Coil Design on the Contrast-to-Noise Ratio, Precision, and Consistency of Quantitative Cartilage Morphology at 3 Tesla: A Pilot Study for the Osteoarthritis Initiative.* Magnetic Resonance in Medicine, 2007. **57**: p. 448-454.

27. Inglis, D., et al., *Brief report: Accuracy and test-retest precision of quantitative cartilage morphology on a 1.0T peripheral magnetic resonance imaging system.* Osteoarthritis and Cartilage, 2007. **15**: p. 110-115.

28. Folkesson, J., et al., *Segmenting articular cartilage automatically using a voxel classification approach.* IEEE Transactions on Medical Imaging, 2007. **26**(1): p. 106-115.

29. Potter, H.G. and L.F. Foo, *Magnetic Resonance Imaging of Articular Cartilage.* American Journal of Sports Medicine, 2006. **34**(4): p. 661-677.

30. Hargreaves, B.A., et al., *Comparison of New Sequences for High-Resolution Cartilage Imaging.* Magnetic Resonance in Medicine, 2003. **49**: p. 700-709.

31. Koo, S., G.E. Gold, and T.P. Andriacchi, *Considerations in measuring cartilage thickness using MRI: factors influencing reproducibility and accuracy.* Osteoarthritis and Cartilage, 2005. **13**(9): p. 782-789.

32. Kass, M., A. Witkin, and D. Terzopoulos, *Snakes: Active contour models.* International Journal of Computer Vision, 1987. **1**(4): p. 321-331.

33. Tek, H. and B.B. Kimia, *Volumetric segmentation of medical images by three-dimensional bubbles.* Computer Vision and Image Understanding, 1997. **65**(2): p. 246-258.

34. Amini, A.A., T.E. Weymouth, and R.C. Jain, *Using dynamic programming for solving variational problems in vision.* IEEE Transactions on Pattern Analysis and Machine Intelligence, 1990. **12**(9): p. 855-867.

35. Sebastian, T.B., et al., *Segmentation of carpal bones from CT images using skeletally coupled deformable models.* Medical Image Analysis, 2003. **7**(1): p. 21-45.

36. Barrett, W.A. and E.N. Mortensen, *Interactive Live-Wire Boundary Extraction.* Medical Image Analysis, 1997. **1**(4): p. 331-341.

37. Falcao, A.X., J.K. Udupa, and F.K. Miyazawa, *An ultra-fast user-steered image segmentation paradigm: live wire on the fly.* Medical Imaging, IEEE Transactions on, 2000. **19**(1): p. 55-62.

38. Song, Y., et al., *Articular cartilage MR imaging and thickness mapping of a loaded knee joint before and after meniscectomy*. Osteoarthritis and Cartilage, 2006. **14**(8): p. 728-737.

39. Wluka, A.E., et al., *How does tibial cartilage volume relate to symptoms in subjects with knee osteoarthritis?* Annals of the Rheumatic Diseases, 2004. **63**(3): p. 264-268.

40. Li, G., et al., *In vivo articular cartilage contact kinematics of the knee: an investigation using dual-orthogonal fluoroscopy and magnetic resonance image-based computer models.* American Journal of Sports Medicine, 2005. **33**(1): p. 102-107.

41. Bowers, M.E., et al., *Effects of ACL interference screws on articular cartilage volume and thickness measurements with 1.5 T and 3 T MRI.* Osteoarthritis and Cartilage, 2007. EPub.

42. Chang, M.C., F.F. Leymarie, and B.B. Kimia, *Surface Reconstruction from Point Clouds by Transforming the Medial Scaffold.* 3-D Digital Imaging and Modeling (3DIM) 2007, 2007: p. 13-20.

43. Folkesson, J., et al., *Accuracy evaluation of automatic quantification of the articular cartilage surface curvature from MRI.* Academic Radiology, 2007. **14**(10): p. 1221-8.

		Femur						Tibia	
Specimen	**Method**	**M1**	**M2**	**M3**	**L1**	**L2**	**L3**	**MT**	**LT**
Cadaver	**Manual**	**4.83**	**3.35**	**4.78**	**3.70**	**4.41**	**6.82**	**2.43**	**2.93**
	LiveWire	**3.66**	**4.72**	**3.00**	**2.73**	**2.16**	**3.48**	**2.15**	**2.23**
	Laser	**1.00**	**1.27**	**2.48**	**0.75**	**1.86**	**1.10**	**1.52**	**2.74**
Volunteer	**Manual**	**2.89**	**0.81**	**1.33**	**3.74**	**3.03**	**3.95**	**4.23**	**1.68**
	LiveWire	**1.59**	**1.48**	**5.45**	**5.80**	**3.84**	**6.43**	**2.54**	**2.08**

Table 4.1: Coefficients of variation (%) for each specimen, method, and region of interest.

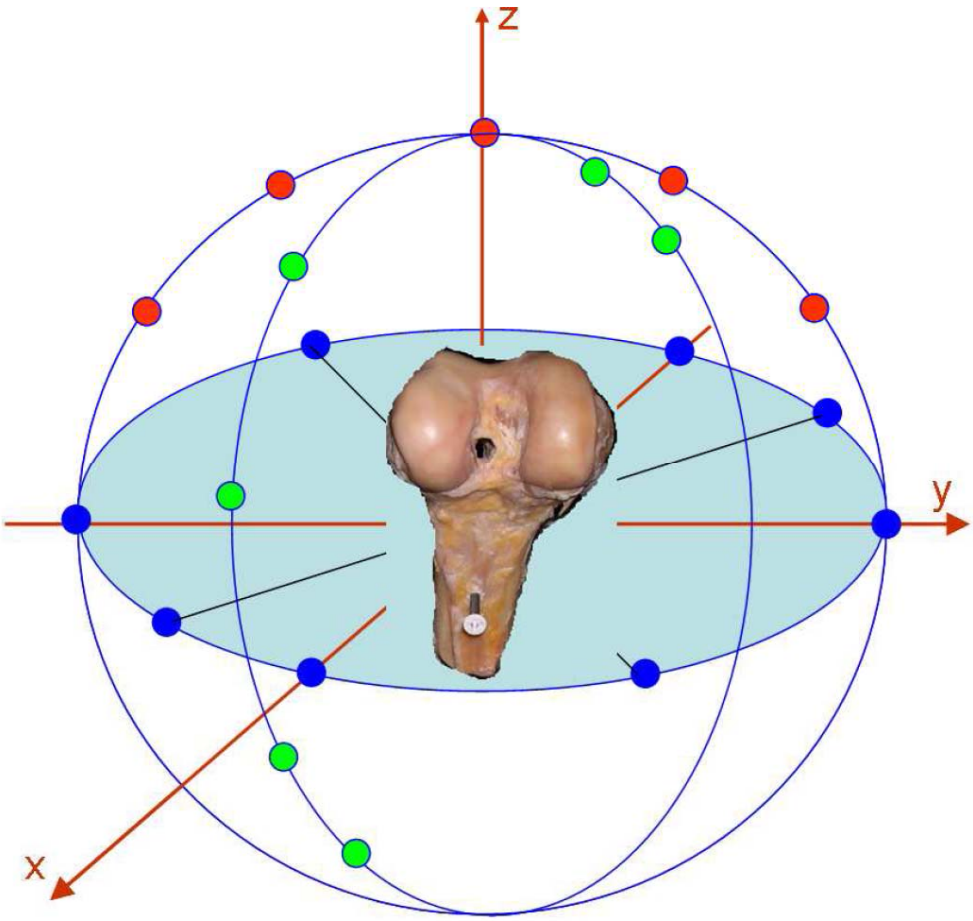

Figure 4.1: Schematic representation of the laser scanning method. Each bone, with and without articular cartilage, was scanned from twenty different views. Each view is represented as a dot in this figure. The views were then merged to create 3D models, from which a cartilage model was extracted.

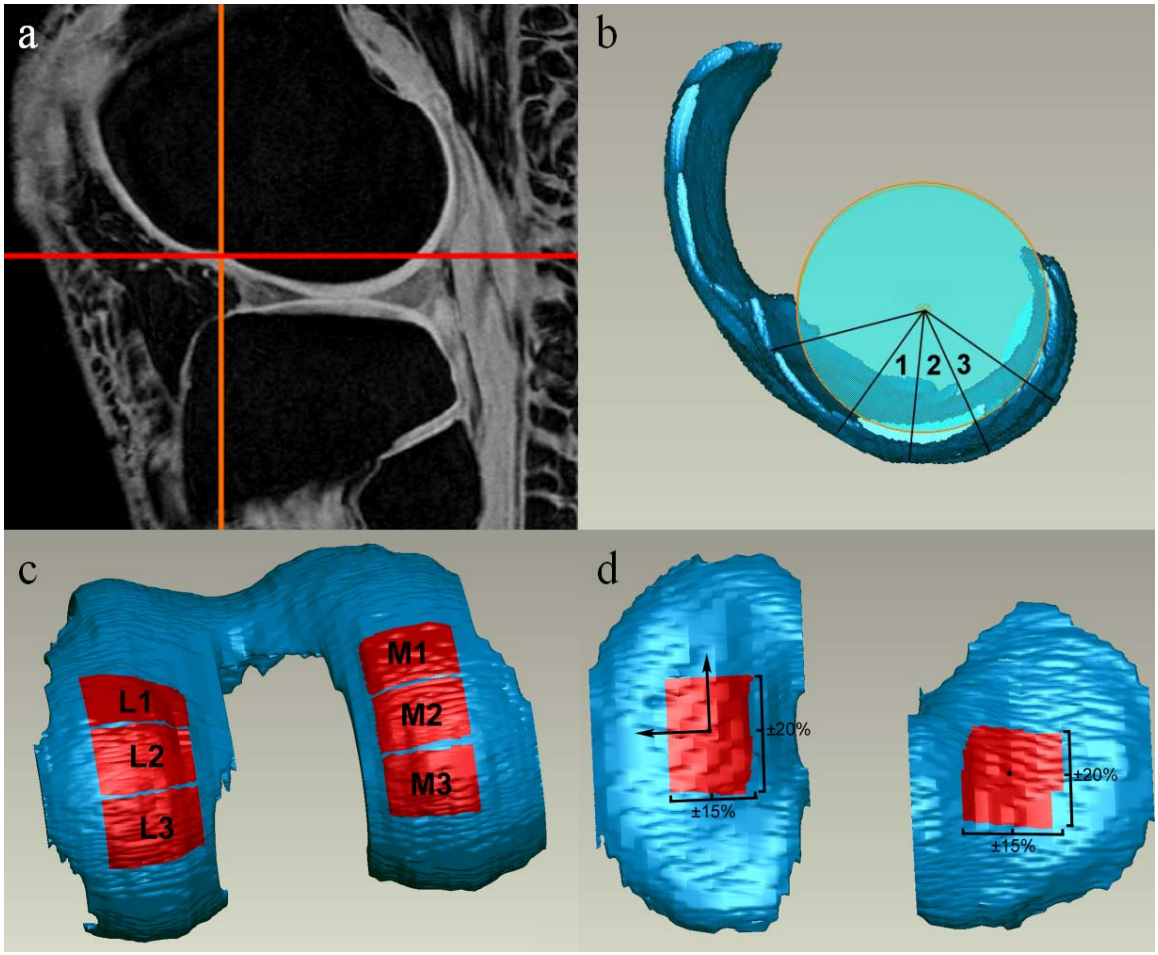

Figure 4.2: Determination of cartilage regions of interest (ROIs) for thickness measurements. ROIs were selected to represent load-bearing regions of TF articular cartilage. Portions of this figure adapted from a previous manuscript with permission [41].

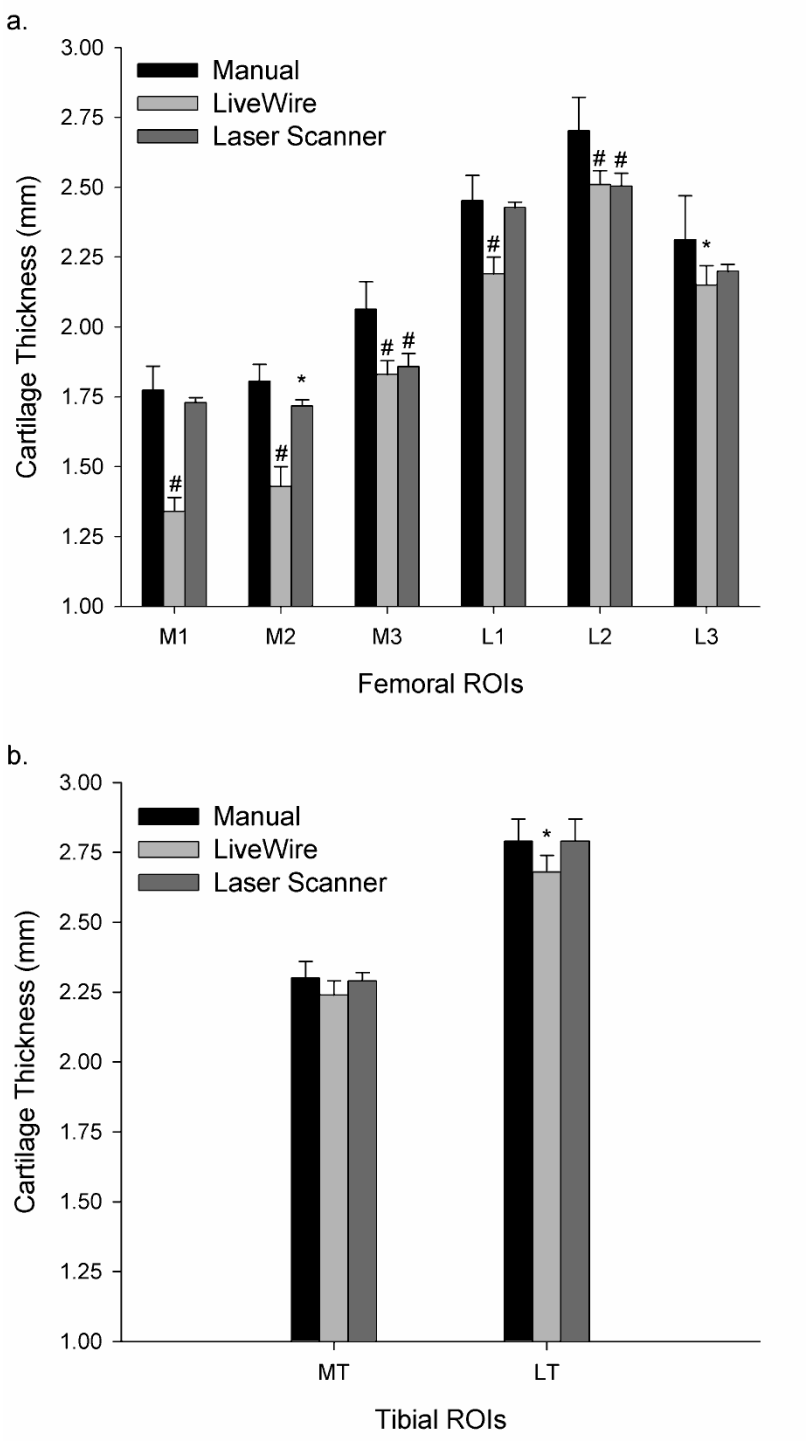

Figure 4.3: *Ex vivo* mean cartilage thickness values (mm) for (a) femoral and (b) tibial regions of interest (ROIs) assessed with each technique. Significant differences between laser scanning and manual segmentation, and between laser scanning and LiveWire, are denoted with * ($p<0.05$) and # ($p<0.01$). Significant differences between LiveWire and manual segmentation are not shown.

Chapter 5

Quantitative Magnetic Resonance Imaging Detects Changes in Meniscal Volume *in Vivo* after Partial Meniscectomy

Megan E. Bowers, Glenn A. Tung, Heidi L. Oksendahl, Michael J. Hulstyn, Paul D. Fadale, Jason T. Machan, Braden C. Fleming

The following chapter was accepted for publication in *The American Journal of Sports Medicine* (In Press).

5.1 Abstract

5.1.1 Background

Quantifying changes in meniscal volume *in vivo* before and after partial meniscectomy (PM) could help elucidate the mechanisms involved in osteoarthritis development after meniscal injury and its surgical treatment.

5.1.2 Purpose/Hypothesis

To determine whether quantitative MRI (qMRI) could detect the immediate reduction in meniscal volume created by PM, while ruling out changes in unresected structures. We hypothesized that qMRI would be reliable for determining meniscal volume within the repeated images of unresected menisci. Additionally, we expected no significant difference in volume between the uninjured menisci of the injured knees and the same menisci of the uninjured knees.

5.1.3 Methods

Ten subjects with meniscal tears were evaluated with 3T MRI before and after arthroscopic PM. Manual segmentation was used to create models of the menisci and to determine the pre- and post-operative meniscal volumes for each subject. The responsiveness and reliability of qMRI for determining meniscal volume *in vivo* were evaluated using these measurements. We expected a decrease in volume of the resected menisci, but not in the uninjured menisci, after surgery.

5.1.4 Results

The mean pre-operative volume of the injured menisci was significantly greater than the mean post-operative volume ($2896\pm277 mm^3$ vs. $2480\pm277 mm^3$; p=0.000). There was no significant difference between the mean pre- and post-operative volumes of the uninjured menisci ($2687\pm256 mm^3$ vs. $2694\pm256 mm^3$; p=1.000).

5.1.5 Conclusions

Manual segmentation demonstrated a significant reduction in the volume of the surgically resected menisci after PM, but no significant change in the volume of unresected meniscal tissue, indicating that the manual segmentation method is responsive.

5.1.6 Clinical Relevance

This approach offers a novel, reliable method to study the relationship between the volume of meniscal tissue removed during PM and subsequent patient outcomes during long-term clinical studies.

5.2 Introduction

The menisci of the knee are fibrocartilagenous load-bearing structures responsible for increasing cartilage contact area and decreasing contact stress within the tibiofemoral (TF) joint [1-6]. These structures are thought to play a role in shock absorption, joint congruity, and articular cartilage nutrition, and are essential for long-term joint function [7-9]. Meniscal injury is known to alter knee joint contact mechanics [10], and may disrupt the load-bearing capabilities of the meniscus, thereby adversely affecting articular cartilage metabolism. Meniscal injuries, therefore, may place the knee joint at risk for early osteoarthritis (OA).

Total meniscectomy, a procedure in which the entire damaged meniscus is excised, was once a standard treatment for meniscal tears, but has since been identified as a risk factor for OA [11-13]. Partial meniscectomy (PM), in which the torn portion of the meniscus is removed, while the unaffected, stable portion is left intact, is routinely performed to eliminate the painful symptoms and dysfunction that can accompany meniscal tears. While regarded as an improvement, it is unknown whether PM decreases OA risk compared with total meniscectomy [13-27].

The relationship between meniscal injury, PM, and OA is poorly understood. The effects of meniscal tears and varying degrees of PM on TF joint contact mechanics have been studied in finite element models and cadaver specimens [10, 28], but the results may differ *in vivo*, and the amount of meniscal tissue removed and subsequent OA risk remain unknown. Of particular clinical interest is whether there is a critical amount of meniscal

tissue that can be removed during PM without compromising the load-bearing, shock-dissipating, and nutritional support capabilities of the meniscus. While the amount of meniscus removed during surgery may not be the only factor associated with the outcome of PM, it almost certainly plays a significant role. Tracking these patients may help determine the existence of such a threshold. These data could help surgeons predict OA risk after PM, and may help determine when the procedure is the best treatment option for meniscal tears, and when alternative treatments should be considered. Such studies necessitate a quantitative method that can reliably assess changes in meniscal volume and dimensions *in vivo* with sufficient accuracy to track changes in patients over time.

Quantitative magnetic resonance imaging (qMRI) has been used to assess morphological changes in knee articular cartilage [29-36], and to estimate meniscus allograft size [37]. Our group recently validated a qMRI approach for evaluating meniscal volume *ex vivo* using phantom and cadaver models [38]. However, in order for this method to be applied in long-term clinical studies, it must first be validated *in vivo*.

The purpose of this study was to assess the responsiveness of qMRI for determining meniscal volume *in vivo* before and after PM in subjects with unilateral meniscal tears. The main focus was to determine whether qMRI could detect the immediate reduction in meniscal volume created by partial resection, while simultaneously ruling out changes in unresected structures. Ten subjects participated; their injured and uninjured knees were imaged before and after PM. The specific aims were: (1) to determine whether qMRI could detect a decrease in the volume of surgically resected menisci *in vivo* following partial resection; (2) to determine the reliability of the method for quantifying meniscal volume *in vivo* by repeated imaging of the uninjured

menisci; and (3) to determine whether the volume of the contralateral uninjured meniscus could be used to estimate the pre-injury volume of the injured meniscus. We hypothesized that there would be a decrease in the volume of the resected menisci, but not in the uninjured menisci, after surgery (Hypothesis 1). We also expected the qMRI method to be reliable for determining meniscal volume within the repeated images of the unresected menisci (Hypothesis 2). Additionally, we expected no significant difference in pre-operative volume between the menisci of the injured knees and the same menisci of the contralateral knees (Hypothesis 3).

5.3 Materials and Methods

5.3.1 Subjects

Study approval was granted by the Institutional Review Boards of Brown University and Rhode Island Hospital prior to subject recruitment. Male and female subjects between the ages of 18 and 50 years who were candidates for arthroscopic PM were eligible for inclusion in the study. Subjects whose injury had occurred more than 12 months before surgery, those with a prior knee injury for which they sought medical attention, or with diseases predisposing them to cartilage damage were excluded from the study. The subjects represented a consecutive sample of those eligible and willing to participate, whose MRIs could be scheduled prior to surgery. No participating subjects were excluded after surgery for any reason.

Ten subjects (9 males, 1 female) with a mean age of 36.2 years (range 22-48 years) were included. The causes of injury varied among subjects. Five subjects underwent unilateral partial medial meniscectomy, 4 subjects underwent unilateral partial lateral meniscectomy, and 1 subject underwent both medial and lateral PM within the same knee.

5.3.2 MR Imaging

MR imaging was performed on both knees of each subject, an average of 11.5 days (range 2 – 44 days) before and 27.2 days (range 14 – 46 days) after surgery; the time between pre- and post-operative MRI assessments averaged 39.7 days (range 18 – 71

days). Each knee was imaged on a 3T MR imaging system (Siemens Trio, Erlangen, Germany), using a commercially available circular polarized knee coil. The medial and lateral menisci of each knee were imaged using the T2*-weighted, 3D-CISS sequence **(Figure 5.1)** [Constructive Interference in the Steady State; TR/TE/FA: 12.5/6.3/35^{o}; FOV: 160mm; matrix: 512x512; in-plane resolution/slice thickness/interslice gap: 0.3125/1.0/0mm; bandwidth: 130 Hz/pixel; averages: 1; acquisition time: 13 minutes, 36 seconds] at both time points [38].

5.3.3 Manual Segmentation

The menisci of each scan were independently segmented in both the sagittal and coronal planes by a single experienced examiner (M.E.B.) using commercial software (Mimics 9.11, Materialise, Ann Arbor, MI). Each subject's scans were segmented consecutively, but the examiner was blinded to operative status and patient information. Because the segmentation process is binary, the external contour of each meniscus was segmented without noting any degenerative signal within the meniscal tissue. Once segmented, the menisci were reconstructed, and a 3D voxel model of each structure was created. Each voxel model was wrapped with a triangular mesh to create a virtual solid model [33-34, 38]. Each virtual model captured both the volume and morphology of each meniscus **(Figure 5.2)**.

5.3.4 Meniscal Volume

Once a virtual solid model of each meniscus was created from manual segmentation, the volume of each model was determined by surface integration [38]. The

volumes of the right medial, right lateral, left medial, and left lateral menisci of each subject were recorded both before and after PM. The pre- and post-operative volumes of the surgically resected menisci were compared to demonstrate that the method could detect the change in volume of the meniscus following PM (Aim 1; **Figure 5.3a**). The pre- and post-operative images of the menisci that were not treated surgically were used to establish the repeatability of the technique (Aim 2; **Figure 5.3a**). Additionally, the pre-operative volumes of the injured and uninjured menisci were compared in order to demonstrate that the volume of the contralateral uninjured meniscus could be used to estimate the pre-injury volume of the injured meniscus (Aim 3; **Figure 5.3b**).

5.3.5 Statistical Analysis

Meniscal volumes were compared using mixed linear modeling. Within-subject, within-knee, and within-meniscus correlations were accounted for by including random effects for the intercept and a term for the interaction of these factors. Additionally, repeated measurements of the same meniscus were modeled with correlated error. A variance components variance-covariance structure was used for both random and repeated effects. Orthogonal contrast statements were used to test the hypotheses associated with each specific aim. P-values for multiple comparisons were adjusted using the Holm test (sequential Bonferroni). The test-retest reliabilities of uninjured meniscal volumes were estimated based on the intraclass correlation coefficient (ICC) for a fixed set of ratings. Statistical analyses were carried out in *SAS* (Version 9.1.3, Service Pack 4; SAS Institute, Cary, NC). Meniscal volumes were normally distributed.

A post-hoc power analysis was conducted to estimate the smallest changes detectable (2-tailed alpha = 0.05) with 10 subjects at powers of 80, 90, and 95% in the uninjured compartments **(Table 5.1)**. This analysis was informed by the standard deviations and the correlations between the pre- and post-operative measurements of the menisci. The detectable changes can be interpreted as the size of changes at or above that which could be effectively ruled out with probabilities 80, 90, and 95%.

5.4 Results

The pre-operative volumes of the injured medial and lateral menisci were significantly greater than the post-operative volumes (adjusted p=0.000 for both; **Figure 5.4**). The post-operative volumes of the injured medial and lateral menisci were a mean of 16.8% and 12.1% less, respectively, than the pre-operative volumes of those menisci (Hypothesis 1).

There was no statistically significant difference between the pre- and post-operative volumes of the uninjured menisci in the operated knees (adjusted p=1.000; **Figure 5.4**). Similarly, there was no significant difference between the pre- and post-operative volumes of the menisci of the contralateral uninjured knees (adjusted p=1.000; **Figure 5.4**). The post-operative volumes of the uninjured menisci differed by a mean of 0.83% from the pre-operative volumes of the uninjured menisci (Hypothesis 2). The ICCs for the uninjured medial and lateral menisci were 0.91 and 0.93, respectively (Hypothesis 2).

There was also no statistically significant difference between the pre-operative volumes of the uninjured medial menisci of the injured knees and the medial menisci of the uninjured knees (mean difference of 13.8%; adjusted p=1.000). The same result was seen for the pre-operative volumes of the uninjured lateral menisci (mean difference of 7.4%; adjusted p=1.000). Additionally, there was no statistically significant difference between the pre-operative volumes of the injured medial menisci and the medial menisci of the uninjured knees (mean difference of 0.6%; adjusted p=0.963). The same result was

seen for the pre-operative volumes of the injured lateral menisci and the lateral menisci of the uninjured knees (mean difference of 18.4%; adjusted p=1.000). Complete results are seen in Table 5.2 (Hypothesis 3).

5.5 Discussion

Although meniscal injury and PM have been correlated with early OA [11, 13, 15, 18, 20-21, 24, 39-46], to date, a cause-effect relationship between these has not been established. An accurate, reliable method that can quantify changes in meniscal volume and dimensions *in vivo* would allow PM patients to be tracked over time, thereby helping to elucidate the mechanisms involved in early OA development. Such a method could also be used to size meniscal allografts. The method proposed in this study would provide a valuable tool for both applications.

By showing statistically significant reductions in the volume of the resected menisci after surgery, the present study demonstrates that qMRI is sensitive enough to detect the surgical removal of meniscal tissue. The measured volume reduction was not a product of bias, since no reduction was detected in the volumes of the uninjured menisci, despite 95% power to detect changes in volume of 97mm^3. These results suggest that the described MR-based imaging and segmentation method is a responsive and reliable tool for determining a change in meniscal volume *in vivo* after PM. This quantitative method may be useful in future long-term studies designed to evaluate the outcome of meniscal injury and PM.

It is possible that a loss of meniscal volume at the time of injury may affect the pre-operative meniscal volumes indicated by our segmentation method. Preliminary data have shown that it is possible to use the volume of the contralateral, uninjured meniscus to estimate the pre-injury volume of an injured meniscus if necessary [38]. In the present

study (Aim 3), the mean pre-operative volumes of the uninjured medial and lateral menisci within the injured knees differed from the mean volumes of the same menisci within the uninjured knees by 13.8% and 7.4%, respectively. Additionally, the mean pre-operative volumes of the injured medial and lateral menisci differed from the mean volumes of the same menisci within the uninjured knees by 0.6% and 18.4%, respectively. It is likely that the lateral menisci that underwent partial resection were more damaged during injury, contributing to the higher percent difference between these menisci and their uninjured counterparts. These differences were not statistically significant, and further suggest that contralateral menisci may be useful to estimate the pre-injury volumes of injured menisci, particularly when an injured meniscus is badly damaged.

Because the relationships between meniscal injury, PM, and OA are not well understood, it is possible that the volume of meniscal tissue removed during surgery may not be as meaningful as the location from which it is removed, and the status of the outer rim of the meniscus. The 3D voxel models created from our manual segmentation procedure capture both volume and morphology, so it will be possible to use these models to assess not only the volume of meniscal tissue removed during surgery, but also the location from which it is removed and the status of the meniscal rim.

Stone et al. used a similar MR-based approach to size meniscal allografts [37]. The technique involved the segmentation of 1.5T MR images in the sagittal plane. MR-based meniscal volumes were compared to water displacement volumes to determine accuracy. Stone et al. reported the water displacement volumes to be approximately 2500mm^3, which align well with the meniscal volumes estimated in the present study.

While precise, their MR-based measurements consistently underestimated actual meniscal volumes by 20 and 44% for the medial and lateral menisci, respectively. In contrast, our group recently completed an *ex vivo* evaluation of the meniscal segmentation approach described in the present study [38]. By segmenting 3T MR images in both the sagittal and coronal planes, we were able to create 3D virtual models of cadaver menisci. We then compared the volumes of these models to water displacement-based volumes of the same menisci, excised from the cadaver knee. We noted coefficients of variation of less than 4% for both medial and lateral menisci, and MR-based volumes that were within 5% of water displacement volumes, indicating the technique was both reliable and accurate *ex vivo*. The responsiveness of this method for measuring meniscal volume has been further confirmed *in vivo* by the present study, wherein pre- and post-operative volumes of the uninjured menisci across subjects showed a difference of only 0.83% (range 0.16-1.57%), while the volumes of the injured menisci showed a difference of 14.4% (range 12.1-16.8%) before and after PM. An *in vivo* assessment was necessary to account for the errors introduced by motion and blood flow artifacts, which were found to be negligible in the present study.

There are several limitations associated with the present study. First, the number of subjects studied was relatively small (n=10). However, we were able to detect statistically significant decreases in meniscal volume after surgery in the treated menisci with this sample size, while simultaneously ruling out changes in the control menisci. Our post-hoc power analysis suggests that with 10 subjects, the study was adequately powered to detect changes in meniscal volume **(Table 5.1)**. Additionally, the purpose of

this study was to validate the described MR-based segmentation method *in vivo* so that the method can be used in the design of future long-term clinical studies.

Second, the design of this study did not allow for any direct accuracy assessment of meniscal volume. The nature of the arthroscopic PM procedure did not allow us to measure the amount of meniscal tissue removed from each subject's knee during surgery. Attempts were made to filter each piece of tissue removed during preliminary studies, but because each arthroscopy involved some shaving and debridement of the injured meniscus, measurement was not feasible. However, our group has conducted studies using phantom and cadaver models to assess the accuracy and reliability of our meniscal segmentation technique *ex vivo* [38]. In future studies, it may prove useful to study accuracy by taking intra-operative measurements of the resected menisci, and comparing those to dimensions of the 3D voxel models created by our segmentation method.

Despite these limitations, the results of the present study, particularly when combined with the *ex vivo* work evaluating the accuracy of the method [38], indicate that MR-based segmentation is a responsive and reliable method for evaluating meniscal volume *in vivo* before and after PM. This method can be applied in future long-term studies of the outcomes of PM, which may begin to elucidate the mechanisms that drive the relationship between meniscal injury, PM, and early OA.

5.6 Acknowledgements

This project was funded by the National Institutes of Health (AR047910; AR047910S1). The authors wish to thank Benjamin B. Kimia, Ph.D., Joseph J. Crisco, Ph.D., Nhon H. Trinh, M.S., and Evan L. Leventhal, B.S., for their technical assistance.

5.7 References

1. Ahmed, A.M. and D.L. Burke, *In-vitro measurement of static pressure distribution in synovial joints - Part I: Tibial surface of the knee.* J Biomech Engin, 1983. **105**: p. 216-225.
2. Haut Donahue, T.L., et al., *A finite element model of the human knee joint for the study of tibio-femoral contact.* Journal of Biomechanical Engineering, 2002. **124**(3): p. 273-280.
3. McKinley, T.O., D.K. English, and B.K. Bay, *Trabecular bone strain changes resulting from partial and complete meniscectomy.* Clinical Orthopaedics and Related Research, 2003. **407**: p. 259-267.
4. Pena, E., et al., *Finite element analysis of the effect of meniscal tears and meniscectomies on human knee biomechanics.* Clinical Biomechanics, 2005. **20**(5): p. 498-507.
5. Sekaran, S.V., M.L. Hull, and S.M. Howell, *Nonanatomic location of the posterior horn of a medial meniscal autograft implanted in a cadaveric knee adversely affects the pressure distribution on the tibial plateau.* American Journal of Sports Medicine, 2002. **30**(1): p. 74-82.
6. Wilson, W., et al., *Pathways of load-induced cartilage damage causing cartilage degeneration in the knee after meniscectomy.* Journal of Biomechanics, 2003. **36**(6): p. 845-851.

7. Fukuda, Y., et al., *Impact load transmission of the knee joint-influence of leg alignment and the role of meniscus and articular cartilage.* Clinical Biomechanics, 2000. **15**(7): p. 516-521.

8. Voloshin, A.S. and J. Wosk, *Shock absorption of meniscectomized and painful knees.* Journal of Biomedical Engineering, 1985. **5:**: p. 157-161.

9. Arnoczky, S.P. and C.A. McDevitt, *The meniscus: Structure, Function, Repair, and Replacement*, in *Orthopaedic Basic Science*, J.A. Buckwalter, Editor. 2000, American Academy of Orthopaedic Surgeons: Illinois. p. 532-545.

10. Lee, S.J., et al., *Tibiofemoral contact mechanics after serial medial meniscectomies in the human cadaveric knee.* Am J Sports Med, 2006. **34**(8): p. 1334-44.

11. Englund, M. and L.S. Lohmander, *Risk factors for symptomatic knee osteoarthritis fifteen to twenty-two years after meniscectomy.* Arthritis & Rheumatism, 2004. **50**(9): p. 2811-2819.

12. McNicholas, M.J., et al., *Total meniscectomy in adolescence: a thirty year follow-up.* Journal of Bone and Joint Surgery - British Volume, 2000. **82**: p. 217 - 221.

13. Roos, H., et al., *Knee osteoarthritis after meniscectomy: prevalence of radiographic changes after twenty-one years, compared with matched controls.* Arthritis Rheum, 1998. **41**(4): p. 687-93.

14. Andersson, C. and J. Gillquist, *Instrumented testing for evaluation of sagittal plane laxity.* Clinical Orthopaedics and Related Research, 1990. **256**: p. 178-184.

15. Andersson-Molina, H., H. Karlsson, and P. Rockborn, *Arthroscopic partial and total meniscectomy: A long-term follow-up study with matched controls.* Arthroscopy, 2002. **18**(2): p. 183-189.

16. Chatain, F., et al., *A comparative study of medial versus lateral arthroscopic meniscectomy on stable knees. 10-year minimum follow-up.* Arthroscopy, 2003. **19**(8): p. 842-849.

17. Chatain, F., et al., *The natural history of the knee following arthroscopic medial meniscectomy.* Knee Surgery, Sports Traumatology, Arthroscopy, 2001. **9**(1): p. 15-18.

18. Cicuttini, F.M., et al., *Rate of knee cartilage loss after partial meniscectomy.* Journal of Rheumatology, 2002. **29**(9): p. 1954-1956.

19. Englund, M., E.M. Roos, and L.S. Lohmander, *Impact of type of meniscal tear on radiographic and symptomatic knee osteoarthritis: A sixteen-year followup of meniscectomy with matched controls.* Arthritis and Rheumatism, 2003. **48**(8): p. 2178-2187.

20. Englund, M., et al., *Patient-relevant outcomes fourteen years after meniscectomy: Influence of type of meniscal tear and size of resection.* Rheumatology, 2001. **40**: p. 631-639.

21. Higuchi, H., et al., *Factors affecting long-term results after arthroscopic partial meniscectomy.* Clinical Orthopaedics and Related Research, 2000. **377**: p. 161-168.

22. Hoser, C., et al., *Long-term results of arthroscopic partial lateral meniscectomy in knees without associated damage.* Journal of Bone and Joint Surgery. British Volume, 2001. **83**(4): p. 513-516.

23. Hulet, C.H., et al., *Arthroscopic medial meniscectomy on stale knees - A 12-year follow-up.* Journal of Bone and Joint Surgery. British Volume, 2001. **83**(1): p. 29-32.

24. Rangger, C., et al., *Osteoarthritis after arthroscopic partial meniscectomy.* American Journal of Sports Medicine, 1995. **23**(2): p. 240-4.

25. Rockborn, P. and K. Messner, *Long term results of meniscus repair and meniscectomy: a 13-year functional and radiographic follow-up study.* Knee Surgery, Sports Traumatology, Arthroscopy, 2000. **8**: p. 2-9.

26. Roos, E.M., et al., *Long-term outcome of meniscectomy: symptoms, function, and performance tests in patients with or without radiographic osteoarthritis compared to matched controls.* Osteoarthritis Cartilage, 2001. **9**(4): p. 316-324.

27. Roos, H., et al., *Osteoarthritis of the knee after injury to the anterior cruciate ligament or meniscus: The influence of time and age.* Osteoarthritis Cartilage, 1995. **3**(4): p. 261-7.

28. Zielinska, B. and T.L.H. Donahue, *3D finite element model of meniscectomy: changes in joint contact behavior.* Journal of Biomechanical Engineering, 2006. **128**: p. 115-123.

29. Eckstein, F. and C. Glaser, *Measuring cartilage morphology with quantitative magnetic resonance imaging.* Seminars in Musculoskeletal Radiology, 2004. **8**(4): p. 329-353.

30. Eckstein, F., *Noninvasive study of human cartilage structure by MRI.* Methods in Molecular Medicine, 2004. **101**: p. 191-218.

31. Burstein, D. and M. Gray, *New MRI techniques for imaging cartilage.* J Bone Joint Surg Am, 2003. **85**(Suppl 2): p. 70-77.

32. Gray, M.L., et al., *Toward imaging biomarkers for osteoarthritis.* Clinical Orthopaedics and Related Research, 2004. **427**(Suppl): p. S175-S181.

33. Bowers, M.E., et al., *Quantitative MR Imaging using "LiveWire" to Measure Tibiofemoral Articular Cartilage Thickness.* Osteoarthritis Cartilage, 2008. **16**: p. 1167-1173.

34. Bowers, M.E., et al., *Effects of ACL interference screws on articular cartilage volume and thickness measurements with 1.5 T and 3 T MRI.* Osteoarthritis Cartilage, 2008. **16**: p. 572-578.

35. Andriacchi, T.P., et al., *Rotational Changes at the Knee after ACL Injury Cause Cartilage Thinning.* Clin Orthop Relat Res, 2006. **442**: p. 39-44.

36. Koo, S., G.E. Gold, and T.P. Andriacchi, *Considerations in measuring cartilage thickness using MRI: factors influencing reproducibility and accuracy.* Osteoarthritis and Cartilage, 2005. **13**(9): p. 782-789.

37. Stone, K.R., et al., *3D MRI volume sizing of knee meniscus cartilage.* Arthroscopy, 1994. **10**(6): p. 641-644.

38. Bowers, M.E., et al., *Quantification of meniscal volume by segmentation of 3T magnetic resonance images.* J Biomech, 2007. **40**(12): p. 2811-2815.

39. Englund, M., *Meniscal tear - a feature of osteoarthritis.* Acta Orthopaedica Scandinavica, 2004. **75**(Suppl 312): p. 8-45.

40. Englund, M. and L.S. Lohmander, *Patellofemoral osteoarthritis coexistent with tibiofemoral osteoarthritis in a meniscectomy population.* Ann Rheum Dis, 2005. **64**(12): p. 1721-6.

41. Englund, M., P.T. Paradowski, and L.S. Lohmander, *Association of radiographic hand osteoarthritis with radiographic knee osteoarthritis after meniscectomy.* Arthritis & Rheumatism, 2004. **50**(2): p. 469-475.

42. Fairbank, T.J., *Knee joint changes after meniscectomy.* Journal of Bone and Joint Surgery. British Volume, 1948. **30**: p. 664-670.

43. Allen, P.R., R.A. Denham, and A.V. Swan, *Late degenerative changes after meniscectomy. Factors affecting the knee after operation.* J Bone Joint Surg Br, 1984. **66**(5): p. 666-71.

44. Benedetto, K.P. and C. Rangger, *Arthroscopic partial meniscectomy: 5-year follow-up.* Knee Surg Sports Traumatol Arthrosc, 1993. **1**(3-4): p. 235-8.

45. Neyret, P., S.T. Donell, and H. Dejour, *Osteoarthritis of the knee following meniscectomy.* British Journal of Rheumatology, 1994. **33**: p. 267-268.

46. Rangger, C., et al., *Partial Meniscectomy and Osteoarthrits: Implications for Treatment of Athletes.* Sports Med, 1997. **23**(1): p. 61-68.

Leg	Meniscus	Compartment Status	Detectable Change (mm^3)		
			80%	90%	95%
Injured	Lateral	Uninjured	71	82	92
Injured	Medial	Uninjured	6	6	7
Uninjured	Lateral	Uninjured	110	127	143
Uninjured	Medial	Uninjured	113	130	146

Table 5.1: Detectable changes in meniscal volume at power as a function of location.

Leg	Meniscus	Compartment Status	Mean (SE) Pre-op Volume (mm^3)	Percent Difference
Injured	Medial	Uninjured	3268 (324)	13.8%
Uninjured	Medial	Uninjured	2817 (205)	
Injured	Lateral	Uninjured	2249 (290)	7.4%
Uninjured	Lateral	Uninjured	2415 (205)	
Injured	Medial	Injured	2833 (265)	0.6%
Uninjured	Medial	Uninjured	2817 (205)	
Injured	Lateral	Injured	2958 (290)	18.4%
Uninjured	Lateral	Uninjured	2415 (205)	

Table 5.2: Pre-operative least squares mean meniscal volumes (mm^3) and their least squares standard errors (SE) as a function of leg (injured vs. uninjured), meniscus (medial vs. lateral), and compartment status (injured vs. uninjured). Direct comparisons were made between the injured and uninjured leg for each group of menisci by calculating the percent difference.

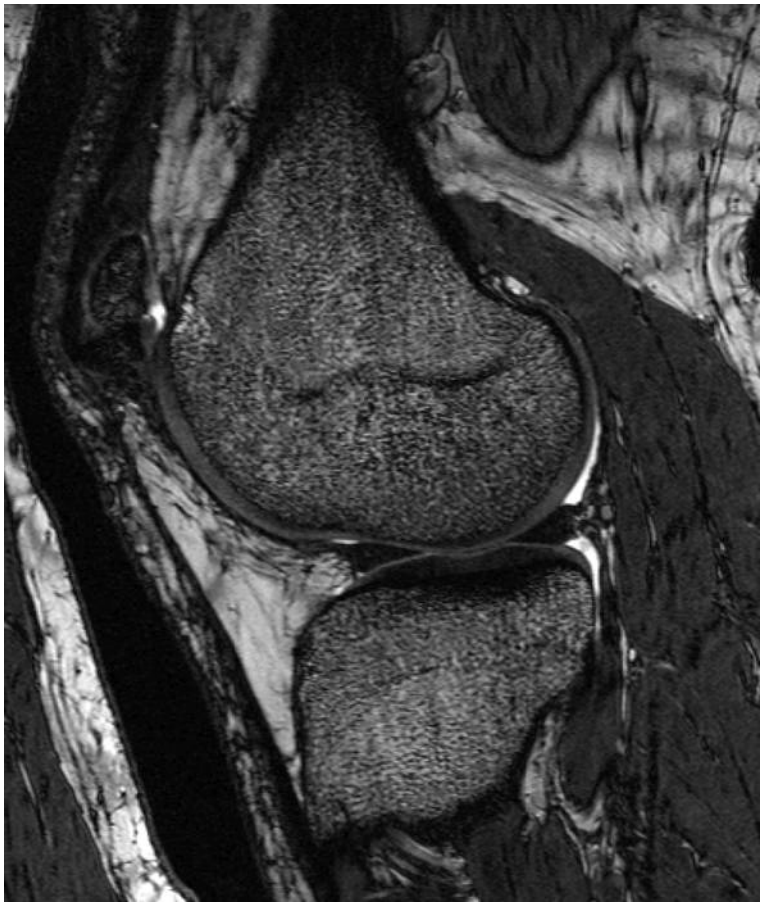

Figure 5.1: Sagittal view of a knee imaged with the Constructive Interference in the Steady State (CISS) sequence, from which the menisci were segmented.

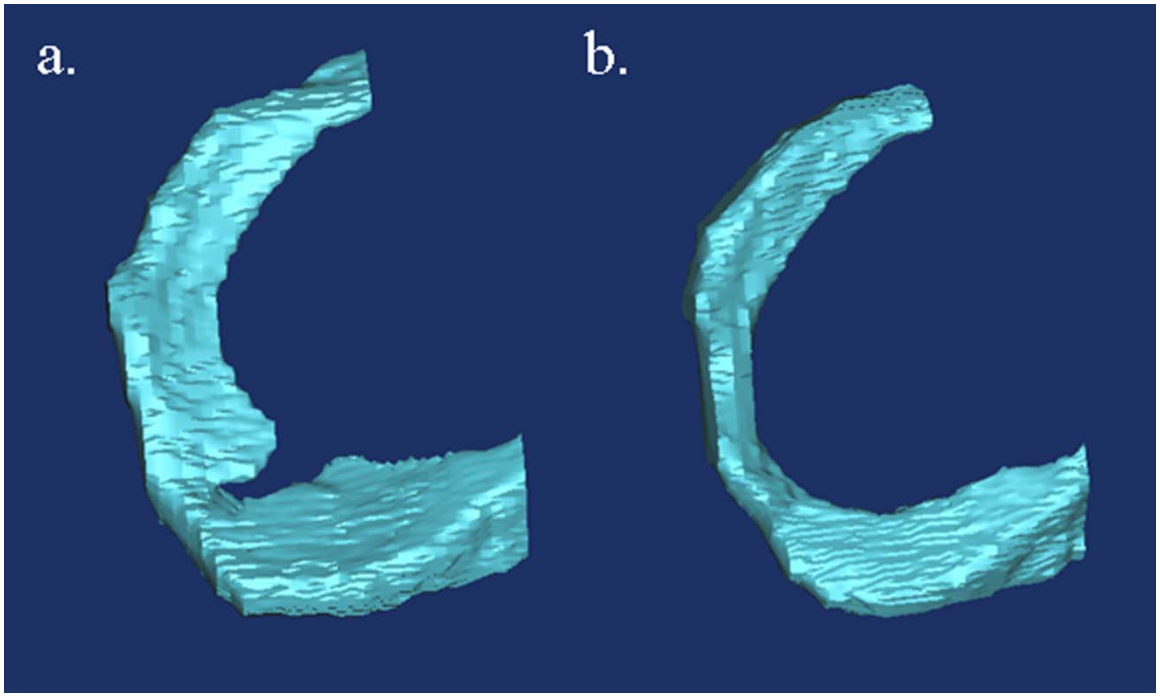

Figure 5.2: MR-based 3D models of a subject's medial meniscus with a radial tear in the posterior region (a) before and (b) after partial meniscectomy. The virtual 3D models created in this study captured both volume and morphology of the menisci.

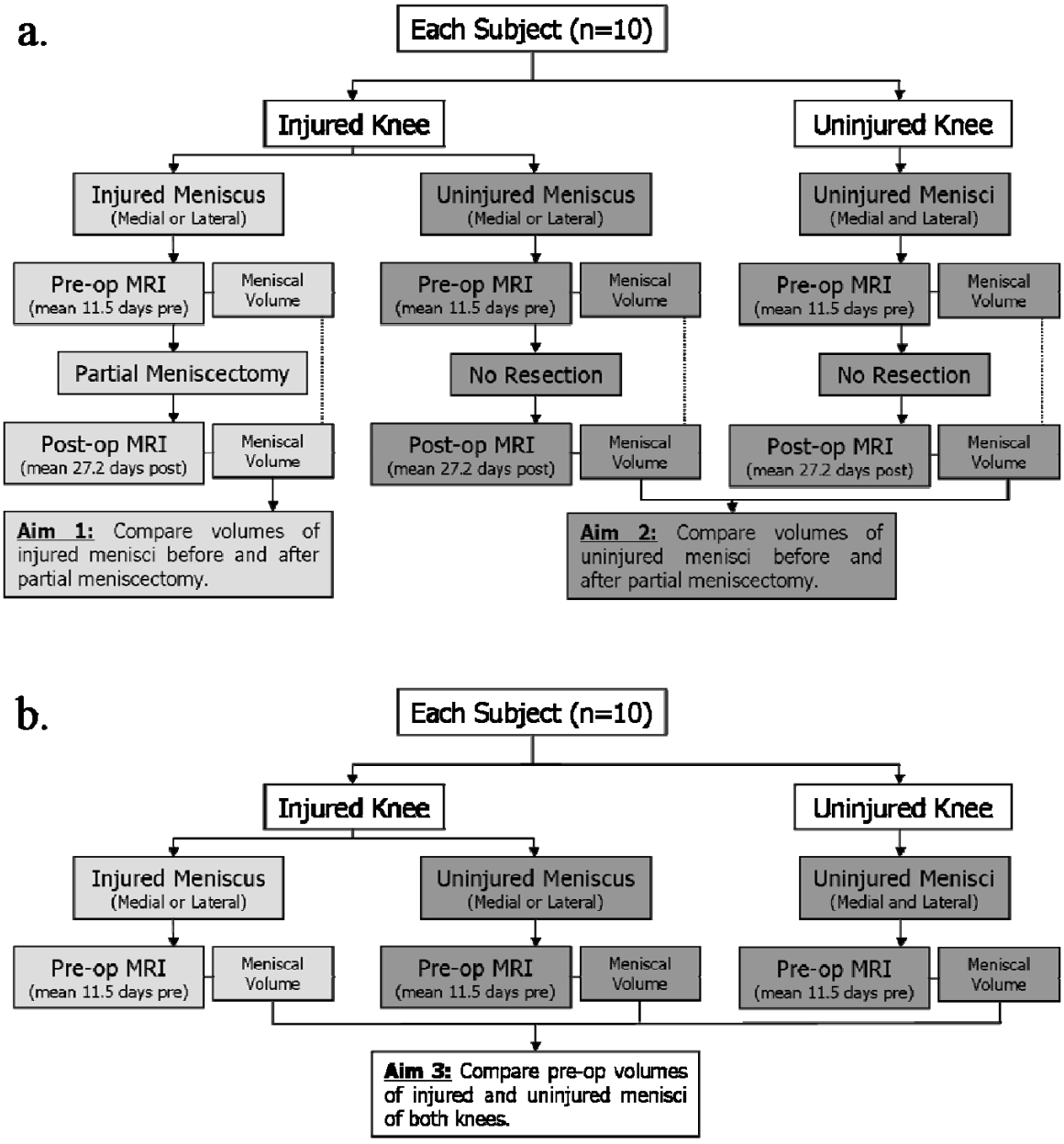

Figure 5.3: Flow charts depicting the use of data gathered from each subject. Each subject had one injured and one uninjured knee, both of which underwent MRI before and after the injured knee underwent arthroscopic partial meniscectomy. (a.) Aims 1 and 2 compared the volumes of the injured and uninjured menisci, respectively, before and after partial meniscectomy. (b.) Aim 3 compared the pre-operative volumes of the injured and uninjured menisci.

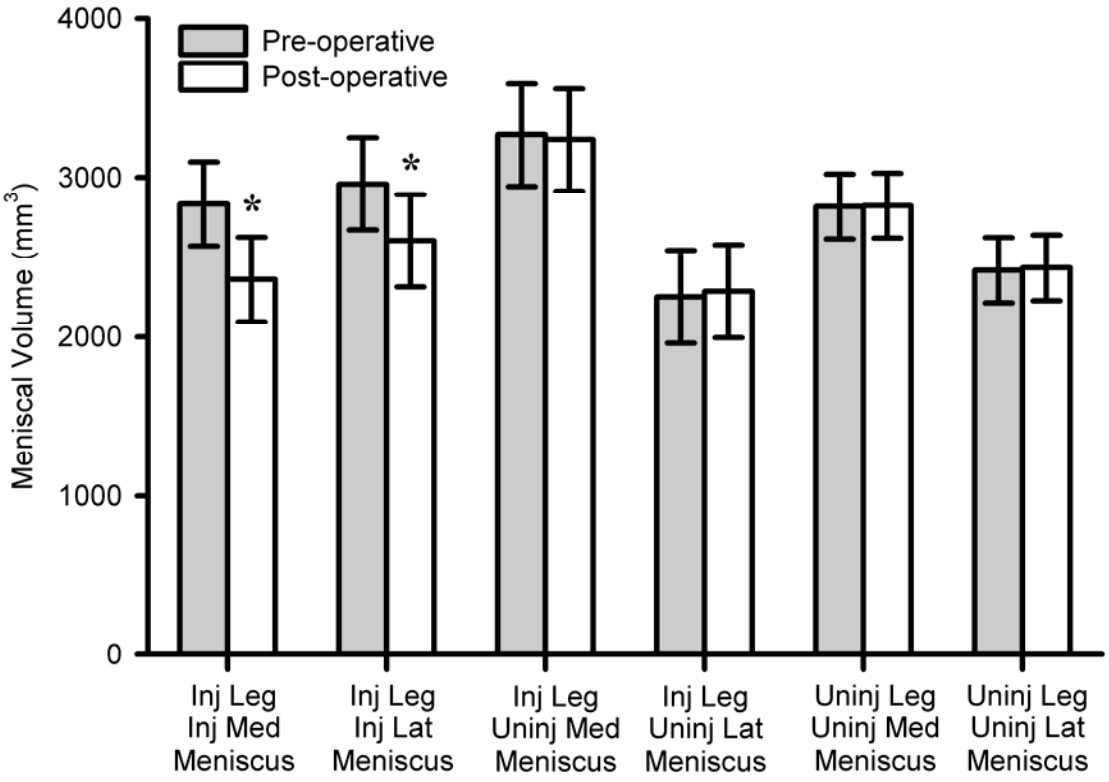

Figure 5.4: Least squares mean volumes (mm^3) of the menisci of the injured (left 4 sets of columns) and uninjured (right 2 sets of columns) legs, before and after arthroscopic partial meniscectomy. Labels "Inj," "Uninj," "Lat," and "Med" denote Injured, Uninjured, Lateral, and Medial, respectively. * denotes adjusted p=0.000. Error bars indicate ± standard errors.

Chapter 6

Quantitative Magnetic Resonance Imaging Can Reliably Determine Tibiofemoral Articular Cartilage Thickness *in Vivo*

Megan E. Bowers, Glenn A. Tung, Heidi L. Oksendahl, Michael J. Hulstyn, Paul D. Fadale, Jason T. Machan, Braden C. Fleming

The following chapter is in preparation for submission to *Journal of Biomechanics*.

6.1 Abstract

Quantifying changes in articular cartilage (AC) thickness *in vivo* may help elucidate the mechanisms involved in the development of osteoarthritis after knee injury. The objective of this study was to validate quantitative MRI (qMRI) as a means for measuring AC thickness *in vivo* before and after partial meniscectomy (PM). We expected no change in AC thickness over the 1-month study interval.

Ten subjects with acute meniscal tears were evaluated with 3T MRI before and after arthroscopic PM. Manual segmentation was used to determine AC thickness for each subject before and after surgery. The reliability of qMRI for measuring AC thickness was evaluated *in vivo*. There was no significant difference between the pre- and post-operative thickness of any AC region ($p=1.00$).

Manual segmentation demonstrated no significant change in the volume of AC thickness. This approach offers a novel method to study the relationship between knee injury, its surgical treatment, and subsequent changes in AC thickness during long-term clinical studies.

6.2 Introduction

Osteoarthritis (OA) of the tibiofemoral (TF) joint is marked by distinct changes in articular cartilage (AC) volume and thickness [1-13]. *In vivo* methods that accurately track these initial changes are crucial for documenting the onset and progression of OA. Quantitative magnetic resonance imaging (qMRI) has shown promise for assessing changes in cartilage morphometry, and may prove to be a valuable measure for OA progression [2, 7, 9, 14-16].

Meniscal injuries, which are common, are thought to place the knee joint at risk for early OA. However, the relationship between meniscal injury and OA is poorly understood. Of particular clinical interest is whether there is a critical amount of meniscal tissue that can be removed during arthroscopic partial meniscectomy (PM) without compromising the load-bearing, shock-dissipating, and nutritional support capabilities of the meniscus, thereby affecting AC function. Tracking cartilage changes in PM patients may help determine the existence of such a threshold. These data could help surgeons predict OA risk after PM, and may help determine when the procedure is the best treatment option for meniscal tears, and when alternative treatments should be considered. Such studies necessitate a quantitative method that can reliably assess changes in meniscal volume and dimensions *in vivo* with sufficient accuracy to track changes in patients over time.

Quantitative magnetic resonance imaging (qMRI) has been used to assess morphological changes in knee articular cartilage [17-24]. Our group recently validated a

qMRI approach for evaluating articular cartilage thickness *ex vivo* using phantom and cadaver models [21-22]. However, in order for this method to be applied in long-term clinical studies, it must first be validated *in vivo*.

The purpose of this study was to assess the validity of qMRI for determining AC thickness *in vivo* before and after PM in subjects with unilateral acute meniscal tears. Subjects undergoing PM were chosen primarily because they offered the opportunity for repeated MR imaging. Ten subjects participated; their injured and uninjured knees were imaged before and after PM. Our specific aim was to determine the reliability of our segmentation method for quantifying TF AC thickness *in vivo* in specific load-bearing regions. We expected qMRI to be reliable for determining AC thickness *in vivo*.

6.3 Materials and Methods

6.3.1 Subjects

Study approval was granted by the Institutional Review Boards of Brown University and Rhode Island Hospital prior to subject recruitment. Male and female subjects between the ages of 18 and 50 years who were candidates for arthroscopic PM were eligible for inclusion in the study. Subjects whose injury had occurred more than 12 months before surgery, those with a prior knee injury for which they sought medical attention, or with diseases predisposing them to AC damage were excluded from the study. The subjects represented a consecutive sample of those eligible and willing to participate, whose MRIs could be scheduled prior to surgery. No participating subjects were excluded after surgery for any reason. Ten subjects (9 males, 1 female) with a mean age of 36.2 years (range 22-48 years) were included; MRI data from these subjects were also used for a separate study of meniscal volume [25].

6.3.2 MR Imaging

MR imaging was performed on both knees of each subject, an average of 11.5 days (range 2 – 44 days) before and 27.2 days (range 14 – 46 days) after surgery; the time between pre- and post-operative MRI assessments averaged 39.7 days (range 18 – 71 days). Each knee was imaged on a 3T MR imaging system (Siemens Trio, Erlangen, Germany), using a commercially available circular polarized knee coil. AC was imaged using the T1-weighted WE-3D-FLASH sequence **(Figure 6.1)** [Water-Excitation, 3D-

Fast Low-Angle Shot; TR/TE/FA: 20/7.6/12^{o}; FOV: 160mm; matrix: 512x512; in-plane resolution/slice thickness/interslice gap: 0.3125/1.5/0mm; bandwidth: 130 Hz/pixel; averages: 1; acquisition time: 8 minutes, 37 seconds] at each time point [21-22].

6.3.3 Manual Segmentation

The AC of each scan was manually segmented in the sagittal plane by a single experienced examiner using commercial software (Mimics 9.11, Materialise, Ann Arbor, MI). Each subject's scans were segmented consecutively, but the examiner was blinded to operative status and patient information. Once segmented, the AC was reconstructed, and a 3D voxel model of each structure was created. Each voxel model was wrapped with a triangular mesh to create a virtual solid model [21-22, 26]. Each virtual model captured both the volume and morphology of each structure.

6.3.4 Articular Cartilage Thickness

The thickness of each of 8 regions of interest (ROIs) within the TF joint was measured before and after surgery for each subject **(Figure 6.2)**. The ROIs were selected to represent load-bearing AC regions [21, 24, 27-28]. With each femoral cartilage model, a cylinder was fit to the bone-cartilage interface of the femoral condyles. A line was drawn from a "notch" point on the lateral condyle, which appears to separate the TF and patellofemoral joints, to the center of the cylinder axis. Six ROIs (3 medial, 3 lateral) were then defined by moving from the "notch" point toward the posterior aspects of the femoral condyles in 30^{0} increments. The mean thickness of each ROI was determined

using a closest point algorithm. Each ROI was labeled M (medial) or L (lateral), and was further denoted 1 (anterior), 2 (middle), or 3 (posterior) **(Figure 6.2a)** [21].

For each tibial cartilage model, the inertial axes of the medial compartment and the centroid of each compartment (medial and lateral) were determined using MATLAB (The Mathworks, Inc., Natick, MA) [21]. The inertial axes of the medial compartment were then projected onto the centroid of each tibial compartment to determine ROI orientation. Once oriented, the ROI of each compartment (1 medial, 1 lateral) was defined as ±20% of the overall anterior-posterior width of that compartment, and ±15% of its overall medial-lateral width **(Figure 6.2b)**. The mean thickness of each tibial ROI was calculated using a closest point algorithm in MATLAB.

6.3.5 Statistical Analysis

Statistical analyses were carried out using *Proc Univariate* and *Proc Mixed* in *SAS* (Version 9.1.3, Service Pack 4; SAS Institute, Cary, NC). AC thickness values were significantly positively skewed. A logarithmic transformation was applied to reduce this skewness (absolute value of coefficient of skewness < 1). Statistical analyses of AC thicknesses were performed on the log-transformed values, with means and confidence intervals reported after back-translation to their original units.

Statistical analyses were carried out using mixed linear modeling. The correlations of measures taken within the same subject, knee, compartment, structure, and ROI were accounted for by including random effects for intercept and the interaction of these factors. The measurements taken for the same region were assumed to be independent from the other structures, and have correlated errors (repeated effects). The

compound symmetry variance-covariance structures were used for both random and repeated effects. Orthogonal contrast statements were used to test the difference between pre- and post-surgery for each region. Type I error was maintained at 0.05 across all comparisons by the Holm test (sequential Bonferroni).

A post-hoc power analysis was conducted to estimate the smallest changes detectable (2-tailed alpha = 0.05) with 10 subjects at powers of 80, 90, and 95% in the uninjured compartments **(Table 6.1)**. This analysis was informed by the standard deviations and the correlations between the pre- and post-surgery measurements of these structures. The detectable changes can be interpreted as the size of changes at or above that which could be effectively ruled out with probabilities 80, 90, and 95%.

6.4 Results

There was no statistically significant difference between the mean pre- and post-operative thickness of any ROI (adjusted p=1.00; **Figure 6.3**). The AC regions showed a mean error of 0.86% between pre- and post-operative thickness values.

6.5 Discussion

Although knee injury has been correlated with early OA [27, 29-42], to date, a cause-effect relationship between these has not been established. An accurate, reliable method that can quantify *in vivo* changes in AC thickness would allow knee-injured patients to be tracked over time, thereby helping to elucidate the mechanisms involved in early OA development.

The present study demonstrates that qMRI can reliably determine TF AC thickness *in vivo*. There was no significant difference in AC thickness between time points, despite 95% power to detect changes in thickness of 0.23mm. These results suggest that our qMRI method is a repeatable tool for determining AC thickness *in vivo*. This quantitative method may be useful in future long-term studies designed to evaluate the outcome of knee injuries and their surgical treatments.

Our group has conducted two separate studies to evaluate the accuracy and reliability of MR-based measurements of AC thickness [21-22]. In each study, the manual MR-based segmentation approach described above was employed, and the same regions of interest (ROIs) were identified. One of the studies compared *ex vivo* mean AC thickness values to those obtained with a laser scanning technique, and showed a mean absolute error of just over 4%. The same study indicated that AC thickness measurements were repeatable *in vivo*, with CVs of less than 3%. These measures of variability align well with a study by Koo et al., in which a semi-automated MR segmentation technique was used to evaluate AC thickness in six femoral ROIs, both *ex vivo*, using porcine

cadavers, and *in vivo*, using human subjects [24]. Their study noted CVs of 2-3% *in vivo*, which are similar to the results of our previous studies [21-22], and of the present study.

Based on the data from this and previous studies, it is unknown whether qMRI will be able to detect the small changes in AC thickness that one would expect during the early stages of OA. Using a similar method, other authors have shown that the cartilage volume of the TF joint decreases 0.3-0.5% per year with natural aging [20], compared to 4-6.5% per year in patients with radiographic evidence of OA [6, 12, 20, 27]. Based on the reliability of AC thickness measurements indicated in the present study, and confirmed by the post hoc power analysis, it is likely that over the course of a long-term, prospective study of the outcomes of PM, our qMRI method would be able to detect significant changes in the AC thickness of subjects with OA when compared to control subjects.

There are several limitations associated with the present study. First, the number of subjects studied was relatively small (n=10). Our post-hoc power analysis suggests that with 10 subjects, the study was adequately powered to detect changes in AC thickness. Additionally, the purpose of this study was to validate the described MR-based segmentation method *in vivo*, so that it can be applied to larger long-term clinical studies in the future.

Second, the design of this study did not allow for any direct accuracy assessment of the AC thickness measurements. Fortunately, our group has conducted several studies using phantom and cadaver models to assess both accuracy and reliability of our qMRI methods *ex vivo* [21-22, 26].

Despite these limitations, the results of the present study, particularly when combined with the *ex vivo* work, indicate that MR-based segmentation is a reliable and valid method for evaluating TF AC thickness *in vivo* before and after PM. This method can be applied in future long-term studies of the outcomes of PM, which may begin to elucidate the mechanisms that drive the relationship between meniscal injury, PM, and early OA.

6.6 Acknowledgements

This project was funded by the National Institutes of Health (AR047910; AR047910S1). The authors wish to thank Benjamin B. Kimia, Ph.D., Joseph J. Crisco, Ph.D., Nhon H. Trinh, M.S., and Evan L. Leventhal, B.S., for their technical assistance.

6.7 References

1. Cicuttini, F.M., A.E. Wluka, and S.L. Stuckey, *Tibial and femoral cartilage changes in knee osteoarthritis.* Ann Rheum Dis, 2001. **60**: p. 977-980.
2. Eckstein, F., D. Burstein, and T.M. Link, *Quantitative MRI of cartilage and bone: degenerative changes in osteoarthritis.* NMR Biomed, 2006. **19**(7): p. 822-854.
3. Amin, S., et al., *The relationship between cartilage loss on magnetic resonance imaging and radiographic progression in men and women with knee osteoarthritis.* Arthritis & Rheumatism, 2005. **52**(10): p. 3152-3159.
4. Jones, G., et al., *Early radiographic osteoarthritis is associated with substantial changes in cartilage volume and tibial bone surface area in both males and females.* Osteoarthritis and Cartilage, 2004. **12**(2): p. 169-174.
5. Graichen, H., et al., *Quantitative assessment of cartilage status in osteoarthritis by quantitative magnetic resonance imaging: technical validation for use in analysis of cartilage volume and further morphologic parameters.* Arthritis & Rheumatism, 2004. **50**(3): p. 811-816.
6. Cicuttini, F., et al., *Longitudinal study of the relationship between knee angle and tibiofemoral cartilage volume in subjects with knee osteoarthritis.* Rheumatology, 2004. **43**(3): p. 321-324.
7. Raynauld, J.P., et al., *Quantitative magnetic resonance imaging evaluation of knee osteoarthritis progression over two years and correlation with clinical*

symptoms and radiologic changes. Arthritis & Rheumatism, 2004. **50**(2): p. 476-487.

8. Cicuttini, F.M., et al., *Longitudinal study of changes in tibial and femoral cartilage in knee osteoarthritis.* Arthritis & Rheumatism, 2004. **50**(1): p. 94-97.
9. Raynauld, J.P., et al., *Reliability of a quantification imaging system using magnetic resonance images to measure cartilage thickness and volume in human normal and osteoarthritic knees.* Osteoarthritis and Cartilage, 2003. **11**(5): p. 351-360.
10. Glaser, C., et al., *Femoro-tibial cartilage metrics from coronal MR image data: Technique, test-retest reproducibility, and findings in osteoarthritis.* Magnetic Resonance in Medicine, 2003. **50**(6): p. 1229-1236.
11. Biswal, S., et al., *Risk factors for progressive cartilage loss in the knee: a longitudinal magnetic resonance imaging study in forty-three patients.* Arthritis Rheum, 2002. **46**(11): p. 2884-2892.
12. Wluka, A.E., et al., *The determinants of change in tibial cartilage volume in osteoarthritic knees.* Arthritis & Rheumatism, 2002. **46**(8): p. 2065-2072.
13. Qazi, A.A., et al., *Separation of healthy and early osteoarthritis by automatic quantification of cartilage homogeneity.* Osteoarthritis and Cartilage, 2007. **15**(10): p. 1199-206.
14. Bauer, J., et al., *Volumetric Cartilage Measurements of Porcine Knee at 1.5-T and 3.0-T MR Imaging: Evaluation of Precision and Accuracy.* Radiology, 2006. **241**(2): p. 399-406.

15. Bolbos, R., et al., *Knee cartilage thickness measurements using MRI: a 4 1/2-month longitudinal study in the meniscectomized guinea pig model of OA.* Osteoarthritis Cartilage, 2007. **15**(6): p. 656-65.

16. Bolbos, R., et al., *Measurement of knee cartilage thickness using MRI: a reproducibility study in a meniscectomized guinea pig model of osteoarthritis.* NMR in Biomedicine, 2007. **EPub**.

17. Eckstein, F. and C. Glaser, *Measuring cartilage morphology with quantitative magnetic resonance imaging.* Seminars in Musculoskeletal Radiology, 2004. **8**(4): p. 329-353.

18. Eckstein, F., *Noninvasive study of human cartilage structure by MRI.* Methods in Molecular Medicine, 2004. **101**: p. 191-218.

19. Burstein, D. and M. Gray, *New MRI techniques for imaging cartilage.* J Bone Joint Surg Am, 2003. **85**(Suppl 2): p. 70-77.

20. Gray, M.L., et al., *Toward imaging biomarkers for osteoarthritis.* Clinical Orthopaedics and Related Research, 2004. **427**(Suppl): p. S175-S181.

21. Bowers, M.E., et al., *Quantitative MR Imaging using "LiveWire" to Measure Tibiofemoral Articular Cartilage Thickness.* Osteoarthritis Cartilage, 2008. **16**: p. 1167-1173.

22. Bowers, M.E., et al., *Effects of ACL interference screws on articular cartilage volume and thickness measurements with 1.5 T and 3 T MRI.* Osteoarthritis Cartilage, 2008. **16**: p. 572-578.

23. Andriacchi, T.P., et al., *Rotational Changes at the Knee after ACL Injury Cause Cartilage Thinning.* Clin Orthop Relat Res, 2006. **442**: p. 39-44.

24. Koo, S., G.E. Gold, and T.P. Andriacchi, *Considerations in measuring cartilage thickness using MRI: factors influencing reproducibility and accuracy.* Osteoarthritis and Cartilage, 2005. **13**(9): p. 782-789.

25. Bowers, M.E., et al., *Quantitative Magnetic Resonance Imaging Detects Changes in Meniscal Volume in Vivo After Partial Meniscectomy.* American Journal of Sports Medicine, In Press.

26. Bowers, M.E., et al., *Quantification of meniscal volume by segmentation of 3T magnetic resonance images.* Journal of Biomechanics, 2007. **40**(12): p. 2811-2815.

27. Cicuttini, F.M., et al., *Rate of knee cartilage loss after partial meniscectomy.* Journal of Rheumatology, 2002. **29**(9): p. 1954-1956.

28. Eckstein, F., et al., *Brief report: Two year longitudinal change and test--retest-precision of knee cartilage morphology in a pilot study for the osteoarthritis initiative.* Osteoarthritis and Cartilage, 2007. **15**: p. 1326-1332.

29. Englund, M., *Meniscal tear - a feature of osteoarthritis.* Acta Orthopaedica Scandinavica, 2004. **75**(Suppl 312): p. 8-45.

30. Englund, M. and L.S. Lohmander, *Risk factors for symptomatic knee osteoarthritis fifteen to twenty-two years after meniscectomy.* Arthritis & Rheumatism, 2004. **50**(9): p. 2811-2819.

31. Englund, M., et al., *Patient-relevant outcomes fourteen years after meniscectomy: Influence of type of meniscal tear and size of resection.* Rheumatology, 2001. **40**: p. 631-639.

32. Englund, M. and S. Lohmander, *Patellofemoral osteoarthritis coexistent with tibiofemoral osteoarthritis in a meniscectomy population.* Annals of the Rheumatic Diseases, 2005. **20**: p. Epub.

33. Englund, M., P.T. Paradowski, and L.S. Lohmander, *Association of radiographic hand osteoarthritis with radiographic knee osteoarthritis after meniscectomy.* Arthritis & Rheumatism, 2004. **50**(2): p. 469-475.

34. Fairbank, T.J., *Knee joint changes after meniscectomy.* Journal of Bone and Joint Surgery. British Volume, 1948. **30**: p. 664-670.

35. Andersson-Molina, H., H. Karlsson, and P. Rockborn, *Arthroscopic partial and total meniscectomy: A long-term follow-up study with matched controls.* Arthroscopy, 2002. **18**(2): p. 183-189.

36. Allen, P.R., R.A. Denham, and A.V. Swan, *Late degenerative changes after meniscectomy. Factors affecting the knee after operation.* J Bone Joint Surg Br, 1984. **66**(5): p. 666-71.

37. Benedetto, K.P. and C. Rangger, *Arthroscopic partial meniscectomy: 5-year follow-up.* Knee Surg Sports Traumatol Arthrosc, 1993. **1**(3-4): p. 235-8.

38. Higuchi, H., et al., *Factors affecting long-term results after arthroscopic partial meniscectomy.* Clinical Orthopaedics and Related Research, 2000. **377**: p. 161-168.

39. Neyret, P., S.T. Donell, and H. Dejour, *Osteoarthritis of the knee following meniscectomy.* British Journal of Rheumatology, 1994. **33**: p. 267-268.

40. Rangger, C., et al., *Partial Meniscectomy and Osteoarthrits: Implications for Treatment of Athletes.* Sports Med, 1997. **23**(1): p. 61-68.

41. Rangger, C., et al., *Osteoarthritis after arthroscopic partial meniscectomy.* American Journal of Sports Medicine, 1995. **23**(2): p. 240-4.

42. Roos, H., et al., *Knee osteoarthritis after meniscectomy: prevalence of radiographic changes after twenty-one years, compared with matched controls.* Arthritis Rheum, 1998. **41**(4): p. 687-93.

Leg	Compartment	Compartment Status	Region	Detectable Change (mm)		
				80%	90%	95%
Injured	Lateral	Uninjured	L1	0.16	0.19	0.21
Injured	Lateral	Uninjured	L2	0.11	0.13	0.14
Injured	Lateral	Uninjured	L3	0.12	0.14	0.15
Injured	Lateral	Uninjured	LT	0.06	0.07	0.07
Injured	Medial	Uninjured	M1	0.15	0.18	0.20
Injured	Medial	Uninjured	M2	0.19	0.22	0.25
Injured	Medial	Uninjured	M3	0.20	0.23	0.26
Injured	Medial	Uninjured	MT	0.24	0.28	0.31
Uninjured	Lateral	Uninjured	L1	0.19	0.22	0.25
Uninjured	Lateral	Uninjured	L2	0.14	0.16	0.18
Uninjured	Lateral	Uninjured	L3	0.19	0.22	0.25
Uninjured	Lateral	Uninjured	LT	0.23	0.27	0.30
Uninjured	Medial	Uninjured	M1	0.27	0.31	0.35
Uninjured	Medial	Uninjured	M2	0.17	0.20	0.22
Uninjured	Medial	Uninjured	M3	0.31	0.36	0.40
Uninjured	Medial	Uninjured	MT	0.16	0.18	0.21

Table 6.1: Detectable changes in tibiofemoral articular cartilage thickness (mm) at power (%) as a function of location.

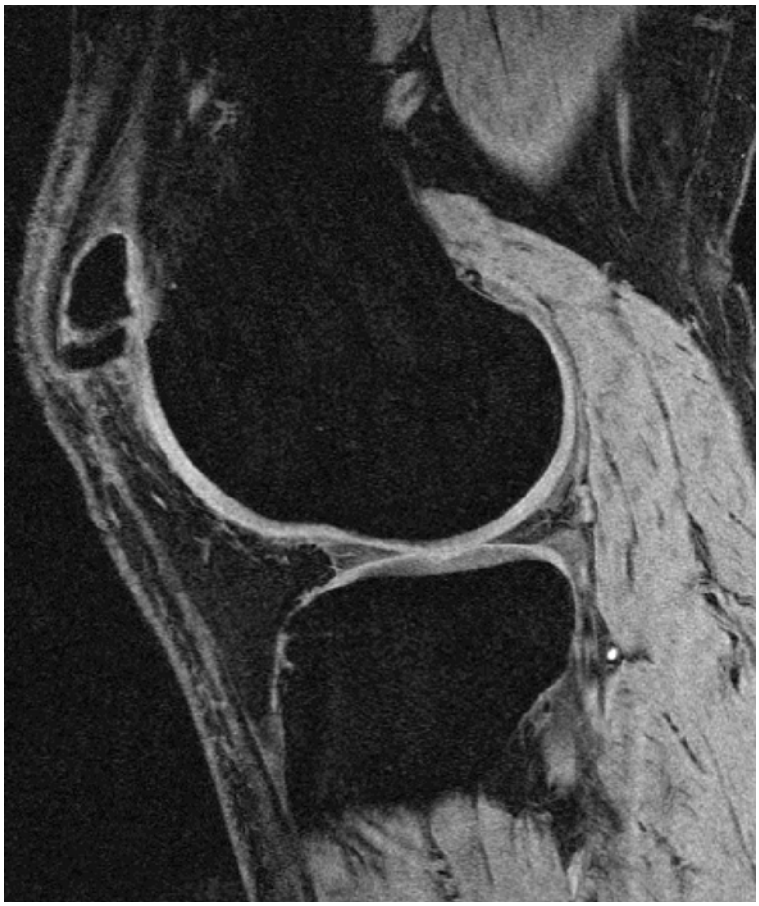

Figure 6.1: Sagittal view of a knee imaged with the Fast Low-Angle Shot (FLASH) sequence, from which the articular cartilage was segmented.

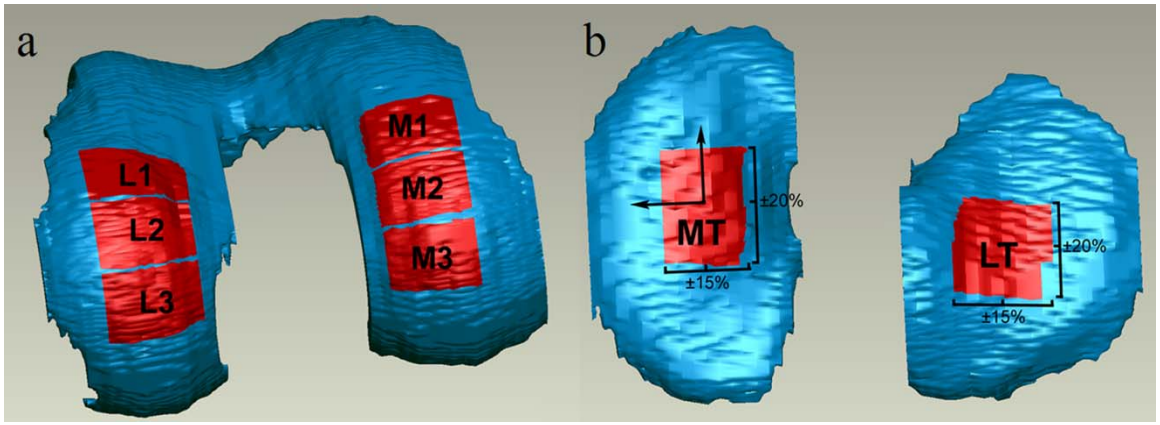

Figure 6.2: Articular cartilage regions of interest (ROIs) defined for thickness calculations. (a) Femoral ROIs were labeled "M" or "L" for medial and lateral regions, respectively. The femoral regions were further denoted as 1 (anterior), 2 (middle), or 3 (posterior). (b) Tibial ROIs were centered about the centroid of each condyle, and each region's size was a percent of the cartilage compartment's overall size. Tibial ROIs were labeled "M" or "L" for medial and lateral regions, and further denoted "T" (tibia). Portions of this figure adapted from a previous manuscript [21].

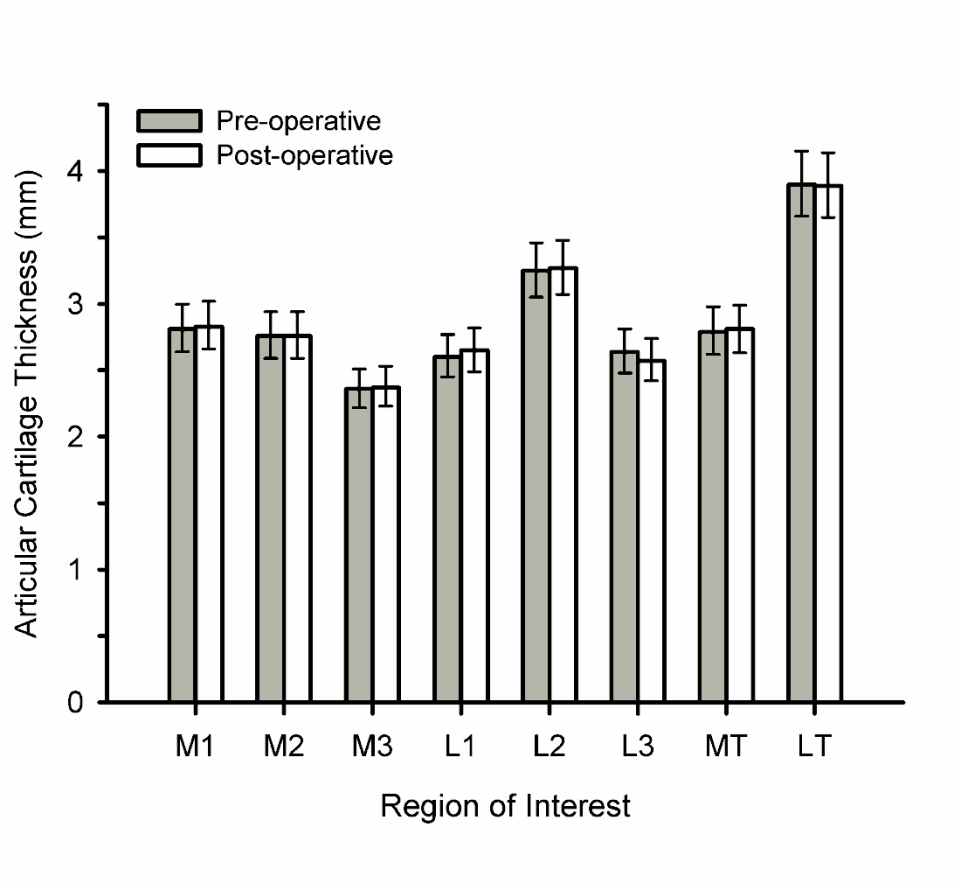

Figure 6.3: Least squares geometric mean articular cartilage thickness values (mm) within each region of interest before and after surgery (combined means from injured and uninjured knees). Error bars indicate standard errors.

Chapter 7

Quantitative Magnetic Resonance Imaging of Tibiofemoral Articular Cartilage in a Porcine Model of ACL Reconstruction

Megan E. Bowers, Glenn A. Tung, Martha M. Murray, Braden C. Fleming

7.1 Abstract

Anterior cruciate ligament (ACL) injury is common, and places the knee at risk for early osteoarthritis (OA). Large animal models are useful for studying disease-modifying interventions. Quantitative MRI (qMRI) of articular cartilage (AC) may be useful for tracking changes in cartilage thickness in such animal models. Our objective was to determine whether 15 weeks of healing would be sufficient for qMRI to detect changes in the AC thickness of ACL-transected and ACL-reconstructed porcine knees, when compared to contralateral control limbs.

Ten mini-pigs were randomized into two groups of five. One group underwent unilateral ACL-transection, and the other underwent allograft ACL-reconstruction. Animals were allowed to heal for 15 weeks before euthanasia. Their hind limbs were harvested and imaged with 3T MRI. A segmentation technique was applied to determine the AC thickness in eight regions of interest (ROIs) within each knee. Surgical limb AC thickness was compared to control limb AC thickness.

The AC thickness in each ROI of the ACL-transected and ACL-reconstructed knees was significantly greater when compared to their respective control limbs. There was no significant difference in AC thickness between the surgical limbs of each group after 15 weeks of healing.

The results suggest that qMRI is able to detect changes in AC thickness in ACL-transected and ACL-reconstructed porcine knees after 15 weeks of healing. This method may be used in future studies to help elucidate the mechanisms involved in OA development after ACL injury and surgical intervention, and could be useful for evaluating potential disease-modifying interventions.

7.2 Introduction

The anterior cruciate ligament (ACL) is the most frequently totally disrupted ligament of the knee joint. The injury is associated with severe functional deficits, and places the knee at risk for early osteoarthritis (OA) [1]. Because the ACL does not heal on its own, ACL reconstruction (ACLR) using an autograft or allograft is typically performed to restore function. While ACLR improves knee joint stability and restores function, the procedure does not eliminate the risk of OA associated with ACL injury.

ACL transection (ACLT), a procedure in which the ACL is surgically transected, mimics many, although not all, aspects of a traumatically ACL-injured knee. ACLT is often used to induce post-traumatic OA to study disease progression and potential treatments in animal models [2-10]. In large animal models, which are crucial for studying disease-modifying interventions before they can be applied to human subjects, data regarding the length of time surgically-induced ACLT takes to precipitate early- and late-stage post-traumatic OA are unclear.

Several magnetic resonance imaging (MRI) studies have demonstrated that while advanced OA is marked by a decrease in articular cartilage (AC) thickness, a focal increase in AC thickness is thought to be one of the earliest detectable indications of OA [11-13]. These studies suggest that the breakdown of proteoglycan, an important structural molecule of cartilage, attracts water into the tissue [12]. The ability to detect these very early changes in AC morphometry may allow researchers to investigate early-stage OA treatments in large animal models.

Quantitative MRI (qMRI) has been used to assess morphological changes in knee articular cartilage [14-21]. Our group recently validated a qMRI approach for evaluating articular cartilage thickness *ex vivo* using phantom and cadaver models [18-19]. We have also studied the method's reliability *in vivo* in human subjects (Chapter 6). The method has not yet been applied to a large animal model that is frequently used to study novel treatment options. Doing so could help determine the length of time between ACLT or ACLR and post-traumatic OA in these animals. The validation of qMRI in a large animal model offers the ability to more comprehensively understand disease progression in these animals.

Therefore, the objective of the present study was to apply our MR-based segmentation technique to porcine stifle joints treated with both ACLT and ACLR. Our specific aim was to determine whether 15 weeks of healing would be sufficient for our qMRI method to detect changes in the TF AC thickness of the ACLT- and ACLR-treated knees, when compared to contralateral control limbs. We hypothesized that after 15 weeks, there would be significant differences in AC thickness between the surgical and control limbs.

7.3 Materials and Methods

7.3.1 Porcine Model of ACL Reconstruction

Ten skeletally mature Yucatan mini-pigs with a mean weight of 50kg (range 31-58kg) were included in the study. 5 pigs underwent unilateral ACL reconstruction (ACLR) using a bone-patellar tendon-bone allograft. The other 5 animals underwent unilateral ACL transaction (ACLT).

In each case, after the induction of anesthesia, the surgical knee was shaved, prepared with a surgical iodine solution and alcohol rinse, and draped. An approximately 8cm incision was made at the medial border of the patellar tendon; the patella was then retracted laterally. The fat pad was partially resected to expose the ACL. The ACL was completely transected at the junction of the proximal and middle thirds of the ligament using a scalpel. ACLT was verified by a positive Lachman examination.

In the animals undergoing ACLR, fresh-frozen allografts were harvested from 5 age-, weight-, and gender-matched donor knees. The entire patellar tendon, approximately 10mm wide, was used. Bone blocks were trimmed to 7mm diameter to allow for smooth graft passage through 8mm osseous tunnels in the femur and tibia. The osseous tunnels were drilled to the insertion sites of the native ACL using a commercial drill guide system (Acufex Elbow Aimer, Smith & Nephew Inc., Andover, MA). Once the tunnels were completed, the graft was introduced intra-articularly through an arthrotomy. One bone block was passed into the femoral tunnel and rigidly fixed using a 6mm bioabsorbable interference screw (CALAXO, Smith & Nephew, Inc.). The graft

was then passed into the tibial tunnel, pre-conditioned using 20 cycles of manual tension, held in maximum manual tension, and secured in the tibia using another 6mm interference screw. The tibial screw was inserted into the tibial tunnel at the distal end of the tunnel, and the screw was countersunk 3mm below the cortical surface of the tibia.

In each case, the retinacular and subcutaneous tissues were closed with interrupted 2-0 Vicryl sutures (Ethicon Inc., Somerville, NJ). A 3-0 Vicryl subcuticular stitch was used to close the skin incision. After surgery, the animals were allowed unrestricted weightbearing. Postoperative pain was managed with narcotics delivered transcutaneously. All animals were monitored closely for signs of discomfort or weight loss. The pigs in each group were euthanized after 15 weeks of healing. The knees were immediately harvested and imaged with the MR imaging protocol describe below.

7.3.2 MR Imaging

MR imaging was performed on both hind limbs of each animal immediately following euthanasia and harvesting. Each knee was imaged on a 3T MR imaging system (Siemens Trio, Erlangen, Germany), using a commercially available circular polarized knee coil. AC was imaged using the T1-weighted WE-3D-FLASH sequence [Water-Excitation, 3D-Fast Low-Angle Shot; TR/TE/FA: 20/7.4/12^{o}; FOV: 140mm; matrix: 512x512; in-plane resolution/slice thickness/interslice gap: 0.3125/0.8/0mm; bandwidth: 130 Hz/pixel; averages: 3; acquisition time: 23 minutes, 16 seconds] [18-19].

7.3.3 Manual Segmentation

The AC of each scan was manually segmented in the sagittal plane by a single

experienced examiner (MEB) using commercial software (Mimics 9.11, Materialise, Ann Arbor, MI). The examiner was blinded to the operative status of each limb. Once segmented, the AC was reconstructed, and a 3D voxel model of each structure was created. Each voxel model was wrapped with a triangular mesh to create a virtual solid model [18-19, 22]. Each virtual model captured AC volume and morphology.

7.3.4 Articular Cartilage Thickness

The AC thickness of each of 8 load-bearing regions of interest (ROIs) within the TF joint was measured for each animal after euthanasia using a standardized anatomic-based coordinate system **(Figure 7.1)**. With each femoral cartilage model, a cylinder was fit to the bone-cartilage interface of the femoral condyles. A line was drawn from a "notch" point on the lateral condyle, which appears to separate the TF and patellofemoral joints, to the center of the cylinder axis. Six ROIs (3 medial, 3 lateral) were then defined by moving from the "notch" point toward the posterior aspects of the femoral condyles in 30^0 increments. The mean thickness of each ROI was determined using a closest point algorithm with custom MATLAB (The Mathworks, Inc., Natick, MA) code. Each ROI was labeled M (medial) or L (lateral), and was further denoted 1 (anterior), 2 (middle), or 3 (posterior) **(Figure 7.1a)** [18]. Because porcine stifle joints have a maximum extension angle of approximately 30^o, the MATLAB code allowed for angle correction to align the vertical axis of the femur with the MRI scan axes.

For each tibial cartilage model, the inertial axes of the medial compartment and the centroid of each compartment (medial and lateral) were determined using MATLAB [18]. The inertial axes of the medial compartment were then projected onto the centroid

of each tibial compartment to determine ROI orientation. Once oriented, the ROI of each compartment (1 medial, 1 lateral) was defined as ±20% of the overall anterior-posterior width of that compartment, and ±15% of its overall medial-lateral width **(Figure 7.1b)**. The mean thickness of each tibial ROI was calculated using a closest point algorithm in MATLAB.

7.4 Results

In the ACLT group, the mean AC thicknesses of the surgical knees were 1.56mm and 1.43mm for the femoral and tibial ROIs, respectively. In the same animals, the mean AC thicknesses of the contralateral control limbs were 1.27mm and 1.11mm, respectively. In the ACLT group, there was a mean 22.8% increase in the femoral thickness within the surgical limbs compared to the control limbs. There was also a mean 29.3% increase in the tibial thickness within the surgical limbs compared to the control limbs. In each ROI, the mean AC thickness of the ACLT limbs was greater than the mean AC thickness of the contralateral limbs **(Figure 7.2)**.

Animals in the ACLR group had mean AC thicknesses of 1.59mm and 1.49mm for the femoral and tibial ROIs, respectively, of the surgical limbs. These animals' mean contralateral control limb AC thicknesses were 1.37mm and 1.16mm for the femoral and tibial ROIs, respectively. In the ACLR group, there was a mean 15.6% increase in the femoral thickness within the surgical limbs compared to the control limbs. There was also a mean 28.6% increase in the tibial thickness within the surgical limbs compared to the control limbs. In each ROI, the mean AC thickness of the ACLR limbs was greater the mean AC thickness of the contralateral limbs **(Figure 7.2)**.

7.5 Discussion

Although ACL injury is associated with the development of early OA, the mechanisms involved in post-traumatic OA development after injury remain poorly understood. An accurate, reliable method that can quantify *in vivo* changes in AC thickness would allow knee-injured patients to be tracked over time, thereby helping to elucidate these mechanisms. The ability to use this method in a large animal model of knee injury would allow researchers to study disease progression, as well as evaluate disease-modifying interventions before they are applied to human subjects.

The present study demonstrates that qMRI can detect a difference between the AC thickness of ACL-transected, ACL-reconstructed, and their respective contralateral control limbs in mini-pigs after 15 weeks of healing. The limbs that underwent ACLT and ACLR had significantly greater AC thicknesses than their respective control limbs, suggesting that our qMRI method can be used to evaluate AC thickness in large animal models. This quantitative method may be useful in future large animal studies designed to evaluate the outcome of knee injuries, their surgical treatments, and potential disease-modifying interventions.

It is particularly interesting to note the marked increase of the AC thickness of each group's respective surgical limbs when compared to control limbs. It is hypothesized that in the very early stages of OA development, AC undergoes a brief swelling period, wherein proteoglycan breakdown draws water into the cartilage tissue [11-13]. It is likely that, after 15 weeks of healing, the animals used in this study were

euthanized while their limbs were undergoing the initial cartilage thickness changes characteristic of early OA. While additional animals must be added to each treatment group before firm conclusions can be drawn, the results of this study may indicate that 15 weeks are not sufficient to observe the cartilage loss one may expect during OA disease progression.

Our group has conducted several studies to evaluate the accuracy and reliability of MR-based measurements of AC thickness [18-19]. In each study, the manual MR-based segmentation approach described above was employed, and the same regions of interest (ROIs) were identified. One of the studies compared *ex vivo* mean AC thickness values to those obtained with a laser scanning technique, and showed a mean absolute error of just over 4%. The same study indicated that AC thickness measurements were repeatable *in vivo*, with coefficients of variation (CVs) of less than 3%. These measures of variability align well with a study by Koo et al., in which a semi-automated MR segmentation technique was used to evaluate AC thickness in six femoral ROIs, both *ex vivo*, using porcine cadavers, and *in vivo*, using human subjects [21]. Their study noted CVs of 2-3% *in vivo*, which are similar to the results of our previous studies [18-19]. When considered in the context of the present study, these results suggest that the MR-based method used to evaluate porcine AC thickness is both reliable and accurate.

There are several limitations associated with this study. First, the number of animals studied was relatively small (n=5 in each group). A power analysis conducted on an *in vivo* study of human subjects (Chapter 6) suggested that 10 subjects provided adequate power to detect changes in AC thickness.

Second, this study did not include any direct accuracy assessment of the AC thickness measurements. Our group has conducted several studies using phantom and cadaver models to assess both accuracy and reliability of our qMRI methods *ex vivo* [18-19, 22].

Despite these limitations, the results of the present study, particularly when combined with the *ex vivo* work, indicate that MR-based segmentation can detect a difference in TF AC thickness in porcine knees 15 weeks after ACLT and ACLR. This method can be applied to future large animal models of knee injury, surgical intervention, and potential disease-modifying interventions. Such studies may begin to elucidate the mechanisms that drive the relationship between ACL injury, surgical intervention, and OA.

7.6 Acknowledgements

This project was funded by a National Football League Charities Medical Research Grant and the National Institutes of Health (R01-AR047910-06). The authors wish to thank Scott McAllister, Lynn Fanella, and Evan Leventhal for their assistance.

7.7 References

1. Daniel, D.M., et al., *Fate of the ACL-injured patient: A prospective outcome study.* Am J Sports Med, 1994. **22**: p. 632-644.
2. Batiste, D.L., et al., *Ex vivo characterization of articular cartilage and bone lesions in a rabbit ACL transection model of osteoarthritis using MRI and micro-CT.* Osteoarthritis Cartilage, 2004. **12**(12): p. 986-996.
3. Brandt, K.D., et al., *Anterior (cranial) cruciate ligament transection in the dog: a bona fide model of osteoarthritis, not merely of cartilage injury and repair.* J Rheumatol, 1991. **18**(3): p. 436-46.
4. Hasler, E.M., et al., *In vivo knee joint loading and kinematics before and after ACL transection in an animal model.* Journal of Biomechanics, 1998. **31**(3): p. 253-262.
5. Johnson, R.G. and A.R. Poole, *The early response of articular cartilage to ACL transection in a canine model.* Exp Pathol, 1990. **38**(1): p. 37-52.
6. Liu, W.H., et al., *Spontaneous and experimental osteoarthritis in dog: similarities and differences in proteoglycan levels.* J Orthop Res, 2003. **21**(4): p. 730-737.
7. Lopez, M.J., et al., *A comparison of joint stability between anterior cruciate intact and deficient knees: a new canine model of anterior cruciate ligament disruption.* Journal of Orthopaedic Research, 2003. **21**(2): p. 224-230.

8. Papaioannou, N., et al., *Optimal timing of research after anterior cruciate ligament resection in rabbits.* Contemp Top Lab Anim Sci, 2004. **43**(6): p. 22-7; quiz 58.

9. Setton, L.A., D.M. Elliott, and V.C. Mow, *Altered mechanics of cartilage with osteoarthritis: human osteoarthritis and an experimental model of joint degeneration.* Osteoarthritis and Cartilage, 1999. **7**(1): p. 2-14.

10. Tashman, S., et al., *Kinematics of the ACL-deficient canine knee during gait: serial changes over two years.* Journal of Orthopaedic Research, 2004. **22**(5): p. 931-941.

11. Calvo, E., et al., *High-resolution MRI detects cartilage swelling at the early stages of experimental osteoarthritis.* Osteoarthritis and Cartilage, 2001. **9**(5): p. 463-472.

12. Calvo, E., et al., *Histopathological correlation of cartilage swelling detected by magnetic resonance imaging in early experimental osteoarthritis.* Osteoarthritis and Cartilage, 2004. **12**: p. 878-86.

13. Qazi, A.A., et al., *Separation of healthy and early osteoarthritis by automatic quantification of cartilage homogeneity.* Osteoarthritis and Cartilage, 2007. **15**(10): p. 1199-206.

14. Eckstein, F. and C. Glaser, *Measuring cartilage morphology with quantitative magnetic resonance imaging.* Seminars in Musculoskeletal Radiology, 2004. **8**(4): p. 329-353.

15. Eckstein, F., *Noninvasive study of human cartilage structure by MRI.* Methods in Molecular Medicine, 2004. **101**: p. 191-218.

16. Burstein, D. and M. Gray, *New MRI techniques for imaging cartilage.* J Bone Joint Surg Am, 2003. **85**(Suppl 2): p. 70-77.

17. Gray, M.L., et al., *Toward imaging biomarkers for osteoarthritis.* Clinical Orthopaedics and Related Research, 2004. **427**(Suppl): p. S175-S181.

18. Bowers, M.E., et al., *Quantitative MR Imaging using "LiveWire" to Measure Tibiofemoral Articular Cartilage Thickness.* Osteoarthritis Cartilage, 2008. **16**: p. 1167-1173.

19. Bowers, M.E., et al., *Effects of ACL interference screws on articular cartilage volume and thickness measurements with 1.5 T and 3 T MRI.* Osteoarthritis Cartilage, 2008. **16**: p. 572-578.

20. Andriacchi, T.P., et al., *Rotational Changes at the Knee after ACL Injury Cause Cartilage Thinning.* Clin Orthop Relat Res, 2006. **442**: p. 39-44.

21. Koo, S., G.E. Gold, and T.P. Andriacchi, *Considerations in measuring cartilage thickness using MRI: factors influencing reproducibility and accuracy.* Osteoarthritis and Cartilage, 2005. **13**(9): p. 782-789.

22. Bowers, M.E., et al., *Quantification of meniscal volume by segmentation of 3T magnetic resonance images.* Journal of Biomechanics, 2007. **40**(12): p. 2811-2815.

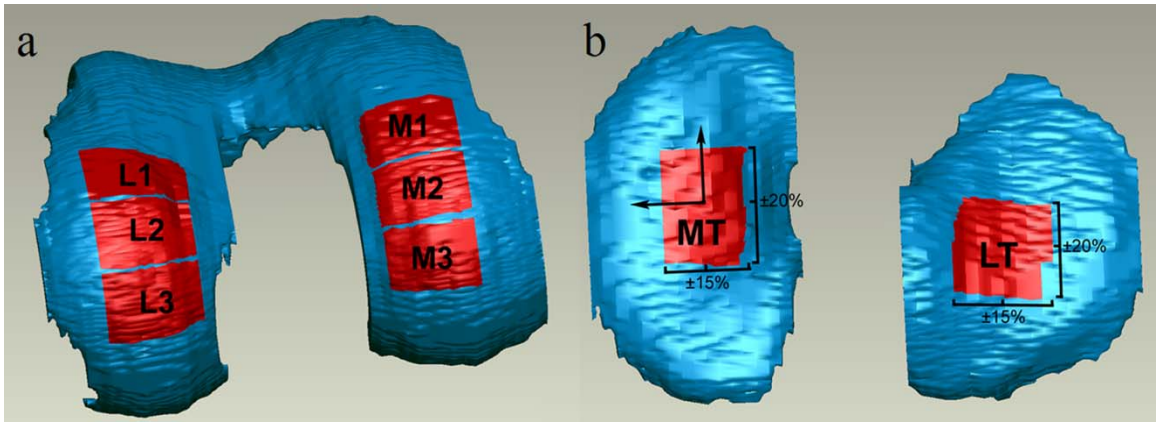

Figure 7.1: Articular cartilage regions of interest (ROIs). ROIs were labeled “M” and “L” for medial and lateral regions, respectively. (a) Femoral ROIs were further denoted as 1 (anterior), 2 (middle), or 3 (posterior). (b) Tibial ROIs were further denoted “T” (tibia). Portions of this figure adapted from a previous manuscript [18].

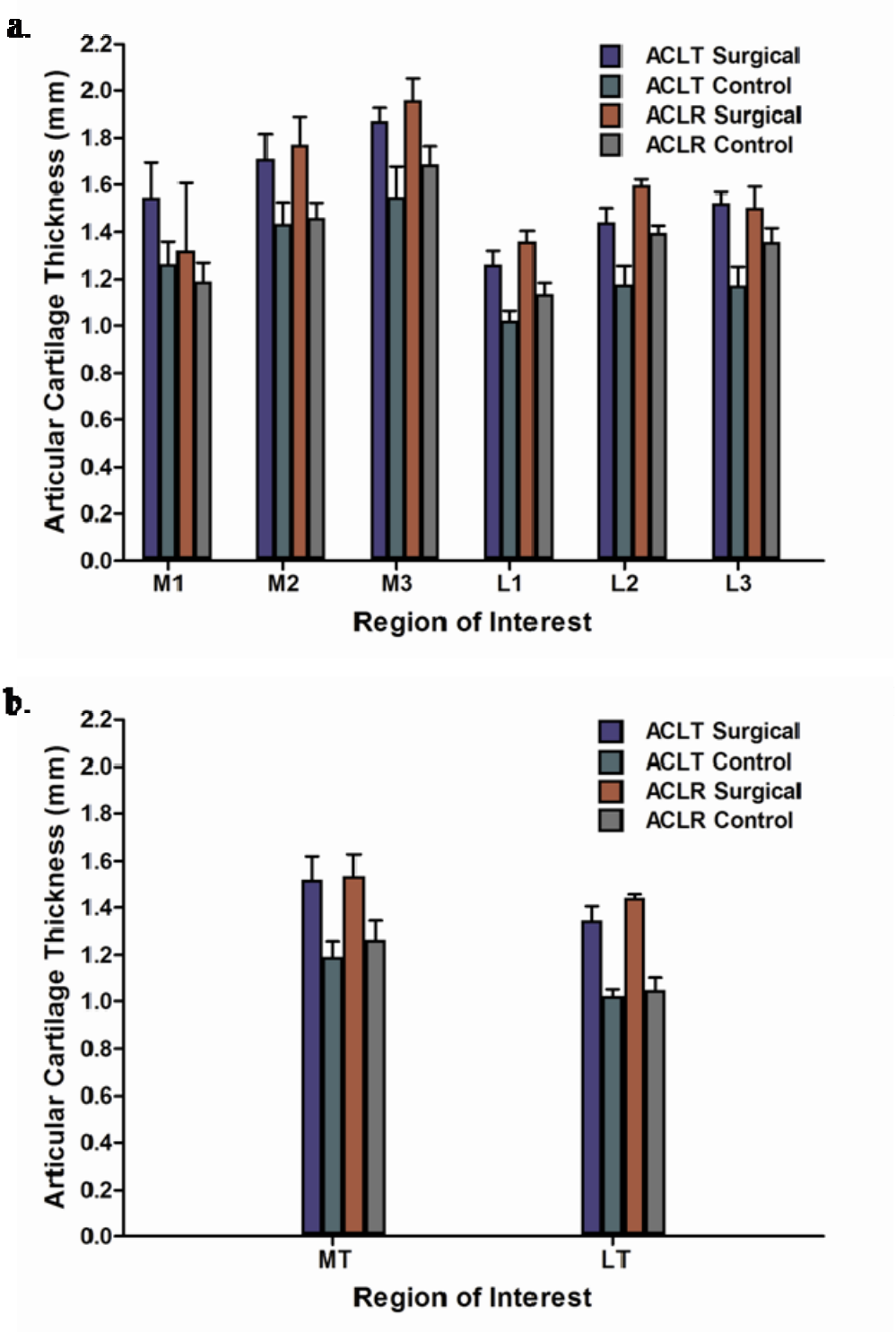

Figure 7.2: Mean articular cartilage thickness values (mm) within the (a) femoral and (b) tibial regions of interest for surgical and contralateral control limbs within each group of animals. Error bars indicate standard errors.

Chapter 8

Conclusions and Ongoing Studies

8.1 Conclusions

The data presented within this dissertation provide the groundwork necessary to develop and justify a long-term prospective controlled cohort study evaluating the development of osteoarthritis (OA) following partial meniscectomy (PM). The long-term objective of this work remains to identify whether a critical amount of meniscal tissue can be removed during PM without compromising the structure's chondroprotective function. Such a threshold may be determined by measuring the volume of meniscal tissue removed from a patient's knee during PM, and then tracking that patient's tendencies toward OA development by using quantitative MRI to assess articular cartilage (AC) thickness. The specific aims of the work presented within the chapters of this thesis were to: (1) refine and validate an image segmentation technique to quantify meniscal volume and AC thickness; (2) apply the segmentation technique to patients with acute meniscal tears; and (3) use the segmentation technique to evaluate outcomes of anterior cruciate ligament (ACL) transection and ACL reconstruction in a controlled

animal model. Chapter 1 describes the significance of our overall goal, and explains our specific aims in detail.

8.1.1 Aim 1: Refine and validate an image segmentation technique to quantify meniscal volume and articular cartilage thickness

Aim 1 of this thesis was accomplished with the studies contained in Chapters 2-4. Chapter 2 describes a series of studies conducted to: (1) evaluate the feasibility of an MR-based segmentation method for determining meniscal volume; (2) determine the method's reliability for repeated measurements; and (3) validate its accuracy *in situ*. In these studies, which included phantom and cadaver specimens, MR images were obtained on a 3T magnet, and each scan was segmented using a biplanar approach. The MR-based volumes of the menisci of each specimen were compared to those measured by water displacement. The overall results of these studies indicated that our biplanar segmentation approach is accurate and reliable. The calculated volumes of the menisci were within 5% of the water displacement volumes, and the coefficients of variation were 4%. The intraclass correlation coefficients for our MR-based measurements were greater than 0.96. These data demonstrated that our segmentation method could be used to measure the amount of meniscal tissue excised during partial meniscectomy to within 126mm^3.

Aim 1 was further examined within Chapter 3, wherein we assessed the effects of interference screws, which are commonly used during ACL reconstruction, and magnetic field strength on AC volume and thickness measurements with quantitative MRI. In this study, we imaged 5 cadaver knees on both 1.5T and 3T scanners, with and without interference screws implanted. The tibiofemoral (TF) AC was segmented and

reconstructed from the MR images, and volume and thickness measurements were made on the resulting 3D models. Although several load-bearing regions of AC showed significant differences in volume and thickness between magnet strengths, most showed no significant difference between screw conditions. The medial tibial cartilage showed a mean decrease in volume of 5.9% and 8.0% in the presence of interference screws at 3T and 1.5T, respectively. At 3T and 1.5T, the medial tibial cartilage showed a mean decrease in thickness of 7.0% and 12.0%, respectively, in the presence of interference screws. From this data, we concluded that caution should be used when interpreting AC volume and thickness at 3T in the presence of interference screws, particularly in the medial tibial compartment. Additionally, we observed that qMRI at different magnet strengths should not be used interchangeably to assess structural changes in TF AC during longitudinal studies.

Chapter 4 describes the final study used to accomplish Aim 1. Within this study, we set out to assess the reliability and accuracy of manual and semi-automated segmentation methods for quantifying knee cartilage thickness. This study employed both manual and LiveWire-based semi-automated segmentation methods, *ex vivo* and *in vivo*, to measure TF AC. In this study, the AC of a cadaver knee and a healthy volunteer's knee were segmented manually and with LiveWire from multiple 3T MR images. The cadaver specimen's cartilage thickness was also evaluated with a 3D laser scanner, which we assumed to be the gold standard. Thickness measurements were made in the ROIs described in previous chapters. The reliability of each segmentation method was assessed both *ex vivo* and *in vivo*, and accuracy was assessed *ex vivo* by comparing segmentation results to those obtained with laser scanning. The cadaver specimen thickness

measurements showed mean CVs of 4.2%, 3.0%, and 1.6%, when evaluated with manual segmentation, LiveWire segmentation, and laser scanning, respectively. The cadaver specimen showed mean absolute errors versus laser scanning of 4.1% and 7.5% for the manual and LiveWire segmentation, respectively. *In vivo* thickness measurements showed mean CVs of 2.7% and 3.7% when segmented manually and with LiveWire, respectively. From this data, we concluded that manual segmentation, LiveWire segmentation, and laser scanning are repeatable methods for quantifying knee cartilage thickness; however, the measurements are technique-dependent. Ex vivo, the manual segmentation error was distributed around the laser scanning mean, while LiveWire consistently underestimated laser scanning by 9%. We ultimately concluded that although LiveWire offers repeatability and decreased segmentation time, manual segmentation more closely approximates true cartilage thickness, particularly in cartilage contact regions.

The data and conclusions offered in Chapters 2-4 were sufficient to satisfy Aim 1, and allowed us to begin applying our refined and validated segmentation method *in vivo*.

8.1.2 Aim 2: Apply the segmentation technique to patients with acute meniscal tears

Aim 2 of this thesis was addressed in Chapters 5 and 6. Within these chapters, we describe a study in which ten subjects with meniscal tears were evaluated with 3T MRI before and after arthroscopic PM. Manual segmentation was used to create models of the menisci and TF AC of each subject's knees before and after surgery. The purpose of this study was twofold. With the meniscal segmentation, we intended to determine whether

qMRI could detect the immediate reduction in meniscal volume created by PM, while ruling out changes in unresected structures. By segmenting TF AC, we evaluated the reliability of qMRI for measuring AC thickness *in vivo*.

Chapter 5 addresses the first purpose of this study. With meniscal segmentation of each subject's injured and uninjured knees at each time point, we determined that the mean pre-operative volume of the injured menisci was significantly greater than the mean post-operative volume (2896±277mm^3 vs. 2480±277mm^3). Additionally, there was no significant difference between the mean pre- and post-operative volumes of the uninjured menisci (2687±256mm^3 vs. 2694±256mm^3). From this data, we determined that manual segmentation demonstrated a significant reduction in the volume of the surgically resected menisci after PM, while simultaneously ruling out changes in the volume of unresected meniscal tissue. We concluded that our manual meniscal segmentation method is responsive *in vivo*.

Chapter 6 addresses the TF AC portion of the study. In each subject's injured and uninjured knees, we observed no significant difference between the pre- and post-operative thickness of any AC region. We did not expect to see any differences between time points, because the study was conducted over a short 1-month interval, and was designed to assess repeatability *in vivo*.

From the data in Chapters 5 and 6, we were able to satisfy Aim 2 by determining that our segmentation method offers a novel, reliable method to study the relationship between the volume of meniscal tissue removed during PM and subsequent changes in AC thickness *in vivo* during long-term clinical studies.

8.1.3 Aim 3: Use the segmentation technique to evaluate outcomes of ACL transection and ACL reconstruction in a controlled animal model

Chapter 7 addresses the final aim of this dissertation. This chapter describes a study in which 10 mini-pigs were randomized into two groups of five. Group 1 underwent unilateral ACL transection (ACLT), and Group 2 underwent unilateral ACL reconstruction (ACLR). The animals in both groups were allowed to heal for 15 weeks, and were then humanely euthanized. Their hind limbs were harvested and imaged with 3T MRI. Our segmentation technique was applied to determine the AC thickness in 8 ROIs within each knee. Surgical limb thickness was compared to control limb thickness in each group, and across groups. We found a marked increase in AC thickness in each ROI of the ACLT and ACLR knees when compared to their respective control limbs. There was no significant difference in AC thickness between the surgical limbs of each group after 15 weeks of healing.

The results presented in Chapter 7 suggest that qMRI is able to detect changes in AC thickness in ACLT and ACLR porcine knees after 15 weeks of healing. We concluded that this method may be used in future studies to help elucidate the mechanisms involved in OA development after ACL injury and surgical intervention. The method could also be useful for evaluating potential disease-modifying interventions in large animal models.

8.2 Ongoing Studies

Our lab has several ongoing studies that seek to further address the aims described within the chapters of this dissertation. Below is a summary of these studies.

8.2.1 One-Year Follow-Up of Partial Meniscectomy Subjects

The subjects described in Chapters 5 and 6 were each treated for meniscal tears with arthroscopic PM. Initially, these subjects were imaged on a 3T scanner shortly before and approximately one month after their surgical resections. We are in the process of obtaining one-year follow-up data from these subjects. Follow-up data includes updates on each subject's perceived knee function, and additional 3T images of both the surgical and control knees. These images will be processed in the manner described above, and both meniscal volume and AC thickness will be determined. Data from these subjects will serve to supplement Specific Aim 2 of this dissertation.

8.2.2 Porcine Model of Biologically Enhanced ACL Reconstruction

In addition to the animal study described in Chapter 7, we plan to apply our segmentation method to several other groups of mini-pigs, each of whom have undergone "biologically enhanced" ACLR. Dr. Martha Murray has developed a method for applying a collagen scaffold and a proprietary platelet-rich plasma (PRP) mixture to traditional ACL grafts to attempt to improve mechanical properties of the resulting ligament. While the primary outcome measure of these studies will involve mechanical testing, we plan to

supplement these data with not only information about the pigs' articular cartilage thickness, but also data on the volume of the ACL grafts. We plan to determine ACL volume in a manner similar to the way we have determined meniscal volume in previous studies.

8.2.3 Delayed Gadolinium-Enhanced MRI of Cartilage (dGEMRIC) After ACL Reconstruction

Delayed Gadolinium-Enhanced MR Imaging of Cartilage (dGEMRIC) has been used to study changes in articular cartilage glycosaminoglycan (GAG) content following ACL injury. GAG is an important structural molecule of cartilage, and its loss is associated with articular cartilage degeneration. dGEMRIC involves the creation of T1 maps of hyaline cartilage after the administration of an IV dose of an anionic gadolinium [$Gd(DTPA)^{2-}$] contrast agent. Because cartilage matrix is composed largely of negatively charged GAG molecules, it repels the negatively charged ions of the contrast agent. Subsequently, the $Gd(DTPA)^{2-}$ concentration is higher in cartilage regions with lower GAG concentration; the cartilage $T1_{gd}$ relaxation time is thereby reduced. The resulting dGEMRIC index is correlated with cartilage GAG concentration.

Using the dGEMRIC method, our lab was able to study 15 subjects with unilateral ACL injuries. Within each subject, each knee (ACL-injured and contralateral) was imaged prior to ACL reconstruction. We observed a significant difference in the mean dGEMRIC indices of the medial compartment between the injured and uninjured knees. There was a mean 13% decrease in the dGEMRIC index of the injured knee compared to

the uninjured knee, indicating that each subject's ACL-injured knee had a lower GAG content than the contralateral knee.

Eight of these subjects returned for a follow-up dGEMRIC scan on each knee approximately one year after ACL reconstruction. Within these one-year follow-up subjects, the dGEMRIC indices of the femoral and tibial AC of the injured knees remained significantly lower than those of the contralateral uninjured knees. In fact, there was no significant difference between the initial (pre-ACL reconstruction) and 12-month follow-up dGEMRIC indices. These findings suggest that cartilage integrity may be jeopardized following ACL injury, and ACL reconstruction does not restore cartilage health in a one-year time frame.

8.3 Summary

The studies described within this dissertation served to develop and assess the tools necessary to quantify cartilage damage and partial meniscectomy, and to provide preliminary data supporting a long-term prospective controlled cohort study evaluating osteoarthritis following partial meniscectomy. Such a study will influence the future care of patients undergoing surgical treatment for meniscus changes. This will be particularly important when a patient and his or her clinician must choose between partial meniscectomy and other more complicated, expensive treatment alternatives, which may include repair, allografts, xenografts, and tissue-engineered replacements, as they become available. Data from a long-term prospective study will also provide a glimpse into the changes in articular cartilage thickness that occur after injury and its surgical treatment, and may allow researchers to elucidate the mechanisms involved in post-traumatic osteoarthritis development.